M.F. Wiegel

Mapping port operability indicators across the world

Screening the suitability of port locations in terms of metocean conditions

TU Delft Deltares

Mapping port operability indicators across the world
Screening the suitability of port locations related to metocean conditions

Cover image
A beautiful ocean scene made by Hokusai. The gigantic wave is about to hit the boats as if it were a huge monster that seems to symbolize the irresistible power of nature and the weakness of man. Yet these fishermen braved the seas on a clearly rough day. I chose this image because the boats can also symbolize a port under the attack of great forces of Mother Nature. To this day, we try to understand these forces and their consequences better and better.

Mapping port operability indicators across the world

Screening the suitability of port locations related to metocean conditions

By

M.F. Wiegel

in partial fulfilment of the requirements for the degree of

Master of Science
in Hydraulic Engineering

at the Delft University of Technology,
to be defended publicly on Thursday September 24, 2020 at 11:00 AM.

Supervisor:	Ir. W.P. de Boer	
Thesis committee:	Prof. dr. ir. M. van Koningsveld,	TU Delft
	Ir. W.P. de Boer,	TU Delft / Deltares
	Ir. A.J. van der Hout,	TU Delft / Deltares
	Prof. Dr. ir. A.J.H.M. Reniers,	TU Delft

An electronic version of this thesis is available at https://repository.tudelft.nl/.

Preface

This master thesis finalizes my program of Master of Science in Hydraulic Engineering at the Delft University of Technology.

First of all, a special thanks goes to Wiebe for giving me the opportunity to do my Master Thesis as a graduation internship at Deltares in Delft. Also, your commitment, enthusiasm, broad view and optimistic ideas against well-founded and realistic goals have given me the confidence from the start that I can bring this project to a successful outcome. In addition, I would like to express my gratitude to the whole team of Deltares for their hospitality, helpful colleagues and extensive knowledge.

Many thanks also to Mark, your critical eye did not always make me walk away satisfied after a meeting, but it did enable us to take this research to another level that I am proud of. You challenged me to go the extra mile. You expanded my perspective to use the power of global datasets and shift our focus on Africa to the world. This did not go without a fight, because what remains underexposed in this report is the worldwide data processing of multiple terabytes before I could apply my method on a selection of (port) locations.

I also want to thank Arne and Ad for their time and energy, both of you could quickly understand what it was about when I got stuck, took time to brainstorm or when I wanted feedback on something I could count on you.

Last but not least, I would like to thank my family, friends and girlfriend for their love and support during this research project. Due to the COVID-19 pandemic the last six months were not really normal. Nevertheless, I had a really enjoyable time and learned a lot of new skills, thank you all!

Matijs Wiegel,
De Zilk, September 2020

Abstract

Ports are crucial nodes in the world's supply chains and can play an important role in the development of local, regional and global economies. The port operability is an important factor for a port's viability as it determines the "uptime" and thus the extent to which a port is available for cargo handling operations. The metocean conditions (e.g., wind, waves, water levels and currents) are crucial indicators for a port's operability. This study investigates if it is possible to use global datasets to analyze and map the metocean conditions as indicators for port operability on a global scale. The aim of this study is to provide insights into which metocean indicators may influence port operability at which locations around the world.

We developed a generic method to analyze port operability indicators based on the (global) ERA5 reanalysis data of metocean conditions for the period 1979 to 2018. We selected the following three metocean parameters that are relevant for port operability: wind, short waves and infragravity (IG) waves. The offshore (short) wave conditions were translated to the nearshore via linear wave theory. Based on these nearshore wave conditions we estimated the bound long (infragravity) wave conditions (which are known to be important for moored vessels). The operability is estimated by the percentage of time that metocean conditions are below their operability threshold, derived from literature. We use a threshold of 13.8 m/s for wind speed, 2.0 m for short waves and 0.05 m for infragravity waves. We introduced the term operability potential (P_{total}) as the amount of time that all these indicators are below their thresholds and the port is potentially available for port operations. We deliberately defined this as "potential", because operability depends on more factors than metocean conditions alone. Based on P_{total} we classified geographical locations into very high (P_{total} > 95%), high (85% < P_{total} ≤ 95%), intermediate (75% < P_{total} ≤ 85%) and low (P_{total} ≤ 75%) operability potential.

To map the metocean indicators globally, we followed a gradual approach in terms of the number of locations included in the analysis. First, we started locally with a single port location (Cape Town) to develop and calibrate our method and to aggregate and visualize our results in a clear and effective way. Secondly, we validated our method for 10 port locations that are known to have serious or limited operability problems. For 9 out of the 10 ports, the (global) indicators correctly predicted whether operability problems due to metocean conditions were expected (or not). Thirdly, we applied our method to 103 (existing) port locations to analyze the statistics of the operability indicators. Finally, we applied our method to 4560 selected locations along the world's coastlines to screen and map the suitability of new port locations in terms of metocean conditions.

Out of the 103 analyzed port locations, 56 (54.4%) are classified as very high operability potential, 31 (30.1%) high, 9 (8.7%) intermediate, and 7 (6.8%) low. The short waves seem to be the most critical indicator for port operability. For all classes the short waves result into the lowest average operability potential, followed by IG waves. For 39 ports (37.9%), short waves are the main driver (the indicator with the lowest operability potential for a certain port location). For 37 ports (35.9%) a combination of short waves and IG waves are the main driver and for 7 ports (6.8%) IG waves. Based on our global analysis, the wind conditions hardly seem to result into operability problems. Still, for 20 port locations (19.4%) wind is the main driver, but the wind conditions hardly exceed the operability threshold for the present wind climate. Ports around the equator generally have a higher operability potential than port locations farther away from the equator. Around inland seas (such as the Red Sea and the Mediterranean) the operability potential is generally higher, which is probably related to their sheltered location for wind and waves. The port locations in the lowest operability class (P_{total} ≤ 75%) are defined as "hotspots" for possible operability issues, These hotspots are situated especially along the southern capes (Cape of Good Hoop & Leeuwin), around the 'Roaring Forties' (strong westerly winds between the latitudes 40 and 50 degrees south of the equator with less land to break the wind) and at exposed locations along the oceans.

Assuming an operability limit of 95%, our analysis indicated that about half (51.2%) of the world's coastline is potentially suitable as a port location in terms of metocean conditions. 1048 ports (23%) have a high operability potential, 491 (10.8%) intermediate and 685 (15%) low. Similar to the port locations, short waves are the most critical indicator for the equidistantly spaced locations, followed by IG waves and wind. The distribution of the indicators and main drivers over the different operability classes is comparable between both sample sets. The geographical differences are similar to the 103 port locations, on the southern hemisphere we observe short waves and IG waves resulting in less suitable port locations around the capes. On the northern hemisphere, wind is playing a larger role, but still mainly short waves and IG waves result in less suitable port locations along the oceans.

The uncertainty in the output of our approach is studied through a sensitivity analysis. We found that our generic method is robust (the operability potential is not changing more than 5%) for different water depths, changing metocean conditions, interannual trends and seasons. Our method is sensitive for different operability thresholds, the distribution of locations across the operability classes changes radically, the majority (36.9%) of the locations is then classified as "low". This means that our method yields similar results in terms of the operability classes for different water depths and changing metocean conditions. When different operability thresholds are applied are method is still applicable, but the results in terms of (global) operability classifications will be different.

Our study demonstrates that port operability estimates based on global metocean data provide realistic first-order insights into the suitability of different geographical locations for port operations. This allows port authorities, operators and designers to quickly scan at which existing port locations operability issues can be expected, which locations are potentially suitable for new port developments and where operability risks change due to changing metocean conditions (e.g., due to climate change), changing water depths (e.g., due to deepening or sea level rise) or changing operability limits (e.g., due to different cargo or ship types). As our results are based on global data, they remain high level. For local applications the operability needs to be verified by more detailed studies accounting for the local bathymetry, the influence of the port layout (wave breaking, sheltering, diffraction and reflections) and details of ship characteristics, cargo and mooring systems. Nevertheless, the results of our study do provide insights into which metocean indicators can influence the operability of ports at which locations around the world. This can help not only operators but also port authorities and designers to identify operability risks for existing port locations, quickly compare (port) locations based on global metocean data, their main drivers, but also find suitable (new) port locations where port operability risks are as low as possible.

Keywords: ports, global approach, port operability, suitability, downtime, metocean, wind, short waves, infragravity waves, ERA5, WPI

Contents

Acronyms and abbreviations

Acronym / abbreviation	Description
CERC	Coastal Engineering Research Center
COVID	Corona VIrus Disease
DAS	Docking Aid System
DJF	December/January/ February
DWT	Dead Weight Tonnage
ECMWF	European Centre for Medium-range Weather Forecasting
ERA5	ECMWF Re-Analysis 5th generation dataset
FN	False Negative
FP	False Positive
GLOSSIS	GLObal Storm Surge Information System
GTSM	Global Tide and Surge Model
ICS	International Chamber of Shipping
IG	InfraGravity
JJA	June/July/August
JMA	Japan Meteorological Agency
JOC	Journal of Commerce
JONSWAP	JOint North Sea WAve Project
JOT	Joint Occurrence Table
JRA-55	Japanese 55-year Re-Analysis
LST	Longshore Sediment Transport
MAA	March/April/May
MarCom	Maritime Navigation Commission
MWD	Mean Wave Direction
NCAR	National Centre for Atmospheric Research
NCEP	National Centers for Environmental Prediction
NOAA	National Oceanic and Atmospheric Administration
PDF	Probability Density Function
PHAROS	Program for HARbour Oscillations
PIANC	Permanent International Commission for Navigation Congresses
POT	Peaks Over Threshold
RMSE	Root Mean Square Error
RQ	Research Question
SLR	Sea-Level Rise
SON	September/October/November
SWAN	Simulating WAves Nearshore
SWH	Significant Wave Height
TEU	Twenty-foot Equivalent Unit
TN	True Negative
TP	True Positive
ULCV	Ultra Large Container Vessel
UNCTAD	United Nations Conference on Trade and Development
USA	United States of America
VTS	Vessel Traffic System
WPI	World Port Index
WG	Work Group

1 Introduction

1.1 Motivation and problem statement

The international shipping industry is vital to the global economy and responsible for the transport of around 90% of the world trade (ICS, 2020). As crucial nodes in the world's supply chains, it is vital that port operations can continue as much as possible independent of ocean and weather conditions. Terminals experiencing downtime due to extreme wave or weather conditions lead to declining revenues for terminal operators, which may also affect other parts of the supply chain. Hence, disruptions in port operations can have a major impact on the local, regional and global economy. Therefore, in addition to other factors such as finance, location, stakeholders, environmental policy and regulations, port operability is an important factor for the viability of ports (see Figure 1.1).

Port operability is the degree to which safe and reliable port operations (e.g., navigation, tugging, mooring, berthing, on/offloading etc.) can be guaranteed. The port operability is determined, among other things, by the physical conditions, availability of infrastructure, ship handling capacity and well-functioning ICT systems. In terms of physical conditions, the port operability depends on the wind, waves, water levels, currents and siltation. High wind speeds can cause limitations for container handling equipment and safety issues for mooring (Van den Bos, 2011). Short waves can affect tugboat navigability and influence the roll motions of the vessels which makes them harder to operate. Long waves can increase the vessel motions and thus increase the risk of breaking mooring lines and hindrance of (off)loading operations (Bellotti, 2007; López & Iglesias, 2014). Currents can influence the maneuverability and so the safety of large vessels and the operations at the berths. Water depth is an important aspect and influences the draft of the ship under which a ship can safely navigate. Many ports suffer from siltation which entails expensive maintenance dredging (Winterwerp, 2005) which are affected by sediment availability and wave influences to mobilize those sediments (Sierra & Casas-Prat, 2014). In this study we focus on operability indicators related to metocean conditions. Metocean is a composite of the words meteorological and ocean, covering physical phenomena such as wind and atmospheric pressure variations, such as waves, water levels and currents. We focus in particular on wind and wave conditions.

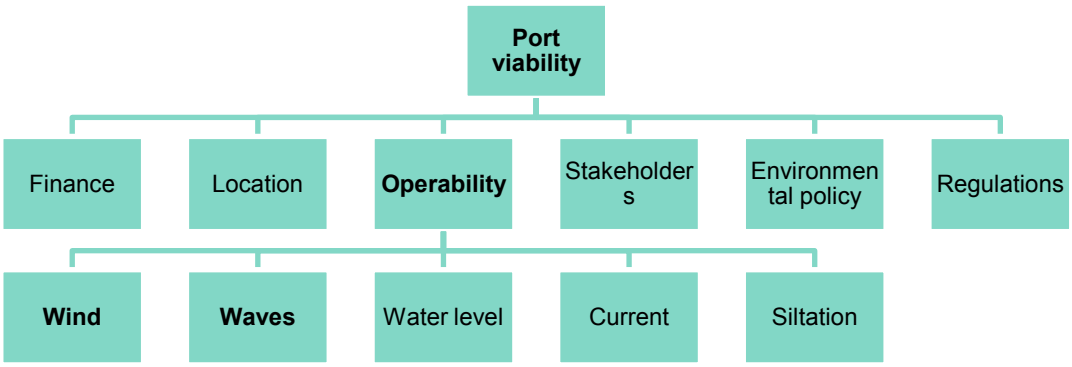

Figure 1.1 Multiple aspects for a viable port and relevant indicators for port operability

When we talk about the operability or, conversely, downtime of ports, all the above mentioned metocean conditions and processes are indicators that can influence the operability of a port. Explicitly, it does not indicate exact downtime, because there are many other factors that can influence downtime that we do not consider. For example, we do not consider the influence of the port layout (wave breakage, shelter, diffraction and reflections), ship characteristics, cargo and mooring systems.

Nowadays, data on metocean conditions is available on a global scale. Compared to local data, this global data has a long-time span and global coverage. This gives us the opportunity to create a global view on port operability based on metocean conditions. This enables us to analyze existing port locations for operability and identify driving conditions for potential operability risks. It also enables us to map the port suitability of (new) locations worldwide including the change over time in terms of metocean conditions, which can be useful information for the site selection of new port developments.

1.2 Scientific gaps

The availability of global databases has made large scale studies on ports possible. For example, a continental scale study on the evolution of sandy beaches around seaports for the African continent (De Boer, Mao, et al., 2019) or a European scale assessment of the impacts of climate change on seaports (Christodoulou et al., 2019). However, global studies on the operability of ports, including the methods to analyze it, have not yet been carried out to the best of our knowledge.

Analyzing port operability on a global scale is not an easy task. Van Marle (2015) stated that it is impossible to compare the performance of ports for multiple ports. One of the main obstacles is to quantify port performance into a single number, given the complexity of port processes. Another obstacle was the willingness of many operators to share data with a third party. Nobody likes the risk of having bad publicity or not being in the top performing ports. Instead of going to port operators the JOC (Journal of Commerce) decided to work with the shipping lines and measure the terminal productivity as the amount of cargo handled from the moment the first mooring line has been tied to the quay until the last line is cast as it departs (JOC, 2014). The JOC productivity database consists of more than 215 million moves at 798 terminals in 451 ports, representing around 54% of global moves in 2017. This has led to a genuine industry benchmark. Multiple shipping lines collect the data and provide it to JOC to compare different terminals. In this scenario, it is still difficult to define why there are differences in berth productivity between port locations or terminals, because we do not have information on the external factors that influence the port operability.

The aim of this study is to provide insight into the differences between (port) locations along the world coastline based on metocean conditions only. Multiple students (Hadijah, 2013; Bakermans, 2014; Kassimi, 2016) have attempted to assess port operability based on global datasets in order to study the feasibility of open seaport layouts while using metocean parameters. These students focused on the extreme conditions (important for port design) rather than the whole timeseries (important for port operations) resulting in a “good” or “bad” location, without quantifying the actual “operability” number. In addition, they studied the metocean parameters individually rather than in conjunction for a relatively small number of port locations (~100, see Figure 1.2). In this study, we will use high-resolution global databases to compare up to 4560 locations along the world’s coastline for a range of metocean parameters (i.e., wind conditions, short waves and infragravity waves) over long timeseries in order to observe the operability indicators, identify the main drivers and map suitable locations for port operations geographically.

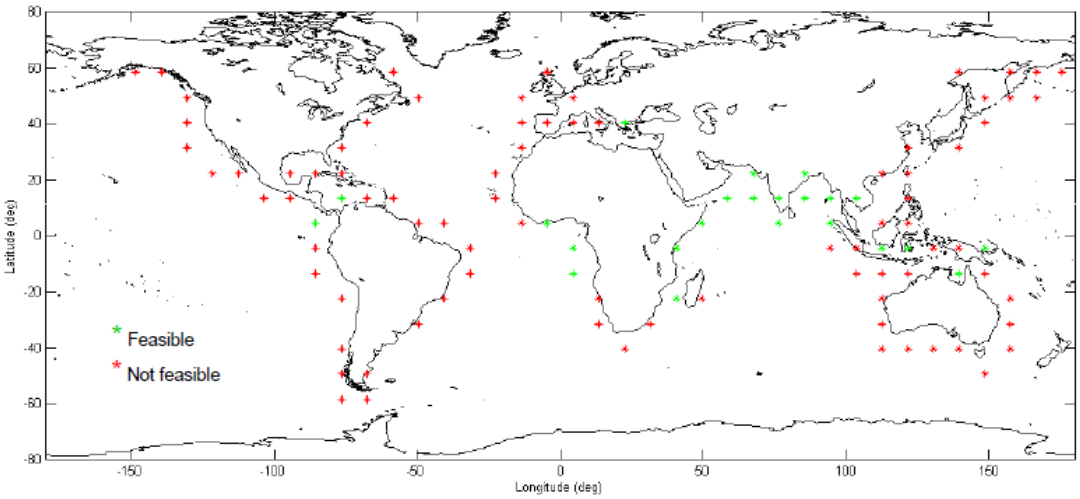

Figure 1.2 Global map for tug effectiveness, Hs < 2.5 m, for approximately 100 locations (Hadijah, 2013)

1.3 Research objectives and questions

In this study, we evaluate a range of metocean indicators for port operability on a global scale to quickly classify, map and compare locations in terms of operability as well as to identify the driving conditions and changes over time. This provides insights into which metocean indicators may influence port operability at which locations around the world. This information enables port authorities, operators and designers to be more effective in identifying potential operability risks, mitigating these risks (protection, mooring systems and relocations) and select locations where operability risks are acceptable for (new) port developments.

The purpose of this study is to:

- Identify which parameters are relevant indicators for port operability
- Develop a generic method to get first insights into port operability indicators based on global data of metocean conditions
- Classify, map and compare the suitability of existing and new port locations in terms of metocean conditions and assess the sensitivity to changes in these conditions
- Asses the global change in the suitability of port locations over time and reveal possible trends

The main research question:
"How can global datasets of metocean conditions be used to assess and compare port locations in terms of port operability?"

To achieve this research objective and answer the main research question, four sub-questions are formulated to systematically work towards it:

1. Which metocean parameters are relevant indicators for port operability?
2. How can we systematically analyze global metocean datasets to provide insights into port operability risks?
3. What are the global hotspots in terms of port operability risks and what are the main causes (or drivers) of these risks?
4. What is the sensitivity of the port suitability to changes in the metocean conditions (e.g., under the influence of climate change)?

1.4 Overall approach

In order to answer the research questions, this study is divided into 5 phases. In phase 1, we carried out a literature review to answer the first research question: 'Which metocean parameters are relevant indicators for port operability?'. For the next research phases, we followed a gradual approach in terms of the number of geographical locations that are analyzed (see the dashed box in Figure 1.3). We started with 1 location and then gradually expanded to 10, 103 and 4560 locations, respectively. In phase 2, we used a single port location (Cape Town) to develop and test our method and to aggregate and visualize our results in a clear and effective way, i.e., the calibration phase. The second research question: 'How can we systematically analyze global metocean datasets to provide insights into port operability risks?' is answered. In phase 3, we validated our method for 10 port locations which are known to have either severe or limited operability issues to determine whether the results derived from global datasets are reliable and meaningful for individual port locations. In phase 4, we classified and analyzed 103 existing ports to answer the third research question: 'What are the global hotspots in terms of port operability risks and what are the main causes (or drivers) of these risks?' This provides insights into how individual metocean conditions can influence the overall operability. Finally, in phase 5, the suitability of 4560 locations along the world coastline are classified, analyzed and compared with the previous subset. Note that the 4560 locations are equidistant spaced along the coast (not too close but also not too far away from the coast), hence, different from the other 3 data samples which are based on actual port locations. The fourth and last research question: **'**What is the sensitivity of the port suitability to changes in the metocean conditions (e.g., under the influence of climate change)?**'** is answered.

1.5 Report outline

This report is structured as follows, see Figure 1.3. The body is divided into four parts. Starting with a literature review in Chapter 2 to answer the first research question. The gradual approach is grouped via the dashed line, introducing the methods in Chapter 3 by answering the second research question. In Chapter 4, the results of this study are presented, answering the third and final research questions. The results are discussed in Chapter 5. Chapter 6 summarizes the most important conclusions and recommendations for further research.

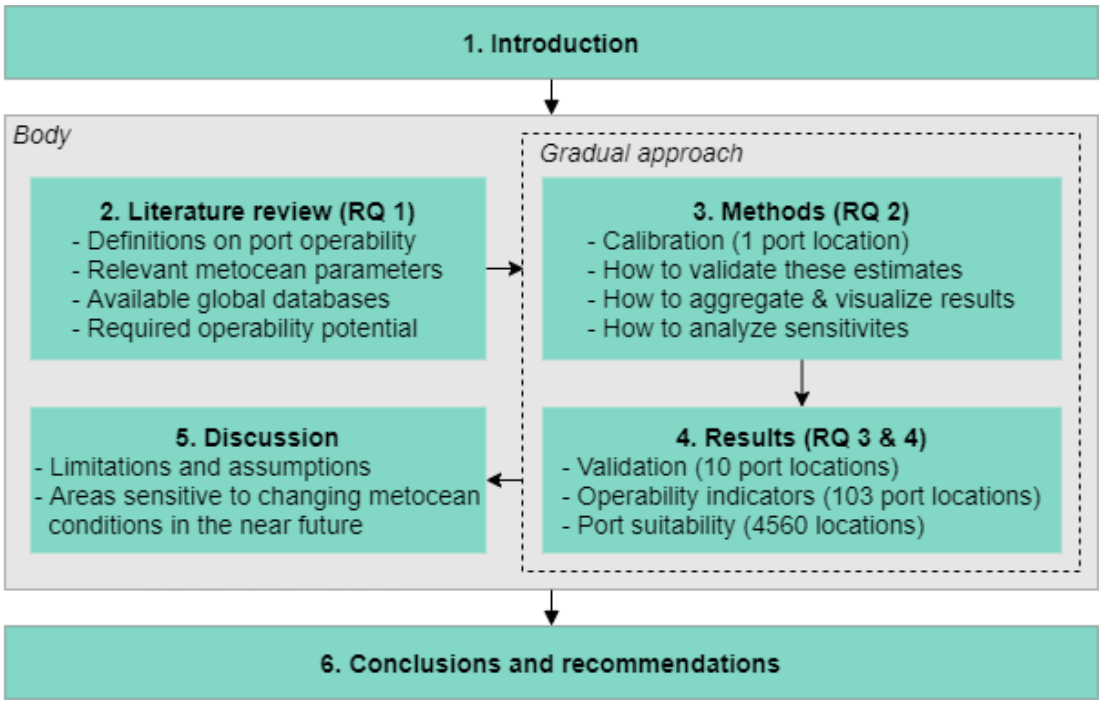

Figure 1.3 Report outline with a gradual research approach in terms of the number of locations (1–10–103–4560). All the research questions are referred to by the abbreviation: RQ.

2 Literature review

2.1 Definitions of port operability

Port operability is the degree to which safe and reliable port operations (e.g., navigation, tugging, mooring, berthing, on/offloading etc.) can be guaranteed. This is often defined in relation to pre-set operational requirements. When these requirements cannot be met, port operations may be interrupted, which results into port downtime and, hence, lowers port operability. There are multiple factors influencing the operability, such as berth utilization, the number of cranes deployed at a berth, the average crane moves per hour, the worker's skills, logistics, infrastructure availability, system failures, the impact of passing ships on moored ships and metocean conditions. High operability and low downtime are key for ship and terminal operators, because waiting ships and underused quays cost a lot of money. In this study we focus on port operability in relation to metocean conditions which we call operability indicators (metocean conditions that are relevant for port operability, see Section 2.2).

As port operability depends on more factors than metocean conditions alone, we use the term "operability potential" in this study. Here, we define operability potential as the amount of time a port is potentially available for operations or, in other words, the time that the metocean conditions are below their operational limits. We also use the term "port suitability" to indicate how suitable a certain (port) location is in terms of metocean conditions.

Section 2.2 discusses the relevant metocean parameters and how they are assessed in terms of port operability. The available and chosen global datasets are discussed in Section 2.3. To evaluate our estimates, the average required availability based on literature is elaborated in Section 2.4. The connection between different literature subjects of this study is visually shown in Figure 2.1.

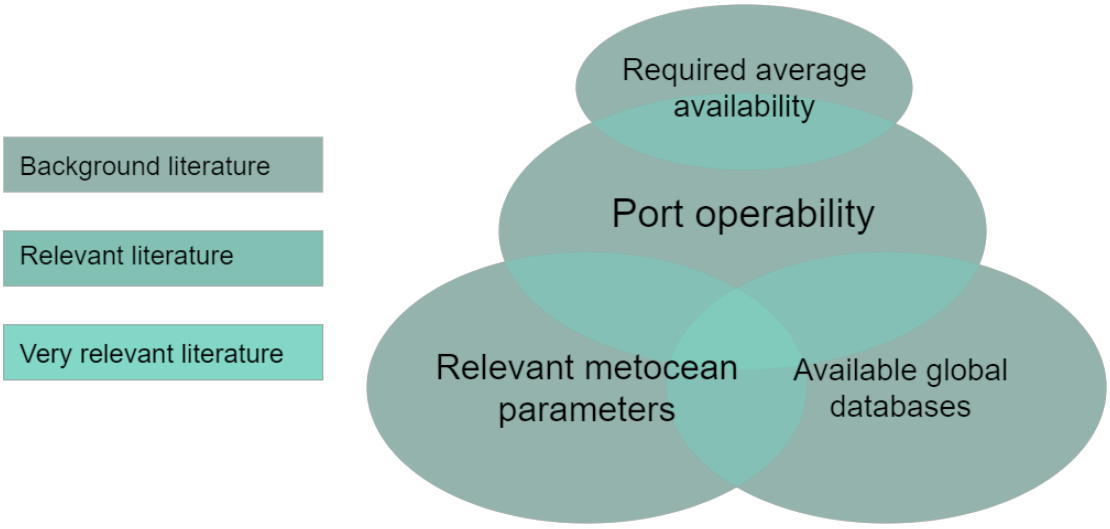

Figure 2.1 Venn diagram to show the connection between the different literature subjects

2.2 Relevant metocean parameters to assess port operability

In general, the operability indicators as a result of the metocean conditions depends on the critical wind, wave and current conditions that could cause unacceptable ship motions or mooring line loads, and/or the inability to operate (Thoresen, 2014). Most of the times a port operability assessment is site and case specific by assessing the local metocean conditions. There are multiple ways of doing this. Typically, long-term metocean data from hindcasted reanalysis datasets are used as boundary conditions for advanced modelling and data assimilation systems to arrive at local estimates of the metocean conditions. In addition, local measurements, such as deployed wave buoys at the port location for a certain (short) period, can be used to verify these model predictions. Due to the global focus of this research, there is a detailed elaboration on available global metocean databases in Section 2.3.

In addition to metocean parameters, the port operability also depends on other factors such as the mooring arrangement, berthing arrangement, size/natural period of the vessel, port layout, characteristics on cargoes, (un)loading equipment, siltation and passing ships. This study on a global scale will focus on the metocean parameters only and not on the specifics of the local infrastructure and mooring arrangements as this information is not available on a global scale. Ships are subject to multiple external conditions. The aim is to resist these forces and respond to these external factors to avoid damage and possible downtime. Downtime for ships is generated by unacceptable ship motions, high mooring line loads and/or limiting circumstances for (un)loading because of the equipment on the berth. It is important to know the influence of external factors as a group on the ship, as well as their significance and relative importance.

The following metocean forces are relevant and explained in more detail below (Bruun, 1989; Ligteringen & Velsink, 2017; PIANC MarCom WG 115, 2012; PIANC MarCom WG 24, 1995; Thoresen, 2014): wind, waves (wind/swell/infragravity waves and seiching), water levels, currents, visibility and ice problems

2.2.1 Wind

Wind can influence the operability via wind forces on the ship and (un)loading equipment. The forces on the ship vary with the exposed area or superstructures. Ships with high superstructures, such as container carriers, oil tankers and car carriers can be expected to have problems controlling the ship with high wind speeds. The wind direction is important for its influence on the ship. Beam winds influence the whole side area of the ship whereas head winds affect only a relatively small surface area of the ship. The mean wind velocity and direction should, in accordance with Beaufort wind scale, be recorded 10 m above the mean sea level and should be based upon the 10 min averaged of the wind velocity and direction (Thoresen, 2014). International standards and regulations for wind speed limits are given for different terminal types in Table 2.1 by (Thoresen, 2014).

Type of ship	Limiting wind speed (m/s)
Container, ro/ro	20 m/s for loading arms, heavy lifting equipment
General cargo	20 m/s for loading arms, heavy lifting equipment
Dry bulk	20 m/s for loading arms, heavy lifting equipment
Tankers	10 m/s for berthing (wind area > 5000m^2)
	15 m/s for berthing (wind area < 3000m^2)
	15 m/s for cargo transfer operations
	20 m/s disconnection of loading arms
	25 m/s leave the berth for open sea
Tugboats	15 m/s for modern mooring boats

Table 2.1 Maximum wind speed per ship type (Thoresen, 2014)

Container terminals reduce their operability significantly for wind speeds above 6 Beaufort (PIANC MarCom WG 24, 1995; Thoresen, 2014; Van den Bos, 2011). An investigation of an Ultra Large Container Vessel (ULCV) shows that at Beaufort scales 6 to 7 the maximum movements of the cell guides for positioning containers are still acceptable, although it already requires special mooring lines and bollards. At Beaufort scale 8 it is recommended to provide storm bollards (Van den Bos, 2011) and stop container handling operations.

Due to high superstructures or freeboard, wind can have a significant influence on the ship. High wind velocities will hinder operations in the port and the safe mooring. A wind beam on or perpendicular or a wind gust can cause extra downtime because it can blow a ship away from the fenders and decreasing the friction while increasing the ship motions. Variable wind speeds can cause oscillations of the vessel and potentially reducing the efficiency. Increasing ship sizes will also increase the size of loading arms and heavy lifting equipment. Larger equipment becomes more sensitive for high winds.

2.2.2 Waves

Waves can be classified into two types (Holthuijsen, 2007; Munk, 1950):

- Wind and swell waves: wind waves are generally short-crested and irregular with short periods (4 – 10 s). When they leave the generation zone, they travel and change due to dispersion into a regular and long-crested waves with relatively longer periods (8 – 30s) called swell waves.
- Infragravity waves and seiching (Van der Molen et al., 2006; Van Dongeren et al., 2016): long-period waves or infra-gravity waves are generated by groups of wind-generated waves, for instance in the surf zone at the beach, where these waves are called surf beat with long periods (30 - 300s). Seiches are standing waves with a frequency equal to the resonance frequency of the basin in which they occur. In a port seiches can have devastating consequences, flooding of low-lying areas, breaking of mooring lines and overall downtime.

2.2.2.1 Wind and swell waves

Ports are in general well protected against wind and swell waves by natural sheltering or breakwaters. Short waves (with periods less than 30 s) can be effectively mitigated by a breakwater to facilitate port operability. The operability due to short waves is determined by the maximum allowable ship movements at berth under which the mooring system and cargo handling equipment can safely operate (see for example the work of Molina-Sanchez et al., 2020). To assess the operability for case specific situations, typically the offshore wave data is transformed to the nearshore via numerical models, such as SWAN (Simulating WAves Nearshore) (Booij, Holthuijsen, & Ris, 1997), STWAVE (Steady-State Spectral Wave Model) (Massey, Anderson, Smith, Gomez, & Jones, 2011) and MIKE 21 SW (DHI, 2017). Other models can be used to assess the wave penetration into the harbor. For example, PHAROS (Program for HARbour Oscillations, (Deltares, 2016), a mild-slope model which can also deal with reflections and diffraction. Even more sophisticated models are phase resolving wave models such as TRITON and CFD which can resolve individual waves.

Table 2.2 shows generally acceptable wave heights for different wave directions and short periods (up to 10 s). There is a correlation between the size of the ship and increasing allowable larger wave. The most sensitive berths are those for container ships and Ro/Ro ships due to safety requirements for (un)loading operations and for gas tankers because of the possibility of ice forming due to condensation of the joints and gas is more dangerous than oil.

Type of ship	Limiting wave height Hs (m)	
	0° (head-on or stern-on)	45-90° (beam-on)
Container, Ro/Ro	0.5	-
General cargo	1.0	0.8
Dry bulk 30000-100000 DWT	1.0	0.8 - 1.0
Dry bulk 30000-100000 DWT	1.5	1.0
Tankers 30000 DWT	1.5	-
Tankers 30000-200000 DWT	1.5 - 2.5	1.0 - 1.2
Tankers >200000 DWT	2.5 - 3.0	1.0 - 1.5
Tugboats	1.5 - 2.0	-

Table 2.2 Maximum significant wave height for different wave directions (Thoresen, 2014)

Elaboration on the maximum significant wave height per ship type (in Table 2.2):

- Container terminals have a significant wave height limit of 0.5 m for proper handling of cargo (Del Estado, 2007; PIANC MarCom WG 121, 2014; Thoresen, 2014). This limit is based on literature without information on the ship size or other characteristics. The natural period of oscillation is in the range of 10 – 15 s, these are in the range of swell periods that mainly induce the vertical ship motions. When the natural period of a ship is not correlated with the short-wave period, the significant wave height may increase to 0.5 – 1.0 m.
- General cargo operating conditions are determined by the type of (un)loading gear, size of the batches, size of the boxes and units handled. These criteria are based on experience and interviews with port and ship operators.
- Dry bulk (un)loading operations are generally carried out by bucket-wheel, elevators, suction devices, conveyors and hoses(grains). The risk of the handling equipment hitting the hatches or ship's bottom is generally lower than the risks for safe container handling. The limiting wave heights for dry bulk are a bit higher and based on practical experience of port and ship operators.
- Oil tankers use loading arms and sometime flexible hoses to (un)load the oil. The safe working criteria are determined by the allowable reach of the loading arms in the longitudinal and transversal direction.
- Tugboats start to lose control and power when there are significant wave heights of more than 1.0 – 1.5 m for ordinary tugboats and approximately 1.5 m for tractor tugboats (Thoresen, 2014). For safe berthing of ships the significant wave height may not be higher than 1.5 – 3.0 m depending on the tug, the skill of the crew and the possibility to attach on the lee side of the vessel (PIANC MarCom WG 121, 2014).

2.2.2.2 Infragravity waves

Infragravity (IG) waves can lead to excessive horizontal ship movements inside ports. This may result in breaking of the mooring lines and possible downtime due to reduced efficiency during (un)loading. There are three main sources responsible for IG waves: bound long waves, free long waves and harbor seiching, Figure 2.2 gives a visualization of the general mechanisms of IG wave generation. Long-period waves, low-frequency waves, surf beat (Munk, 1949) or infragravity waves (Herbers, Elgar, & Guza, 1994, 1995) have typical periods of 30 s till several minutes. Infragravity waves cause large hindrance for operations in a port. IG waves are generated due to non-linear interactions between wind and swell waves. IG waves are classified based on their generation mechanisms.

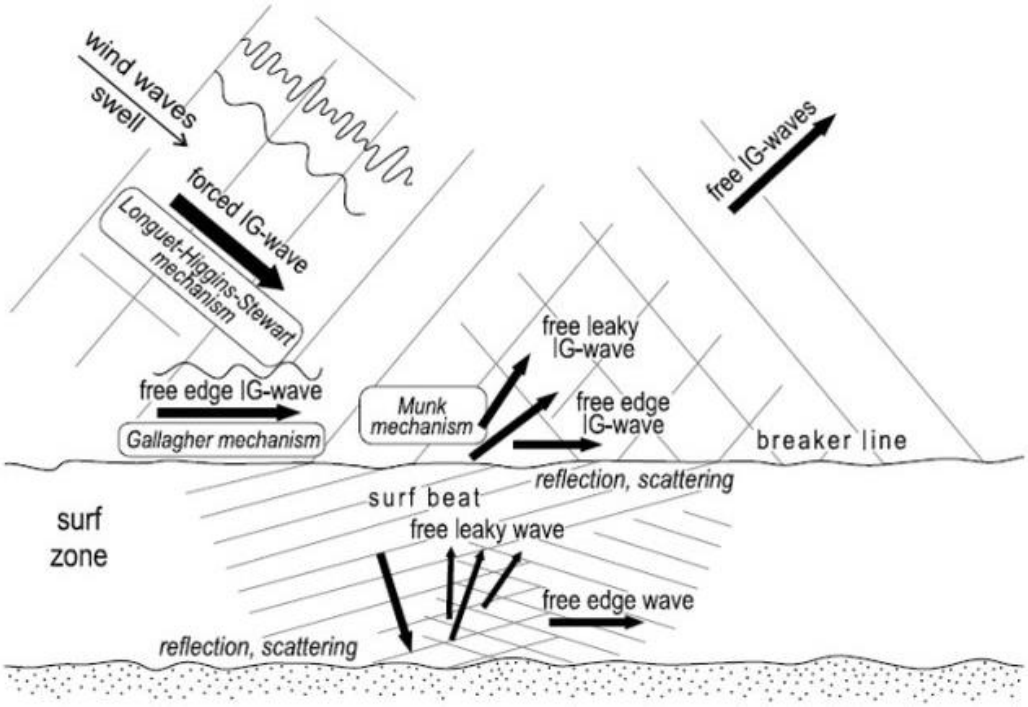

Figure 2.2 General mechanisms of infragravity wave generation in the coastal zone (Rabinovich, 2009)

- *Bound (forced) infragravity waves*: wind and swell waves towards shore propagate and shoal with the wave group celerity due to the superposition of two different short-wave trains with frequency and length similar to each other the generating infragravity waves bound to groups of higher-frequency waves (Longuet-Higgins & Stewart, 1962). An effect of wave grouping is the creation of set-down under larger waves because larger waves transport more momentum, the water pressure will decrease. Under smaller waves a set-up is created because of less momentum the water pressure increases. Under constant air pressure, the mean water level will fluctuate, bound to the wave group and 180° out of phase.
- *Free infragravity waves*: when short waves reach the breaker zone they break, the breakpoint can vary (Symonds et al., 1982). Larger short waves break farther offshore than the smaller waves in the group. The bound infragravity waves locked to the wave group are released because the groupness of the short waves disappears. These free long waves propagate in shoreward and seaward direction and leaving a depression in between. Free infragravity waves reflect of the beach and propagate seawards creating consecutive elevations and depressions of the mean sea level, which is called 'surf beats' (Munk, 1949).

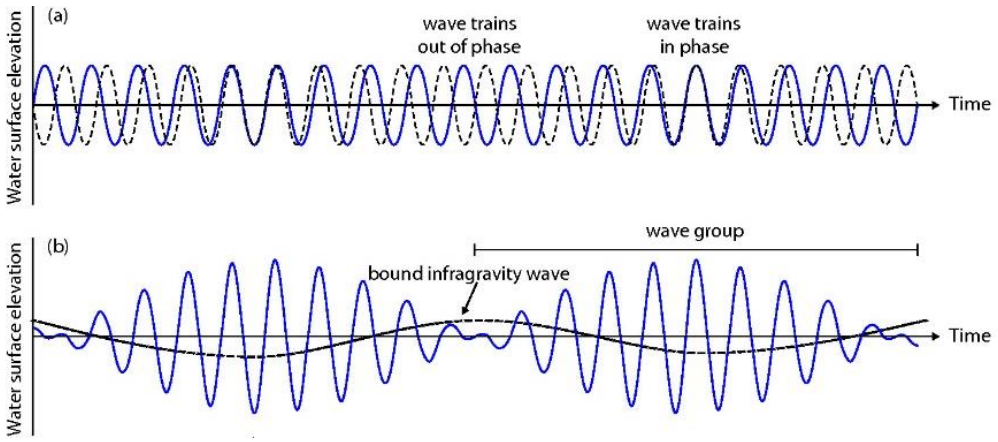

Figure 2.3 a) Merging of two wave trans of slightly different wave lengths, but the same amplitude's) Two wave trains form wave groups and induce a long bound wave (The Open University, 1999)

Out in the open deep sea the infragravity waves are small, up to a few decimeters but when water depths decrease and wave periods of the primary (sea/swell) waves that make up the wave groups increase, infragravity waves will increase too. The total height of infragravity waves consists of the wave height of the bound infragravity and the free outgoing infragravity wave height. The amplitude of infragravity waves could be amplified in port basins because of natural oscillations may develop resulting in port seiches. The period of these infragravity waves is close to the natural periods of large moored ships (Bont et al., 2010; PIANC MarCom WG 115, 2012; Thoresen, 2014; Van der Molen et al., 2006). These standing waves are a resonance phenomenon where the basin size in relation to the wave length is an important factor and can cause horizontal water displacements which can cause mooring difficulties. The limiting significant wave height of infragravity waves at the berth is 0.05 m, based on an empirical relation (Mol, Ligteringen, & Waanders, 1986) and international guidelines (PIANC MarCom WG 115, 2012).

Infragravity waves are hard to reduce because they will go around sea defenses or other hard structures (Bruun, 1989). Elongating breakwaters who narrow the port entrance could even increase the change of severe infragravity wave problems inside a port which is called a 'harbor paradox' (Miles & Munk, 1961). Changing the mooring arrangement could result in a change in natural periods of the ship. Measures against seiches are usually based on size restrictions of ports basins and on the use of irregularly shaped basins (PIANC MarCom WG 115, 2012). For port planners an estimate of the infragravity wave climate can be made but detailed numerical modelling needs to be done when there is a high expectation of infragravity waves because it is correlated with the port basin/layout. Therefore, high quality long-wave data (preferably from field measurements) is necessary to perform high quality simulations inside the basin (PIANC MarCom WG 115, 2012).

2.2.3 Water levels

Water level is the storm surge combined with the tide. The tide consists of two components: astronomical and meteorological effects. The ebb and fall tides cause vertical rise and fall of the ship's in a port and will have an influence on the forces in the mooring arrangement. Meteo-tsunamis are water level oscillations which are similar to waves generated by seismic activity, but with a meteorological origin instead of generated through seismic activity, causing damage to ships and ports. The water depth in the approach channel and port basin should be enough for safe maneuvering. Water levels are not of high importance because it will not have a direct influence on the motions of a vessel on time scales relevant for the efficiency of (un)loading ships but should be considered by port planners/designers, also the risks in terms of sea-level rise must be considered.

2.2.4 Currents

Currents in and around ports are the result of the tidal current and the wind generated current. The magnitude and direction must be evaluated to investigate the influence on maneuvering, (un)berthing and (un)loading operations and can be modelled via the Global Tide and Surge Model (GTSM) from GLOSSIS (Verlaan et al., 2015). The tidal current during rising and falling tide must be measured at various depths over a long time period because the direction of the current can vary. Also, the water clearance beneath the keel and direction of the current relative to the vessel is of significant influence. A safe limit for current velocities (measured at a depth of half the vessel's draught, as a 1-minute average) is 0.5-1.0 m/s (PIANC MarCom WG 121, 2014; Thoresen, 2014). Current forces could be minimized by orientating the terminals parallel to the main current direction.

2.2.5 Visibility

Fog, heavy rain and snow could reduce the visibility. Fog is a weather condition for which the visibility is less than 1000 m. By reduced visibility the ship's velocity should be reduced and if possible, with tugboat assistance. Most oil and gas terminals maintain a general rule to close for (un)berthing if the visibility is less than 1000 – 2000 m. Nowadays with improved navigation via VTS (Vessel Traffic System) and DAS (Docking Aid System) the reduced visibility will rarely lead to downtime (Thoresen, 2014).

2.2.6 Ice problems

Ice does not occur on most port locations. But a port designer should always think of possible consequences because it could result in a lot of downtime. Artic sea routes are gaining popularity due to global warming because it will bring Asia closer to Europe which will also increase the interest in ice issues in and around ports.

2.2.7 Selection of port operability indicators (based on metocean conditions)

The selection of relevant metocean parameters that are included as strong indicators for port operability in this study are: wind speed, short waves and infragravity waves. For port operability all the metocean parameters are important but downtime in ports is often related to excessive ship motions at the berth (PIANC MarCom WG 24, 1995). Reducing those forces as much as possible to facilitate a high operability is the goal of port authorities, operators and designers. Excessive short waves can result in unacceptable ship motions or mooring line loads, affecting the cargo-handling or i.e., the operational availability. The same holds for extreme winds and infragravity waves at the berth. Infragravity waves have relatively small amplitudes compared to other waves, but the amplitude will increase by decreasing depths and may amplify inside port basins and cannot be reduced by defense structures.

2.3 Available global databases

There are multiple global metocean databases available, ranging from buoy wave height data and tidal range levels or widely used reanalysis hindcast datasets which combine model data with satellite observations. The global approach of this study supports the choice for a reanalysis metocean database which are used extensive for climate services and research. Multiple global reanalyzes are carried out by different research institutes. First, a longlist of possible reanalysis metocean database are given in Table 2.3 after which a dataset is chosen for further study.

Name	Source	Period	Output timestep	Resolution
ERA-Interim	European Centre for Medium-Range Weather Forecast (ECMWF, 2019) https://cds.climate.copernicus.eu/	1979 to present	6-hourly	1.0° x 1.0°
ERA5	European Centre for Medium-Range Weather Forecast (ECMWF, 2019) https://cds.climate.copernicus.eu/	1979 to present	hourly	0.5° x 0.5°
MERRA	NASA Global Modelling and Assimilation Office (Rienecker et al., 2011) https://disc.gsfc.nasa.gov/	1979 to present	3-hourly	1.0° x 1.25°
NCEP/NCAR	National Centers for Environmental Prediction (NCEP) created in cooperation with the National Centre for Atmospheric Research (NCAR) (Kalnay, 1996) https://psl.noaa.gov/data/gridded/index.html	1948 to present	6-hourly	2.5° x 2.5°
JRA-55	Japan Meteorological Agency Reanalysis (JMA, 2013) https://rda.ucar.edu/	1958 to present	3-hourly	1.25° x 1.25°

Table 2.3 Overview of atmospheric reanalysis metocean databases

For our study it is essential to look at the mean wave climate instead of an extreme wave climate, because we are interested in all the events over a very long time to estimate the average port operability potential. At the moment, the ERA5 dataset has the highest resolution in time and space and is sufficiently long to analyze the port operability. The ERA5 significant wave height shows a good agreement with measured buoy data in coastal and deep waters but during tropical cyclones the significant wave height is underestimated (Muhammed Naseef & Sanil Kumar, 2020). Another study showed that the wave characteristics of ERA5 during monsoon and post-monsoon do not suffice yet to adequately describe wave fields generated by the interaction of monsoon and local winds (Bruno et al., 2020). However, due to positive experience from researchers at Deltares and the fact that ECMWF is continuously improving the dataset, convinced us to use the ERA5 dataset for this study. ERA5 is a 5th generation of atmospheric reanalyzes of the global climate from 1 January 1979 to present hourly, developed by European Centre for Medium-Range Weather Forecast (ECMWF, 2019). Spatial resolution on regular latitude-longitude grids at 0.25° x 0.25° on land and 0.5° x 0.5° on the ocean.

The World Port Index (WPI, 2019) consists of port characteristics, for example the location, size, known facilities and services of ports. The WPI database is used to extract coordinates (longitude and latitude) from ports to collect the specific data from ERA5. A shapefile from Natural Earth Data (2020) is used to draw the coastlines and extract longitude and latitude coordinates to analyze the suitability of locations across the world, this is further explained in Section 3.3 and 3.4.

2.4 Required average port operability potential

Previous studies to asses port operability for open layouts based on metocean conditions (Bakermans, 2014; Hadijah, 2013; Kassimi, 2016) used an extreme wave climate to determine whether or not the port location is suitable for operations. We will go a step further and analyze the whole timeseries and quantify the operability potential of a (port) location in a percentage to compare (port) locations, identify the main drivers and analyze the change over time. To this end, we need a reference value to determine whether a location is suitable or not. In this study, we use the 95th percentile (p_{95}) as a theoretical threshold. This 95th percentile is chosen based on international standards and recommendations (PIANC MarCom WG 115, 2012; Thoresen, 2014). The p_{95} value indicated that a (port) location is suitable for port operations when the metocean conditions are below their operational threshold for 95% of the time, which is further explained in Section 4.1. This 95th percentile is adjustable throughout this study, because different cargo types require different availability limits at the berth. For oil and gas terminals the availability limit is lower, 90% berth availability per year (Thoresen, 2014). For container terminals it will be slightly higher, 98% availability based on general experience. But is mainly chosen to give an example of the possibilities, quantify the outcomes and analyze sensitivities with a certain point of reference.

3 Methods

The emphasis in this chapter is on the development of a generic method to get first-order insights into port operability by studying global data on wind speed, short waves and infragravity waves in relation to thresholds. The overall method is visualized in Figure 3.1 and divided into 5 phases.

In every phase we make use of different methods. In phase 2 “calibration”, we use a threshold-based approach combined with 4 characterizations of operability to estimate the operability potential for a single port location. In phase 3 “validation”, 10 port locations which are known for either facing serious or almost none operability issues are defined, to determine whether the results derived from global datasets are reliable and meaningful for individual port locations. For each location, we check the goodness of fit for the port operability estimate via a true or false positive (or negative) compared to what is known from literature. In phase 4 “operability indicators”, we analyzed 103 (existing) port locations to study the main causes/drivers for port operability risks and define “hotspots”. In the last phase “suitability”, we map out 4560 locations along the world coastline in terms of port suitability including a sensitivity analysis. Our methods are discussed in more detail in the paragraphs hereafter. At the beginning of each paragraph we explain how we selected the port locations and at the end how we visualize the results.

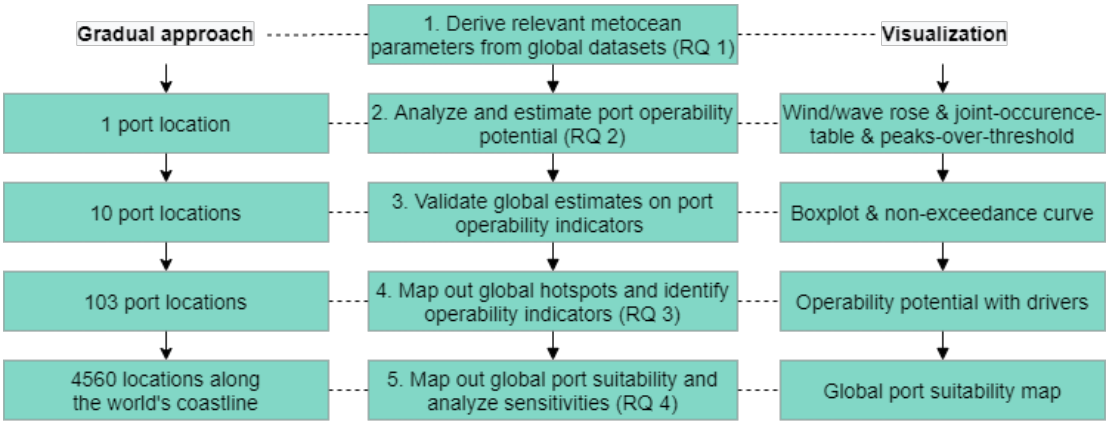

Figure 3.1 Research method representing a gradual approach divided into 5 phases from top to bottom. All the research questions are referred to by the abbreviation: RQ.

In our gradual approach we perform an operability assessment for an increasing number of geographical locations (i.e., 1, 10, 103 and 4560) introduced in Section 1.4 and visualized in Figure 3.2. In phase 2, 3 and 4, we make use of the World Port Index (WPI, 2019) to extract the coordinates (longitude and latitude) from the selected ports. In phase 5, we make use of the WPI database and a shapefile for the coastline consisting of coordinates to draw the coastlines (Natural Earth Data, 2020).

For each location in the selected sample sets, the grid point nearest to the location coordinates are selected from ERA5 (ECMWF, 2019) to derive the relevant metocean data. Each grid point is selected at least 0.1° away from the port/coastline coordinate and not farther away than 0.8°. In this way we ensure that the ERA5 information is sufficiently far away not to be influenced by small-scale geomorphological features such as islands, flats, ridges or troughs (which are not well captured in the ERA5 resolution), yet sufficiently close to the coast to have reliable nearshore conditions.

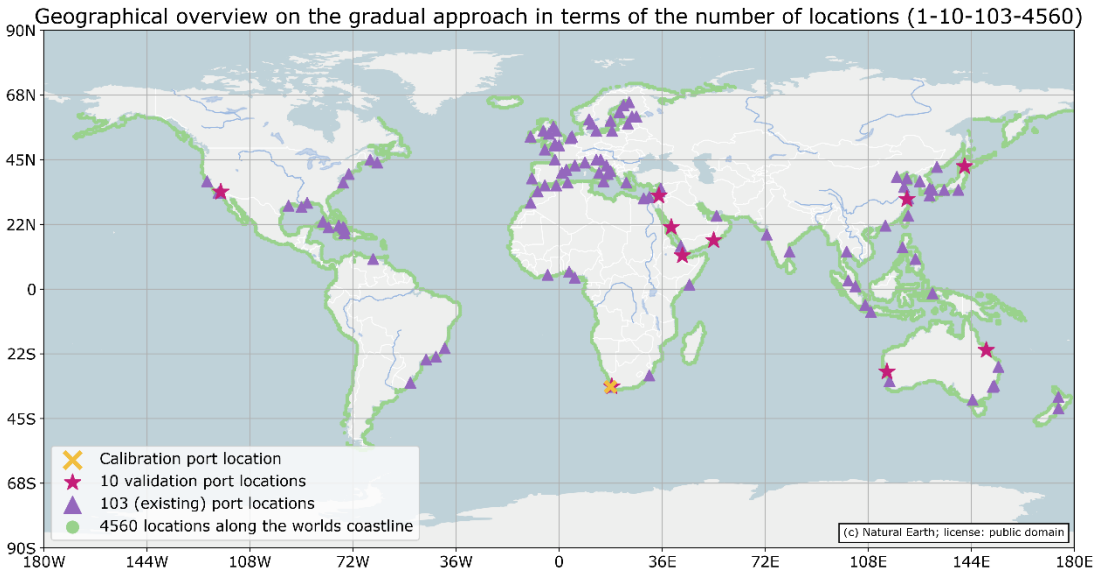

Figure 3.2 Outlining the different locations used in this research to visualize the gradual approach

3.1 Analyzing and estimating port operability potential

3.1.1 Generic method for port operability potential estimates

To derive the operability potential based on metocean conditions for each of the selected locations we use a threshold-based approach. This approach computes the amount of time each metocean parameter exceeds its thresholds as well as the interval between and frequency and duration of exceedance (visualized in an illustrative way in Figure 3.3). We use the following definitions:

1. *Availability*: the probability that a metocean parameter remains below its operability threshold (% per year)
2. *Interval*: the average time between threshold exceedance events (time interval between events)
3. *Frequency*: the average number of operability threshold exceedance events (events per year)
4. *Duration*: the average time of exceedance events (time duration in hours per event)

First, we elaborate on the availability for each individual operability indicator. For availability we classify values above the operability threshold as unavailable and values below it as available. This threshold approach is simplistic, because it assumes that operability can be estimated from an aggregated metocean condition only without accounting for the characteristics of the ship and mooring system. Nevertheless, it is effective to distinguish to which the port operability potential is most sensitive. This port operability potential is seen as a good indicator of whether and which metocean conditions play a role in the operability of a port.

Second, we complement the threshold-based approach by evaluating the interval between exceedance events (i.e., the time between a down-crossing and subsequent up-crossing as shown in Figure 3.3) from the idea of Campos et al. (2019). It is expected that port operators will probably not resume their operations when there is a high probability that the threshold will be exceeded again on short term. Therefore, we assume short-intervals less than or equal to 4 hours (purple lines in Figure 3.3) as ‘unavailable’. Hence, a long period of multiple short interval exceedances is treated as one exceedance event. The remaining non-exceedance events we call operability potential (green line in Figure 3.3).

The frequency and duration are used to analyze port operability potential in more detail. By analyzing the frequency, we generate insights into the number of times port operations need to shut down and restart again which limits the uptime. The average time of exceedance events (per year) gives insights into how long a period of potential unavailability last. In which we can differentiate ports with short periods of downtime and long periods of downtime. Short periods of downtime could be compensated for more quickly than longer periods of downtime. After determining the duration of an exceedance event, it is also possible to define how many exceedance events have a duration larger than 24 hours which can be denoted as storm events.

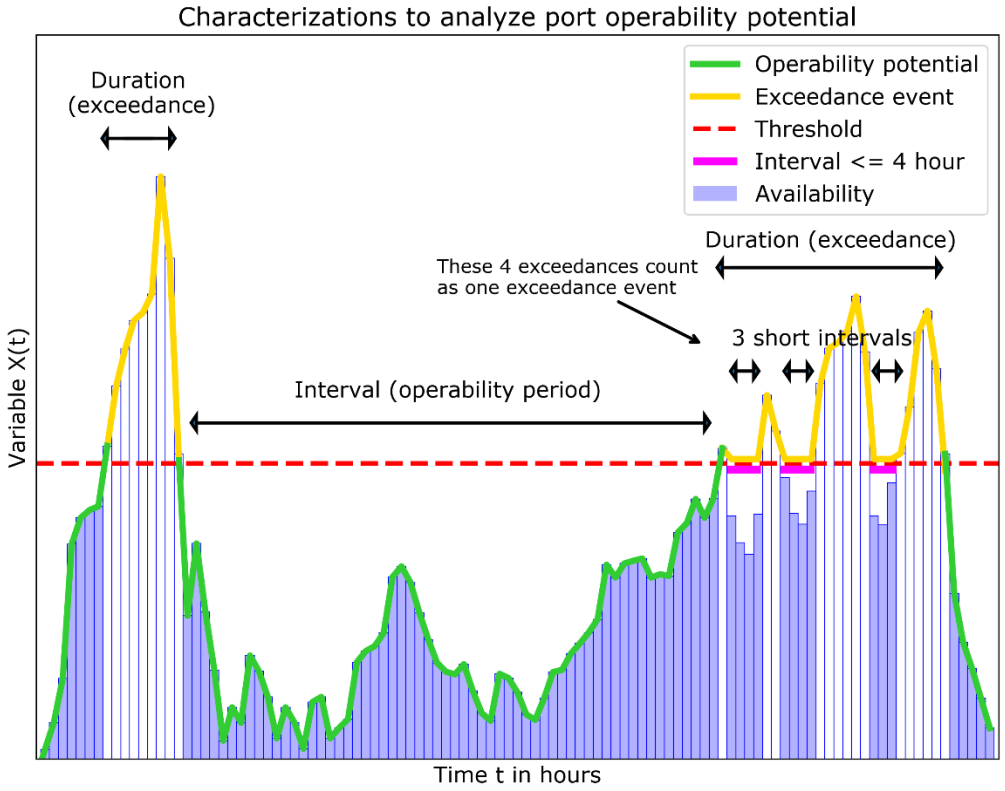

Figure 3.3 Explanation of port operability characterizations via an illustrative plot

The 4 different characterizations could also be given in an algebraic form together with the illustrative plot from Figure 3.3. $X(t)$ is a random variable consisting of observations $X_1, \ldots, X_n$ with n as total number of observations. Suppose N observations from X exceed the threshold u. The probability of exceedance (P) of that threshold is then $^N/_n$ and the probability of non-exceedance (1-P) is then $1 - {}^N/_n$. Let the indexes $\{t_i : X_{t_i} \geq u\}$ denote the locations of up/down-crossing the threshold with f as total number of up/down-crossings. Then $D_i = t_{i+1} - t_i \ (i = 1,3,5,\ldots,f-1)$ denotes the duration of an exceedance event (note that the index of D_i is with steps of 2) and $I_i = t_{i+1} - t_i \ (i = 2,4,6,\ldots,f-1)$ denotes the time of an interval between the exceedance events (note that the index of I_i is with steps of 2). The frequency is the number of exceedance events denoted as $F = {}^f/_2$ and reduced by short-intervals, less than or equal to 4 hours.

The overall operability potential (P_{total}) is directly based on the availability and calculated by combining the operability potential for each individual indicator (P_{wind}, P_{waves} and $P_{IGwaves}$) (dotted lines) in Figure 3.4. Considering that if one of the indicators is above the threshold or the interval between exceedance event is ≤ 4 hours, we assume the port is no longer available in that period. This will result in a combined or unique port operability potential percentage which allows us to compare different locations, find hotspots and define main drivers of these risks. This approach may also be helpful for decision makers to assess the sensitivity of the operability potential to changes in the operability thresholds, water depth and metocean conditions (see Section 3.4).

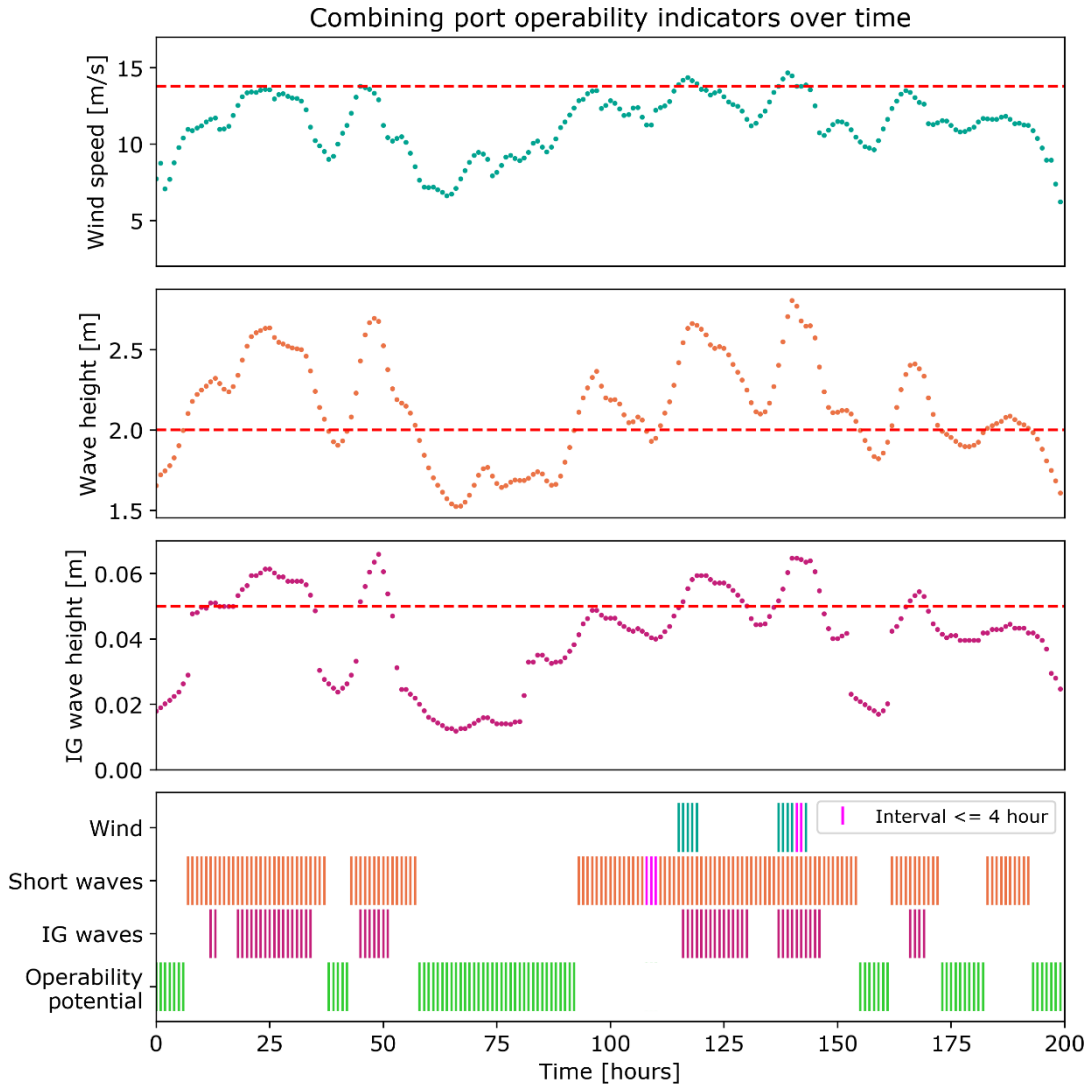

Figure 3.4 Explanation how port operability parameters are combined over timeseries. The dashed line is the threshold. In the bottom figure the persistence of operability is given in green.

In Table 3.1 an overview is given for the individual operability potential indicators including the input values and sources, methods to calculate and the accompanying thresholds. In the following sub-sections, we elaborate further on the different parameters.

Parameter	Input values/source	Methods	Threshold
Wind	Offshore wind climate: U_{10}, V_{10} (m/s) (ERA5)	Calculate the wind speed	13.8 m/s
Short waves	Offshore wave climate: Hs (m) / MWD (°) / Tm (s) / h0(m) / h(m), shoreward (ERA5). Physical coastline vectors to derive the shoreline orientation (°) Natural Earth Data (2020)	Linear Wave Theory (Airy, 1845). Automatic Shoreline Orientation calculation (Natural Earth Data, 2020)	2.0 m
IG waves	Nearshore wave climate for all direction: Hs (m) from short waves. Tp (s) (ERA5)	Herbers et al. (1994) and the model of Van Dongeren et al. (2003)	0.05 m

Table 3.1 Overview of parameters, input values/sources, methods and thresholds for estimating port operability potential

3.1.2 Wind

The wind conditions are derived from the global ERA5 dataset (ECMWF, 2019). We assume that the offshore wind climate is representative for the port location. This is likely to be a conservative estimate, as possible wind speed reductions due to the presence of land mass or infrastructures are not accounted for. International standards and regulations for wind speed limits are given for different terminal types in Table 2.1 by Thoresen (2014).

Because of the large differences in ship size and orientation, we focus on quantifying the wind forces in terms of wind speed (without the wind direction) as input parameter for the operability. The global operability estimates for the wind are derived from the ERA5 database: 10-meter U and V wind component. U_{10} is the Eastward component of the 10 m wind. It is the horizontal speed of air moving towards the east, at a height of 10 meters above the surface of the Earth, in meters per second. This component is combined with the V_{10} component of 10 m wind moving towards the north, to give the wind speed (m/s) of the horizontal 10 m wind (ECMWF, 2019):

$$wind\ speed = \sqrt{V_{10}^2 + U_{10}^2} \qquad (3.1)$$

For the availability in terms of wind speed we use Beaufort scale 6 (13.8 m/s) as the operability threshold, because at higher wind speeds the container terminals will significantly reduce their operability (PIANC MarCom WG 24, 1995; Thoresen, 2014; Van den Bos, 2011). Wind speeds < 6 Beaufort are considered as high operability and > 6 Beaufort as low operability.

3.1.3 Short waves

For analyzing the port operability, we are interested in the hourly rather than extreme wave conditions. The following wave characteristics are derived from the ERA5 database: significant height of combined wind waves and swell (m), mean wave direction (°), mean wave period (s) and the offshore water depth (m). Because the wave conditions are obtained from ERA5 grid points offshore, the wave conditions come from multiple directions (including from land). In the first place we are only interested in the short waves with a direction towards the port/coast. Short waves directing seaward are removed before analyzing the port operability in terms of short waves.

The mean wave period, water depth offshore and nearshore are used to translate the wave climate nearshore via Linear Wave Theory (Airy, 1845). For this we assume a nearshore water depth of 20 m which is compatible with the large vessel sizes (over 20,000 TEU container ships) and port depths of the largest seaports. Because we screen the port operability based on offshore data on a global scale, we neglect detailed processes that are influenced by port layout and infrastructure, such as reflection and diffraction. We do include processes in which the wave motions are affected by the seabed resulting in alteration of the direction of the wave crests (refraction) and wave height (shoaling) and finally breaking (wave-breaking criterium). This is further elaborated in Appendix 7A.

The output consists of the nearshore significant wave height (m). Ports are in general well protected against wind and swell waves by sea defenses like breakwaters therefore we will not follow the criteria from Table 2.2 in terms of the stringent conditions for container terminals, but we will use the navigability limits of tugboats. Following the guidelines (PIANC MarCom WG 121, 2014) the significant wave height may not be higher than 1.5 – 3.0 m for safe berthing of ships. This can be combined with the criteria for tanker terminals from Table 2.2 which are usually located close to the mouth of the port or offshore. Based on this information we selected a significant wave height threshold of 2.0 m.

3.1.4 Infragravity waves

To provide an estimate of the infragravity (IG) wave conditions with a frequency of 0.04 – 0.004 Hz that could be expected in the port, we estimated the incoming bound (forced) IG wave conditions at a nearshore water depth of 20 m. Because IG waves go around defense structures like breakwaters, therefore all wave directions will be considered. IG wave height is determined for relevant combinations between the nearshore significant wave height H_s (m) and the peak period T_p (s) calculated in Section 3.1.3 for hourly input values covering the whole timeseries.

For this study a JONSWAP (JOint North Sea Wave Project) spectrum (Hasselmann et al., 1973) is assumed. Therefore, we need to define the wave directional spreading and peak enhancement factor. Peak wave periods larger than 10 s consist mainly of swell waves with an assumed directional spreading coefficient of s = 7, peak wave periods smaller than 10 s mainly consists of wind waves with a corresponding s = 2. Small spreading coefficients indicate large spreading with lots of different directions and a larger spreading coefficient indicate a single direction implicating a more concentrated IG wave energy resulting in higher IG waves. The peak enhancement factor γ is defined using Torsethaugen et. al. (1984), which provides an estimate for the value of γ as a function of the significant wave height and the peak wave period. A standard JONSWAP spectrum corresponds to γ = 3.3 to increase the peak of the Pierson-Moskowitz spectrum (γ = 1).

The nearshore wave climate is used as spectral input for evaluating the infragravity waves by Herbers et al. (1994) who stated that second-order non-linear theory from Hasselmann (1962) accurately predicts locally forced infragravity motions. Non-linear interactions of two surface gravity waves (with slightly different frequencies f_1=f and f_2 = f+Δf) excites a forced secondary wave with the difference-frequency Δf.

The energy of the secondary forces surface elevation $E_{forced}(\Delta f)$ for one pair of interacting primary waves is computed with the following expression described by Van Dongeren et al. (2003):

$$E_{forced}(\Delta f) = 2\int_{\Delta f}^{\infty}\int_{0}^{2\pi}\int_{0}^{2\pi} D^2\,(f+\Delta f, -f, \Delta\theta+\pi)\,E(f+\Delta f,\theta_1)\,E(f,\theta_2)\,d\theta_2\,d\theta_1\,df \qquad (3.2)$$

$E_{forced}(\Delta f)$ is the bound long wave energy (m²/Hz). $E(f,\theta)$ is the 2D frequency-directional spectrum of primary (swell and sea) waves (m²/Hz). Subscripts 1 and 2 refer to the two interacting primary waves. $D(f+\Delta f, -f, \Delta\theta+\pi)$ is the difference-interaction coefficient with a difference in propagation directions of the interacting pair of primary wave components with directions: $\Delta\theta = |\theta_1 - \theta_2|$. This difference-interaction coefficient for the surface elevation energy is defined as:

$$\begin{aligned} D(-f_1, f_2, \Delta\theta+\pi) &\equiv \frac{g k_1 k_2 \cos(\Delta\theta+\pi)}{8\pi^2 f_1 f_2}\frac{\cosh(k_3 h)}{\cosh(k_1 h)\cosh(k_2 h)} \\ &- \frac{g(-f_1+f_2)}{[g k_3 \tanh(k_3 h) - (2\pi)^2(-f_1+f_2)^2]f_1 f_2} \\ &\times\left\{(-f_1+f_2)\left[\frac{(2\pi)^4(f_1 f_2)^2}{g^2} - k_1 k_2\cos(\Delta\theta+\pi)\right]\right. \\ &\left. - \frac{1}{2}\left[\frac{-f_1 k_2^2}{\cosh^2(k_2 h)} + \frac{f_2 k_1^2}{\cosh^2(k_1 h)}\right]\right\} \end{aligned} \qquad (3.3)$$

In this equation the wave number, k_3 of the bound IG wave is equal to the difference in wave number of the two short waves:

$$k_3 \equiv \left|\overrightarrow{k_1} - \overrightarrow{k_2}\right| = \sqrt{k_1^2 + k_2^2 - 2k_1 k_2\cos(\Delta\theta)} \qquad (3.4)$$

From the estimated bound waves, the representative wave height $H_{m0,Low}$ and mean wave period $T_{m01,Low}$ are determined based on the zeroth-order and first-order moments of the spectral density. The equivalent expression described by Van Dongeren et al. (2003) is used but estimating the infragravity wave height for all (hourly) input values is computationally intensive. To tackle this problem, we developed a look-up table for 250 x 250 combinations between the nearshore significant wave height and peak period with step size: 0.05 m and 0.1 s ranging from 0 – 12.50 m and 0 – 25 s.

It must be noted that IG waves in the nearshore not only consist of bound infragravity waves determined from local wave conditions. Rawat et al. (2017) showed that free infragravity waves radiating from coastlines along the eastern boundaries of ocean basins are the origin of the largest energy bursts in the infragravity band. IG waves are therefore not limited to a certain area. The calculated IG wave height in this study is probably underestimated.

The limiting significant wave height of infragravity waves at the berth is 0.05 m, based on an empirical relation (Mol et al., 1986) and international guidelines (PIANC MarCom WG 115, 2012). IG waves above this limit is classified as low operability and below this limit as high operability.

3.1.5 Calibrating operability estimates for a single port location

The first port that is analyzed is the Port of Cape Town because it is known for its challenges with respect to operability (Van der Molen & Moes, 2009). The main cause for unavailability were infragravity waves and mooring problems due to strong winds. Due to the predominant container cargo throughput, the operations are limited by the stringent metocean thresholds.

The operability of a single port location is in an early design phase visualized and analyzed in multiple ways, Appendix 7B gives an overview on visualizations of metocean parameters and operability indicators. A wind/wave rose gives a better understanding of the wind/wave climate. This gives an idea on how wind speed and wave height including the direction are distributed at one location. To show the likelihood of the joint occurrence of two parameters with bins, a joint-occurrence-table (JOT) (see Figure 3.5) is used. The JOT gives a data visualization in more detail than a wind/wave rose and gives also a better inside into extreme sea states. It can also give a first insight into operability, because it allows you to see at a glance the impact of the waves heading seaward/shoreward (waves travelling seaward are visualized between the two red vertical lines and vice versa). You can also evaluate the height of the waves in a glance (short waves larger than 2.0 m are shown above the red horizontal line and below 2.0 m). Together with the peaks-over-threshold (POT) (see Figure 3.6) the extreme conditions, their magnitude and frequency are identified under which port operations are hindered. Via the threshold approach the operability or availability in terms of metocean conditions is derived. All the visualization methods described are used for a single location but are applicable to all locations and operability indicators. On a global scale we need to look at ways to aggregate and visualize results in a clear and effective way.

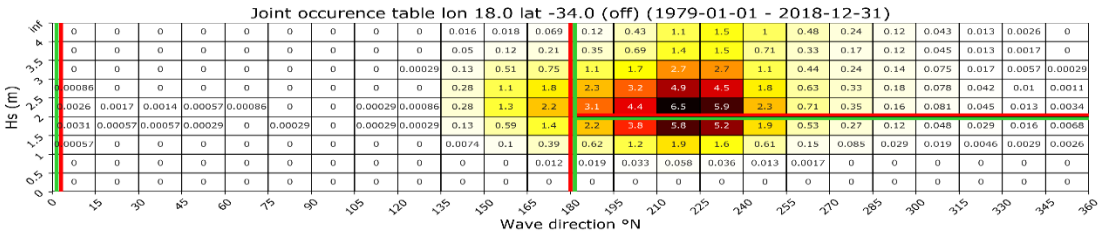

Figure 3.5 Joint-occurrence-table for port of Cape Town with offshore wave data

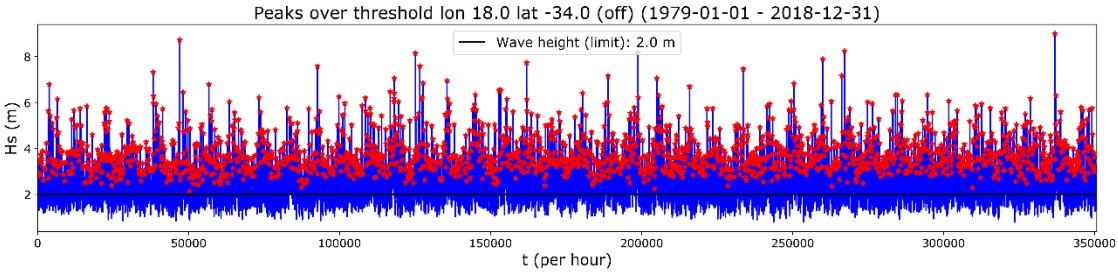

Figure 3.6 Peaks-over-threshold for port of Cape Town with offshore wave data

3.2 Validating global estimates on port operability indicators

To validate the global operability estimates we validate the results for 10 port locations which are known for either having serious or limited operability issues. Preferably we would have actual port operability or downtime data from port operators to validate our global estimates. However, port authority or operators are not eager to share that kind of sensitive information. There is also very little literature available about downtime or operability studies on ports. Therefore, we take a different approach and try to validate our method via literature based on problems related to metocean condition in ports and open layouts.

The following port locations, for example, are known for their downtime based on literature:

- Cape Town (Van der Molen, 2009) in South-Africa suffered from mooring problems in the port. The main cause for this is the occurrence of long waves and, to some extent, harbor seiching. With later modifications to the layout of Duncan Dock and the construction of Schoeman Dock, and proper and numerical model testing the problems in the port of Cape Town have almost disappeared.
- Salalah (Carr, Yavary, & Yavary, 2004) in Oman is suffering also from long waves and extreme high energy wave conditions during the summer monsoon season can result in adverse vessel motions and reduce the efficiency of cargo transfer operations.
- Geraldton (Van der Molen, 2015) in Australia is exposed to high energy long wave conditions reducing the berth operability.
- Long Beach (Mesa & Wesley, 2018) in California (USA) suffers from hurricanes and long waves.
- Tomakomai (Van der Molen, 2006) in Japan is also suffering from long waves resulting in large ship motions occur at relatively low offshore wave heights.

Hereafter, locations with an open port layout is analyzed under the assumption that the port designer has chosen deliberately for an open layout because of the mild wave climate. Port locations that are known for an open layout based on literature and Google maps are:

- Doraleh in Djibouti has an open layout, the landscape of Djibouti is dominated by a series of high, arid plateaus and low coastal plains with coral reefs in front of the coast (African Development Fund, 2008).
- Jeddah in Saudi Arabia located on the Red Sea has an open layout while looking at satellite images. In front of the container terminal a small kind of natural breakwater is located.
- Hadera in Israel has an offshore deep-water coal unloading terminal which started in the 90s. From 2012 a deep-water LNG terminal was constructed. This offshore terminal is in an unprotected environment
- Port of Yangshan in Shanghai, China has an offshore deep-water container terminal which consists of multiple islands in front of the coast in combination with land reclamations.
- Hay Point in Australia is an offshore coal terminal, the project was commissioned in 1975 and continues to operate well beyond its design life, servicing ships well above the original design capacity.

After analyzing these 10 locations they are classified in a confusion matrix via True vs. False and Positive vs. Negative. A True Positive (TP) is an outcome where the model correctly predicts the positive class. Similarly, a True Negative (TN) is an outcome where the model correctly predicts the negative class. A False Positive (FP) is an outcome where the model incorrectly predicts the positive class. And a False Negative (FN) is an outcome where the model incorrectly predicts the negative class.

For a proper validation study the outcomes are analyzed but due to the large amount of data there is a trade-off between the amount of detail/insight in the data and the number of locations to compare. A boxplot (see Figure 3.7) is used to give an idea of the shape of the distribution, its central value and its variability (including extremes). With a quick look you can see a normal distribution for the wind speed. The dash dotted line represents the limit: 13.8 m/s for wind speed which is above the 95th percentile which indicates a high availability in terms of wind speed for the location of Cape Town. The same is done for the other parameters: short/infragravity wave height. It is also very well possible to have multiple boxplots for the same parameter, for example 10 port locations in the same figure allowing us to compare different port locations quickly and reliably.

To gain more insight into the availability we use a cumulative frequency analysis to analyze the frequency of occurrence of values of a phenomenon less than a reference value also called frequency of non-exceedance. By ranking the data, you get the probability estimate from the cumulative frequency analysis. From Figure 3.8 you can read the availability for a given wind speed limit and vice versa. ~80% of the time this location has a wind speed smaller than 10 m/s. If you want to increase your availability in terms of wind speed by increasing the maximum wind speed limit you can look up what the availability is for a higher limit which allows you to decide if an investment in for example better cranes in terms of wind speed is feasible. This visualization method can give insights into the availability for multiple locations for a single parameter related to thresholds.

Box plots and port availability curves are suitable for our validation study of 10 port locations. It can give insights into the availability for multiple locations for single parameters related to threshold which will be shown in Section 4.1. But it is no longer feasible if you want to display more than 10 locations in the same figure. For this global study we will need to go a step further.

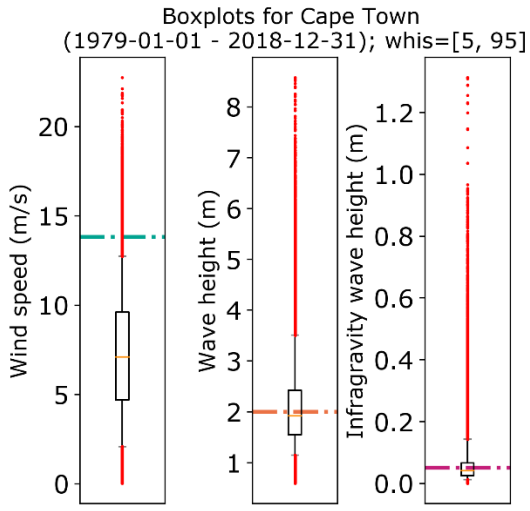

Figure 3.7 Boxplots for the port of Cape Town including the limits for wind, waves and IG waves

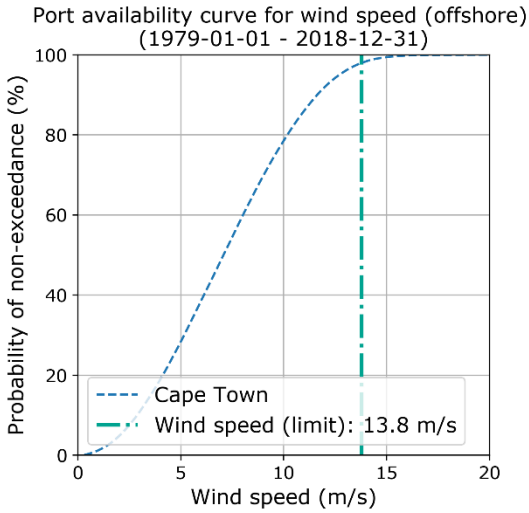

Figure 3.8 Port availability curve for the port of Cape Town including the limiting wind speed

3.3 Classify and map existing port locations in terms of operability indicators

From the World Port Index (WPI), the exact coordinates (longitude and latitude) in terms of harbor size (based on several applicable factors, including area, facilities and wharf space) are selected to collect the specific data from ERA5. Ports located further than 1.0° from the nearest ERA5 grid point (e.g., the Port of Hamburg is located 1.1° from its mouth on the North Sea and 2.0° from the nearest ERA5 grid point) are removed and the same applies to ports located in the vicinity of the same nearest ERA5 grid point (e.g., the ports of Helsinki and Tallinn located opposite of each other in the Gulf of Finland and only 0.7° a part). This has resulted into a list of 103 unique global port location coordinates.

For every port location the overall operability potential (P_{total}), individual operability indicators (P_{wind}, P_{waves} and $P_{IGwaves}$), frequency, duration and the main driver to identify potential risks are estimated. In order to analyze the statistics, the 103 port locations are classified and averaged in different operability classes: $P_{total} > 95\%$ (very high), $85\% < P_{total} \leq 95\%$ (high), $75\% < P_{total} \leq 85\%$ (intermediate) and $P_{total} \leq 75\%$ (low) to say something about the suitability of existing port locations. Potential risks are identified for each operability class via the most critical (averaged) operability indicator and for every port location via the main driver (lowest operability indicator for a certain port location). Port locations with a low ($P_{total} \leq 75\%$) overall operability potential are referred to as “hotspots”, including the main causes of these risks. Hereafter, 103 (existing) port locations are mapped out to analyze the global distribution in terms of port operability indicators based on metocean conditions.

In order to map 103 ports, analyze and define hotspots in terms of port operability and associated drivers, we have chosen to visualize 103 ports using bar graphs including overall port operability potential and operability indicators. From these we can easily select hotspots and identify the main driver for potential risks. Another way to map port operability is via a map for the port operability potential or the main driver. On this map, the dots indicate the locations and the color of a dot indicates the suitability of that location relating to the port operability classes. This gives the opportunity to quickly screen the suitability of existing port locations all over the world.

3.4 Classify, compare and map port suitability across the world

To analyze the suitability of 4560 locations along the word’s coastline, we first need to derive coordinates (longitude and latitude) to collect the specific data from ERA5. This is achieved by using a shapefile for the coastline (1:10.000.000) from Natural Earth Data which is publicly available consisting of 342.070 coordinates to draw the coastlines (Natural Earth Data, 2020). We used the same conditions as in the first three steps, the coordinates do not have to be too close to the coast, but also not too far away from it. Hereafter, some manual adjustments have been made by removing grid points on the open ocean around small islands. Grid points within large estuaries are also removed due to the assumed large uncertainties from the ERA5 datasets in those areas. The final grid points consist of 4560 locations off the coast with a distance between 0.1° - 0.8°. We apply the same method as in Section 3.3 for all (4560) locations to compare with 103 (existing) port locations. This provide insights into the suitability in terms of port operability based on metocean conditions around the world.

4560 locations are mapped out to screen the suitability in terms of port operability based on metocean conditions. This is done for individual operability indicators but also combined to give an overview of the overall port operability potential. The dots indicate the locations and the color the degree of suitability. For each location, the main driver for port operability risks is visualized to quickly screen the coast for the main driver for the operability risks. The dots indicate the locations and the color the main driver.

3.5 Analyzing sensitivities

To verify the effects of the key assumptions on the results, we analyze the inter- and intra-annual trends and perform a sensitivity analysis. This is split into 5 different sensitivity types/variables which are shown in Table 3.2. The focus of the sensitivity analysis is on 4560 locations around the world's coastlines instead of 103 port locations because we look at the performance of our generic method on a global scale.

First, our assumptions on operability thresholds based on literature are analyzed. It is difficult to say when a port operator will shut down the operations, because port operators are reluctant to share this kind of sensitive information. Or, different operability thresholds for different types of cargo are distinguished, and therefore the chosen thresholds are based on literature. Therefore, ± 1 Beaufort for the wind speed, ± 0.5 m short wave height and ± 0.01 m for IG wave height are used (see Table 3.2).

Secondly, we do not have reliable information about the bathymetry in the nearshore and the current nearshore water depth of 20 m is mainly chosen for the world's leading ports, but there are many ports with smaller water depths. Therefore, a changing water depth is used to analyze the sensitivity of the results between 20, 17, 16 and 15 m water depth.

Thirdly, the assumed nearshore wave conditions are subject to uncertainty in metocean conditions and wave transformation. Therefore, we increase the metocean conditions from ERA5: wind speed and short-wave height by an arbitrary +5%.

Fourthly, the global ERA5 database of historical hourly output values is studied over time to analyze the port operability potential with all its characterizations and metocean conditions over time. Interannual variations are identified with intervals of one year and a trendline with the average of 5 years.

Finally, intra-annual time scale is studied via the seasonality. Do the 'exceedance events' take place in the same season or are they evenly distributed over the seasons and how is the operability distributed over the different seasons? Ports need to achieve a certain degree of operability every season because the global economy does not take a break in a particular season. The timeseries are divided into 4 separate seasons: boreal winter: December, January and February (DJF), spring: March, April and May (MAM), summer: June, July and August (JJA) and autumn: September, October and November (SON) to evaluate the dependence of port operations.

Sensitivity type	Analyzed time period	Water depth (m)	Metocean conditions	Threshold		
				Wind speed (m/s)	Short waves (m)	IG waves (m)
Benchmark	1979-2018	20	ERA5	13.8	2.0	0.05
Thresholds	1979-2018	20	ERA5	13.8 ± 1 Beaufort	2.0 ± 0.5	0.05 ± 0.01
Water depth	1979-2018	15-16-17-20	ERA5	13.8	2.0	0.05
Metocean conditions	1979-2018	20	ERA5 + 5%	13.8	2.0	0.05
Interannual variations	1979-2018 in 1-year intervals + 5-year trendline	20	ERA5	13.8	2.0	0.05
Intra-annual variations	1979-2018 in seasons	20	ERA5	13.8	2.0	0.05

Table 3.2 Input variables for the sensitivity analysis

4 Results

4.1 Validating global estimates on port operability indicators

The reliability of our global approach is verified by means of a validation study of 10 port locations (see Table 4.1) that are known to have serious or limited operability problems due to metocean conditions: Doraleh (Djibouti), Jiddah (Saudi Arabia), Hay Point (Australia), Shanghai (China), Hadera (Israel), Long Beach (USA), Tomakomai (Japan), Cape Town (South Africa), Salalah (Oman) and Geraldton (Australia). For these locations we first look at 3 individual metocean parameters (i.e., wind speed, short-wave height and infragravity-wave height) compared to their operability limits obtained from literature (Figure 4.1). In the following, the overall operability potential is estimated for 10 validation port locations in order to conclude whether our approach is capable of providing reliable first-order estimates of the port's operability due to wind and waves.

For none of the 10 locations, the 95th percentile of the wind speed exceeds the operability limit. In terms of short waves, the boxplots in Figure 4.1 show a clear distinction between the two sets of locations with and without experienced operability issues. The 95th percentile short-wave heights for the locations with known operability issues are close to or well above the wave height limit. In contrast, 4 out of 5 locations with limited operability problems due to metocean conditions are well below the wave height limit. The Port of Hadera is only just below the short-wave height limit with the 95th percentile. There is also a clear distinction for the infragravity waves, 4 out of 5 locations known for downtime are close to or well above the infragravity wave height limit. The port of Salalah is a slight outlier. Literature suggests that this port suffers from infragravity waves (Carr et al., 2004), but our approach estimates a 95th percentile of 0.03 m which is well below the 0.05 m limit. This can perhaps be explained by resonance effects due to lay-out of the port that may play a role but is not included in our global approach. Another possible explanation could be that the monsoon conditions, which generally lead to unavailability, are not well represented in the global metocean dataset.

Port	Main cause	Cargo type	Natural shelter / protections	Port lay-out
Doraleh		Container	Bay with fringing reefs	Open
Jiddah		All types	Open coast with fringing reefs	Open
Hay Point		Dry bulk	-	Open
Shanghai		Container	Open coast with islands in an estuary	Open
Hadera		Liquid and dry bulk	-	Open
Long Beach	Long waves and hurricanes	Container and bulk	Large island in front of the coast and breakwaters	Semi-enclosed
Tomakomai	Long waves	All types	Bay and breakwaters	Semi-enclosed and elongated
Salalah	Long waves and monsoon period	All types	Bay and breakwaters	Semi-enclosed and elongated
Cape Town	Long waves	All types	Bay and breakwaters	Semi-enclosed and elongated
Geraldton	Long waves	Bulk and general cargo	Bay and breakwaters	Semi-enclosed

Table 4.1 Classification of (validation) port locations including the main cause, cargo type, shelter and lay-out

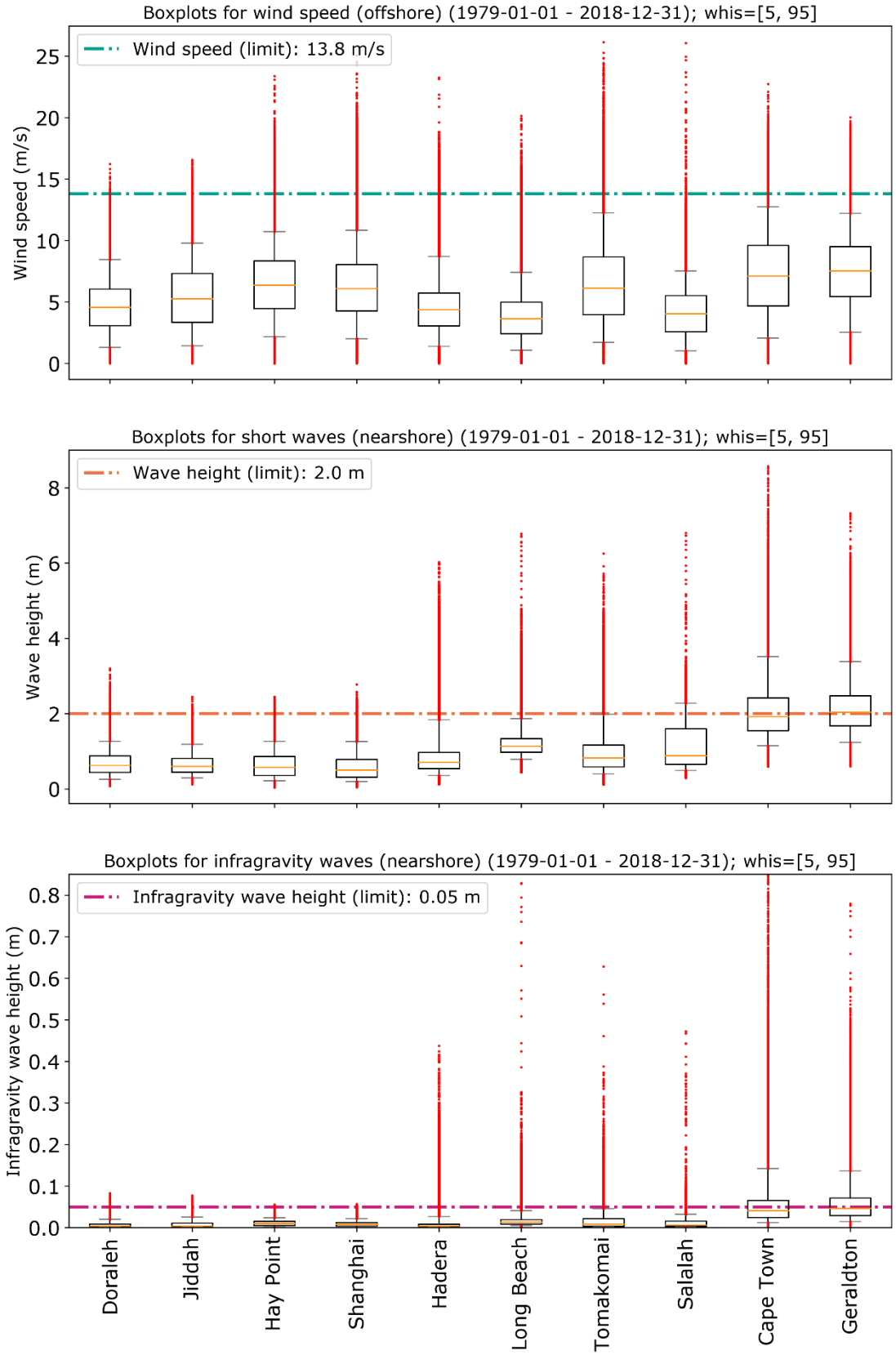

Figure 4.1 Boxplots for 10 validation port locations in terms of wind speed, short-wave height and infragravity wave height including their operability limits

Our method combines the individual operability indicators into an overall operability potential (Table 4.2). For 9 out of 10 cases, our approach is able to correctly predict the presence/absence of operability issues when using the 95% operability potential as separation point (visualized via a confusion matrix in Figure 4.3). We conclude that our approach is able to make reliable first-order estimates of port operability due to wind and waves.

Port	Mean wave period (s)	Wind speed p95 (m/s)	Short-wave height p95 (m)	IG-wave height p95 (m)	Wind operability (%)	Short wave operability (%)	IG wave operability (%)	Overall operability potential (%)	Frequency (events/year)	Duration (average) (hours)
Doraleh	4.33	8.44	1.27	0.02	100.0	99.9	99.9	99.9	1.5	8.6
Jiddah	4.45	9.79	1.19	0.03	99.9	100.0	99.9	99.8	1.4	9.8
Hay Point	3.41	10.72	1.26	0.02	99.7	99.9	100.0	99.7	2.2	10.9
Shanghai	3.24	10.83	1.26	0.02	99.4	99.9	100.0	99.4	5.4	9.5
Hadera	5.12	8.69	1.83	0.03	99.7	96.2	98.0	96.2	12.5	27.1
Long Beach	9.66	7.42	1.86	0.04	99.9	96.5	97.1	95.9	16.5	21.9
Tomakomai	6.55	12.25	1.98	0.05	97.9	97.0	96.2	**94.9**	31.8	14.1
Salalah	7.43	7.54	2.28	0.03	100.0	**87.8**	99.4	**87.8**	17.9	60.0
Cape Town	9.50	12.73	3.51	0.14	97.8	**60.9**	**61.3**	**54.1**	81.3	49.5
Geraldton	10.12	12.20	3.38	0.14	98.8	**47.9**	**54.6**	**46.3**	86.6	54.4

Table 4.2 Output of the validation study for 10 port locations

The Port of Long Beach forms a misclassification with an operability potential of 95.9% which is higher than we would expect based on literature and could mean that our method is a little too optimistic. Figure 4.2 shows that short/infragravity waves are the main cause of the operability problems. It is important to understand why this port is misclassified as it can provide us with information on the conditions for which our approach may or may not be valid. In the case of Long Beach, this port is sheltered by a large offshore island (see Table 4.1). This island and its effects on the wave propagation (e.g., sheltering, refraction and diffraction) are not included in our approach. This can be the cause of the overestimation of the wave heights compared to the actual wave climate. We therefore conclude that our approach does not always provide reliable operability estimates in locations with islands or other (large-scale) geomorphological features offshore or in the nearshore.

4 of 5 port locations known for an open layout (first 5 locations in Table 4.2) have an extremely high operability potential ≥ 99.4%. The Port of Hadera has a port operability potential estimate of 96.2%, which is a small outlier but still exceeds the chosen limit (95%). Looking at Figure 4.2, this is mainly due to short waves. The offshore deep-water terminal in front of the coast of Hadera handles liquid and dry bulk cargo (see Table 4.1), the other 4 port locations handle all kinds of cargo including containers that require strict conditions. The short-wave height limits for tankers and dry bulk vessels (see Table 2.2) may exceed the chosen 2.0 m short-wave height limit. The estimate of the operability potential for the Port of Hadera is therefore indicated as conservative. We can therefore conclude that our approach does not always provide reliable operability estimates for ports with less stringent conditions (i.e., liquid and dry bulk terminals) and possibly offshore located.

The relative difference in terms of frequency between the locations with an open layout and those known for their downtime is an order of magnitude (from 1.4 until 86.6 events/year). The average duration of an exceedance event has also an order of magnitude difference (from 8.6 till 60 hours). It seems that if the threshold is exceeded, even if only a few times per year, the port is unavailable for at least ~8 hours. The frequency of the Port of Salalah is significantly lower than the average for ports known for their downtime, but the average duration of an exceedance event is the highest of all. This can be explained by the monsoon season which is active for only a couple of months a year, but the weather conditions are much more extreme than the average conditions during that period. Another difference can be observed when looking at the mean wave period in Table 4.2. The 5 open layout locations (first 5 locations in Table 4.2) have a mean wave period of 3 – 5 s which is indicative for a wind wave climate, the 5 locations known for their downtime have a mean wave period of 7 – 10 s which is more indicative for a swell wave climate. So we can show that in addition to the operability potential, there are more differences between locations with an open layout and locations known for their downtime, which can provide interesting insights.

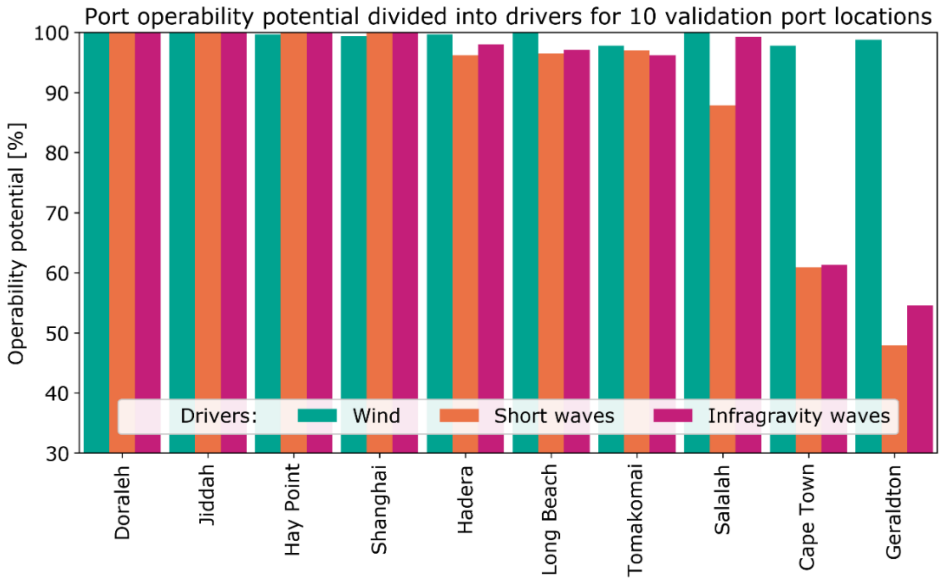

Figure 4.2 Port operability divided into drivers for 10 validation port locations

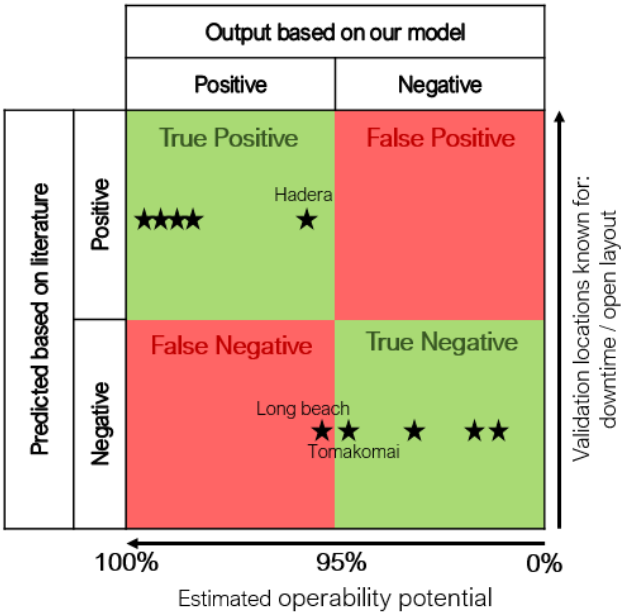

Figure 4.3 Confusion matrix classification: True or False Positive (or Negative)

4.2 Classify and map existing port locations in terms of operability indicators

We applied our approach to 103 existing port locations selected from the World Port Index (see Section 3.3) to analyze the statistics of the operability indicators for existing ports. In Figure 4.4 we visualized the overall operability potential (P_{total}) (i.e., the percentage of time that all operability indicators are below their threshold), as well as the operability potential for the individual indicators (P_{wind}, P_{waves} and $P_{IGwaves}$). The main cause or driver for operability issues is defined as the indicator with the lowest operability for a given port location (i.e., the highest percentage of time an indicator exceeds its threshold). Figure 4.4 shows that short waves and infragravity waves are the main causes for a reduced operability for the 103 port locations. In most cases, the blue-colored bar is close to either the operability line for the short or IG-waves, which means that this operability indicator is exceeded during almost all exceedance events for a given location. The other operability indicators may also show a decreased operability potential which indicates that exceedance events for the other operability indicators are happening at the same time as the lowest operability indicator. When this is not the case and there is a difference between the lowest operability indicator and the blue-colored bar (for example at the Port of Cape Town (1) and Durban (5)) the individual operability indicators are not exceeding at the same time/event and can therefore act more independently of each other. Note that the input/thresholds are given in the lower right corner of Figure 4.4.

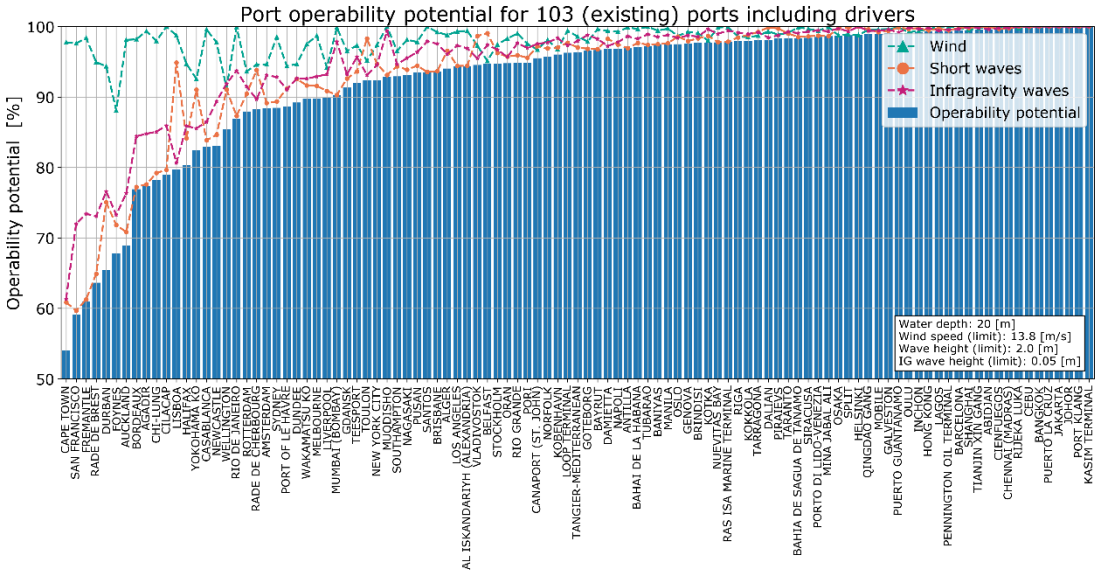

Figure 4.4 Overall operability potential (P_{total}), the % of time that a port is available for port operations (blue-colored bar) and operability indicators (P_{wind}, P_{waves} and $P_{IGwaves}$) (dotted lines) for 103 ports across the world

The 103 existing port locations are classified into different operability classes based on their overall operability potential (P_{total}). Table 4.3 shows the statistics for the following P_{total} classes: $P_{total} > 95\%$ (very high), $85\% < P_{total} \leq 95\%$ (high), $75\% < P_{total} \leq 85\%$ (intermediate) and $P_{total} \leq 75\%$ (low). Of the 103 ports, 56 (54.4%) have a very high operability potential, 31 (30.1%) ports high, 9 (8.7%) intermediate, and 7 (6.8%) low. Note that the ports that are classified as having a low probability potential based on our method, do not necessarily have to experience downtime as the capacity of the port, possible wave sheltering and mitigating measures have not been considered. The classification merely provides information about the suitability of the port location in terms of metocean conditions. Table 4.3 indicates that the majority of the ports (54.4%) are located in suitable metocean conditions for port operations. Table 4.3 also allows us to analyze which metocean conditions are the most critical for the port operability. For all classes, the short waves result in the lowest operability potential. The IG waves, which are derived from the short waves, show slightly higher operability percentages. Wind conditions hardly result into operability problems for the ports analyzed.

The difference between the overall average operability potential and the lowest individual operability indicator increases as the operability classes decrease. This indicates that the lower operability classes are associated with more independent exceedance events. The frequency of exceedance events (number of events per year) increases rapidly with decreasing operability classes (10.8 for very high operability potential and 75.3 for low). The same applies to the duration of an exceedance event, which increases with decreasing operability classes (12.5 for very high operability potential and 45.5 for low). An increase in frequency and duration could hamper the overall operability potential even more than estimated, due to numerous shut down and restart actions and the inability to make up for unavailable operation periods compared to the short durations of unavailability. Consequently, more than half (56 or 54.4%) of the 103 port locations show a suitable port location in terms of metocean conditions with an overall average operability potential of 98.4%.

Operability classes (%)	Port locations (#)	Overall average operability potential (%)	Operability indicators			Frequency (events/ year)	Duration (hours)
			Wind (%)	Short waves (%)	IG waves (%)		
P_{total} > 95	56 (54.4%)	**98.4**	99.3	98.9	99.1	10.8	12.5
85 < P_{total} ≤ 95	31 (30.1%)	**91.7**	97.2	93.5	94.9	39	20.8
75 < P_{total} ≤ 85	9 (8.7%)	**80.0**	97.6	83.6	85.3	52.4	35.7
P_{total} ≤ 75	7 (6.8%)	**62.8**	95.6	66.4	72.3	75.3	45.5
Total/average	**103 (100%)**	**92.3**	**98.3**	**93.7**	**94.8**	**27.3**	**19.3**

Table 4.3 Overview of the results for 103 port locations across the world in different operability classes. Note that the overall operability potential is always lower than the potential for each individual parameter, as not all parameters exceed their threshold at the same point in time.

Our approach also allows us to study the main potential drivers of operability issues (see Table 4.4). The main driver is defined as the indicator with the lowest operability for a given port location. Due to the correlation between short waves as input for the IG waves estimation, we have created an overlapping main driver for short waves and IG waves with a maximum relative difference of 1 percent. For the majority of the ports (39 or 37.9%) short waves are the main driver for ports, closely followed by a combination of short waves and IG waves which is the main driver for 37 ports (35.9%). Of the 103 ports, 20 (19.4%) have wind as their main driver and 7 (6.8%) IG waves. Table 4.4 shows that, in contrast to the average operability indicators from Table 4.3, wind does have a significant impact on the operability of ports that are mainly classified as very high operability potential.

Operability classes (%)	Main drivers			
	Wind (#)	Short waves (#)	Short & IG waves (#)	IG waves (#)
P_{total} > 95	19 (18.5%)	8 (7.8%)	27 (26.2%)	2 (1.9%)
85 < P_{total} ≤ 95	1 (1%)	18 (17.5%)	9 (8.7%)	3 (2.9%)
75 < P_{total} ≤ 85	0 (0%)	7 (6.8%)	0 (0%)	2 (1.9%)
P_{total} ≤ 75	0 (0%)	6 (5.8%)	1 (1%)	0 (0%)
Port locations (#)	**20 (19.4%)**	**39 (37.9%)**	**37 (35.9%)**	**7 (6.8%)**

Table 4.4 Overview of the main drivers for 103 port locations across the world in different operability classes

The port operability potential varies considerably geographically (Figure 4.5). Ports around the equator generally have a higher operability potential (indicated by the green dots) than port locations farther away from the equator (more orange and red dots). Around inland seas (such as the Red Sea and the Mediterranean) there is often a higher operability potential, which is probably related to their sheltered location for the swell waves. By zooming in on the lowest operability class ($P_{total} \leq 75\%$) in Table 4.3 and Table 4.4, we can identify ports with large potential operability risks due to the ambient metocean conditions. We define those 7 ports in the lowest class as “hotspots”. Figure 4.5 shows that the hotspots (indicated by the red dots) are mainly located along the southern capes around the ‘Roaring Forties’ and at exposed locations along the oceans. Short waves are the main cause of lower operability potential due to the highest percentage of time this driver exceeds its threshold.

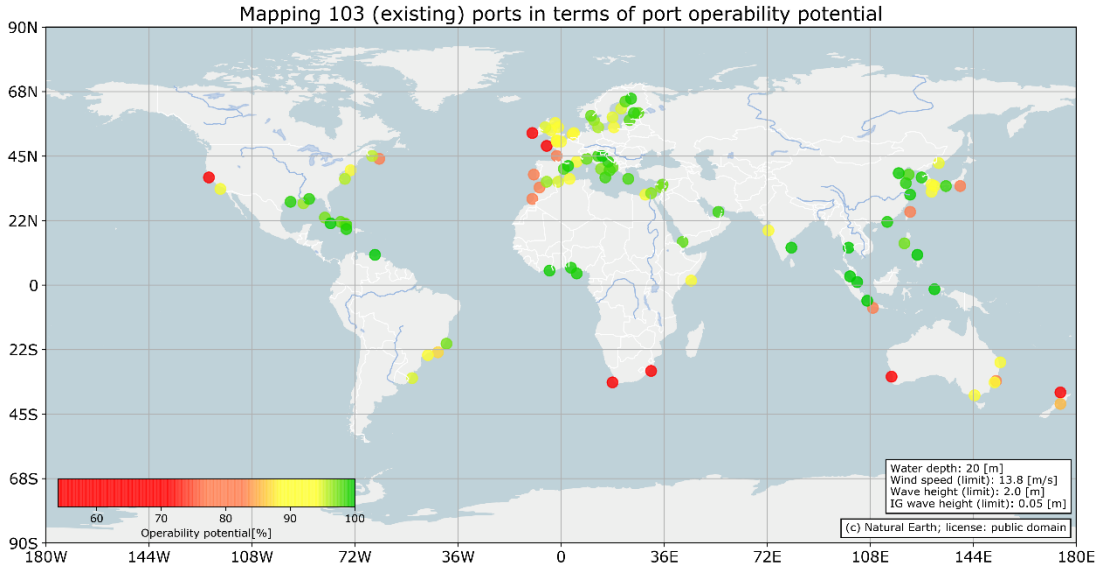

Figure 4.5 Geographical overview on port operability potential for 103 existing port locations

4.3 Classify, compare and map port suitability across the world

To explore the suitability of potential port locations worldwide, we have classified 4560 locations across the world's coastline in operability classes, in a similar way as for the 103 existing port locations in Section 4.2 (see Table 4.5). Of the 4560 locations, 2336 (51.2%) have a very high operability potential, 1048 (23%) high, 491 (10.8%) intermediate and 685 (15%) low. Hence, about half (51.2%) of the world's coastline is thus potentially suitable as a port location in terms of metocean conditions with an overall average operability potential of 98.7%. The average port operability potential for 4560 locations is 88.9% which is lower than the average for 103 port locations which is 92.3% (Table 4.5). This suggests that the 103 port locations are generally better located in terms of metocean conditions than the equidistantly spaced locations along the world's coastline.

Short waves are the most critical indicator, as short waves result in the lowest operability potential for all operability classes. IG waves, which are derived from the short waves in our approach, result in slightly higher operability percentages. Wind conditions are relatively less important compared to the other operability indicators. The difference between the overall average operability potential and the lowest individual operability indicator is greater for 4560 locations than for 103 port locations. This indicates that for 4560 locations the exceedance events act more independent of each other. The distribution of operability indicators over the different classes is comparable with the distribution of the 103 port locations. Compared to the results from Section 4.2, the frequency (number of exceedance events per year) increased only slightly from 27.3 to 28. However, the average duration of the exceedances increased considerably. The most critical operability indicator, short waves, is therefore comparable between the two sample sets, but slightly lower for the 4560 locations.

Operability classes (%)	Locations (#)	Overall average operability potential (%)	Operability indicators			Frequency (events/ year)	Duration (hours)
			Wind (%)	Short waves (%)	IG waves (%)		
P_{total} > 95	2336 (51.2%)	**98.7**	99.7	99.1	99.2	7.2	13
85 < P_{total} ≤ 95	1048 (23%)	**90.7**	97.7	93.2	93.8	35.1	25
75 < P_{total} ≤ 85	491 (10.8%)	**80.6**	95.7	85.4	85.5	54.5	35.7
P_{total} ≤ 75	685 (15%)	**58.3**	93.6	64.8	66.7	69.0	55
Total/average	**4560 (100%)**	**88.9**	**97.9**	**91.1**	**91.6**	**28**	**24.5**
Existing ports	**103**	**92.3**	**98.3**	**93.7**	**94.8**	**27.3**	**19.3**

Table 4.5 Overview of the results for 4560 locations across the world in different operability classes.

The main driver (wind, short waves and infragravity waves) for port operability risks per class are approximately equal to the 103 port locations (see Table 4.6). 1792 (39.3%) locations have a combination of short & IG waves as their main driver, closely followed by short waves for 1433 (31.4%) locations. The number of locations with IG waves as main driver is 897 (19.7%) which is about twice as many as for the existing port location. For 438 (9.6%) locations wind is the main driver, this percentage is twice as small compared to the 103 (existing) port locations. Despite these small differences, the distribution of drivers over the operability classes is comparable between the two sample sets.

Operability classes (%)	Main drivers			
	Wind (#)	Short waves (#)	Short & IG waves (#)	IG waves (#)
$P_{total} > 95$	421 (9.2%)	271 (5.9%)	1503 (33.0%)	141 (3.1%)
$85 < P_{total} \leq 95$	14 (0.3%)	493 (10.8%)	215 (4.7%)	326 (7.1%)
$75 < P_{total} \leq 85$	2 (0.0%)	251 (5.5%)	43 (0.9%)	195 (4.3%)
$P_{total} \leq 75$	1 (0.0%)	418 (9.2%)	31 (0.7%)	235 (5.2%)
Total	**438 (9.6%)**	**1433 (31.4%)**	**1792 (39.3%)**	**897 (19.7%)**

Table 4.6 Overview of the main drivers for 4560 locations across the world in different operability classes

Using the global character of the dataset, we can geographically map the port suitability of coastal locations in terms of metocean conditions geographically (Figure 4.6). Locations around the equator and inland seas are generally more suitable for port locations. There is much variation around the Arabian Sea, with some locations less suitable for port locations due to the monsoon period. From Appendix 7B we can geographically analyze the different operability indicators (wind, short waves and IG waves). In the southern hemisphere we observe short waves and IG waves resulting in less suitable port locations around the capes (Figure 7.4 & Figure 7.5). In the northern hemisphere wind plays a larger role (Figure 7.3), but it is mainly short waves and IG waves that result in less suitable port locations along the oceans.

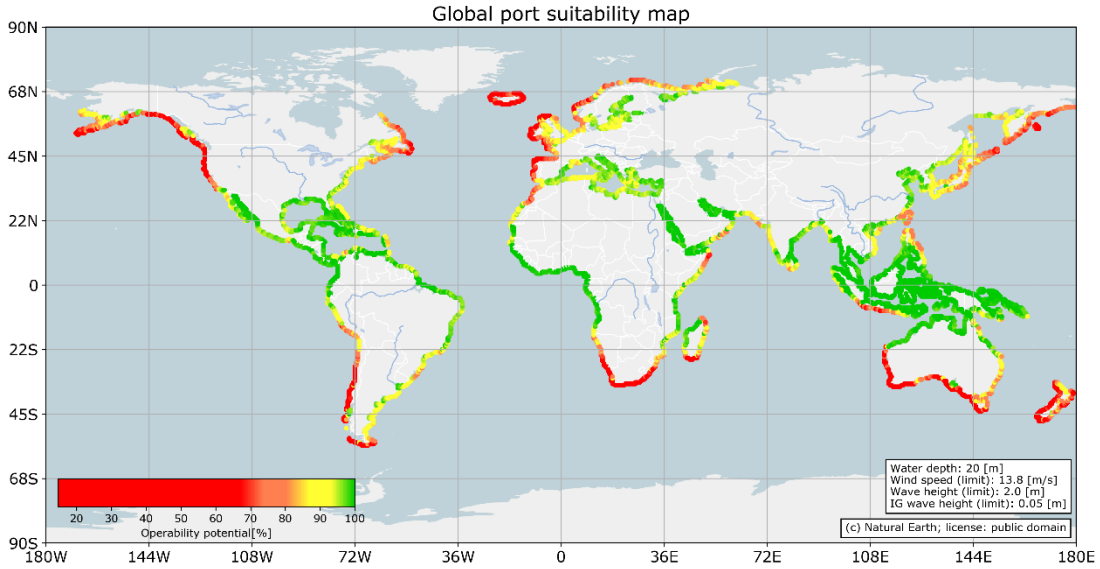

Figure 4.6 Geographical overview on port suitability across the world

Figure 4.7 shows the main operability drivers on a global map. Because of the high correlation between the operability of short and IG waves, the yellow dots represent locations with a maximum relative difference of 1 percent between the two. Along the Pacific Ocean coastline, our approach shows that IG waves are the (potential) main driver for operability issues. Along the Atlantic Ocean coastline, a combination of multiple drivers is important, except for the east coast of South America where short waves are the dominant driver. For the coastline along the Indian Ocean short waves are also the main driver. Around inland seas and mainly Indonesia we see locations where the wind acts as the main operability driver.

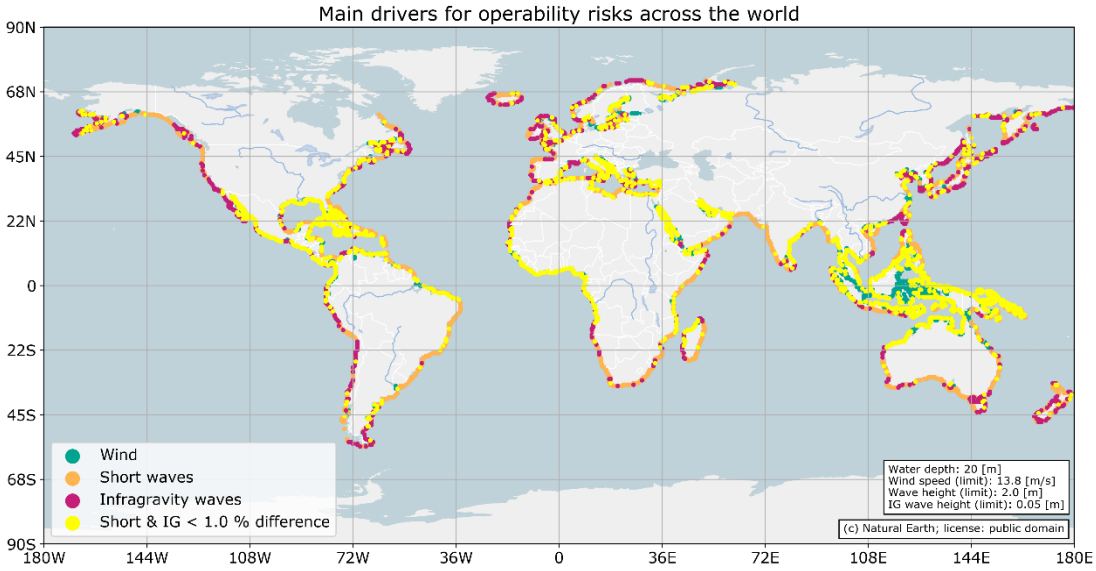

Figure 4.7 Geographical overview for the main causes for port operability risks

4.4 Sensitivity analysis

To analyze the uncertainty in the output of our approach, we determine the impact of a changing variable through a sensitivity analysis. We change the operability thresholds, water depths and metocean conditions and look at the inter- and intra-annual trends through a sensitivity analysis. This analysis is applied to 4560 equidistant spaced locations along the world coastline. For each parameter, we first mention the scenarios/values we tested. After this we make a comparison with the previous results to analyze the implications of changing variables in order to finally reflect on which outcomes are sensitive to changes and which are not.

4.4.1 Operability thresholds

Cargo types are changing due to the growth of the dominant cargo (increasing containerization of world trade). Also, the time the ship spends at berth in the port has decreased significantly compared to, for example, earlier breakbulk operations. This is accompanied by stricter metocean conditions and the ports are more critically dependent on the productivity of the port and efficient supply chains.

The operability thresholds applied in this study are based on rough experience figures. Furthermore, we have not distinguished between different operability thresholds for different types of cargo. In order to examine the influence of these assumptions on the results in Section 4.2 and 4.3, we performed a sensitivity analysis in which we lowered and raised these thresholds by ~20-25% compared to the benchmark (see Table 3.2). For wind speed we used: 13.8 ± 1 Beaufort (m/s), short waves: 2.0 ± 0.5 (m) and IG waves: 0.05 ± 0.01 (m). The results of this sensitivity analysis are shown in Table 4.7 and Table 4.8. The average port operability potential for 20 m water depth and the benchmark thresholds is 88.9%, for the lowered thresholds it decreases to 76.7% (-12.2) and for the raised thresholds it will increase to 93.5% (+4.6). The results show that the thresholds have a positive correlation with the port operability potential. In other words, by raising the thresholds (i.e., lenient operability criteria), the port operability potential will increase and by lowering the thresholds (i.e., stricter operability criteria) it will decrease. Hence, the results are sensitive for changing the thresholds. There is a difference between the relative change in operability, as we can see that the results are more sensitive to decreasing the thresholds than to increasing the thresholds, especially for the classes with very high and low operability in terms of the number of locations per class. In those cases, the rate of change in operability is in the same order of magnitude as (or higher than) the rate of change of the threshold. Hence, when applying stricter operability criteria, the conclusions from Section 4.3 change radically: while in the benchmark the majority of the ports was classified as “very high”, now the majority is classified as “low”. The results are less sensitive to raising thresholds, with the exception for the “very high” category, which has risen to 66.5%. This suggests that the majority of the locations in the “very high” class of the benchmark are very close to the originally chosen threshold. The shift in the number of locations per operability class translates to the individual operability indicators. The ranking remains the same for the stricter thresholds, but there is a shift for the raising thresholds. For all operability classes, IG waves becomes the critical operability indicator.

Operability classes (%)	Locations (#)	Overall average operability potential (%)	Operability indicators		
			Wind (%)	Short waves (%)	IG waves (%)
P_{total} > 95	1187 (-1149) (26%)	**98.2 (-0.5)**	99.1 (-0.8)	98.8 (-0.3)	99.5 (+0.3)
85 < P_{total} ≤ 95	999 (-49) (21.9%)	**90.4 (-0.3)**	95.1 (-2.6)	93.4 (+0.2)	96.8 (+3.0)
75 < P_{total} ≤ 85	691 (+200) (15.2%)	**80.0 (-0.6)**	90.1 (-5.6)	85.5 (+0.1)	91.6 (+6.1)
P_{total} ≤ 75	1683 (+998) (36.9%)	**52.1 (-6.2)**	84.7 (-1.1)	58.7 (-6.1)	73.1 (+6.4)
Total/average	**4560 (100%)**	**76.7 (-12.2)**	**91.5 (-6.4)**	**80.8 (-11.3)**	**88.0 (-3.6)**

Table 4.7 Overview of the results for decreasing/stricter thresholds (wind speed: 10.8 m/s, short-wave height: 1.5 m and IG-wave height: 0.04 m)

Operability classes (%)	Locations (#)	Overall average operability potential (%)	Operability indicators		
			Wind (%)	Short waves (%)	IG waves (%)
P_{total} > 95	3031 (+695) (66.5%)	**99.0 (+0.3)**	99.9 (+0.2)	99.4 (+0.3)	99.1 (-0.1)
85 < P_{total} ≤ 95	842 (-206) (18.5%)	**91.0 (+0.3)**	99.5 (+1.8)	94.8 (+1.6)	91.6 (-2.2)
75 < P_{total} ≤ 85	358 (-133) (7.9%)	**80.4 (-0.2)**	99.0 (+3.3)	87.4 (+2.0)	81.6 (-3.9)
P_{total} ≤ 75	329 (-356) (7.2%)	**62.8 (+4.5)**	98.5 (+4.9)	73.2 (+8.4)	64.4 (-2.3)
Total/average	**4560 (100%)**	**93.5 (+4.6)**	**99.7 (+2.2)**	**95.8 (+4.7)**	**93.8 (+2.2)**

Table 4.8 Overview of the results for increasing/lenient thresholds (wind speed: 17.1 m/s, short-wave height: 2.5 m and IG-wave height: 0.06 m)

The conclusion in Section 4.3 that about half (51.2%) of the world's coastline is potentially suitable as a port location is sensitive to changes in the different operability thresholds. Table 4.8 shows the change in the number of locations per operability class. For lower thresholds only 26% and for raising thresholds 66.5% of the world's coastline is potentially suitable as a port location if one assumes an operability potential of more than 95%. When cargo types in a port change (from breakbulk to container terminal), the metocean conditions can become stricter, resulting in a decrease in port's operability potential. This can be mitigated through protection, mooring systems and possibly relocations, but will undoubtedly involve large investments.

4.4.2 Water depth

By analyzing the sensitivity in terms of water depth, we can see how sensitive the results are to changing water depths, because we do not have reliable nearshore depth information for the 4560 locations along the coast. The assumed nearshore water depth of 20 m has also been chosen for the world's leading ports, but there are many ports with smaller water depths. A changing water depth has a positive correlation with the overall average operability potential for 20, 17, 16 and 15 m water depth, 88.9%, 87.7%, 86.8% and 85.8%. We can conclude that our method is robust for changing water depths and that the operability potential for smaller water depths will decrease.

From Section 4.3 we can conclude that short waves are the most critical indicator and the combination of short & IG waves is the main driver for operability risks. By zooming in on the cause of lower operability due to smaller water depths, Table 4.9 shows that the driving factor for changing operability potential are IG waves. The chosen wind speed is based on an offshore location and in our method is not subject to changing water depth. The short-wave height will slightly decrease relative to offshore due to an initial small increase of the group velocity in intermediate water depth, resulting in a small increase in operability potential. The generation of IG waves is quadratically dependent on the water depth and will therefore increase significantly with decreasing water depths, which is known from literature. The average operability potential in terms of IG waves for 20, 17, 16 and 15 m water depth is 91.6%, 88.9%, 87.7% and 86.3%.

Operability classes (%)	Locations (#)	Overall average operability potential (%)	Operability indicators		
			Wind (%)	Short waves (%)	IG waves (%)
P_{total} > 95	2104 (-232) (46.1%)	**98.6 (-0.1)**	99.7 (0)	99.3 (+0.2)	98.8 (-0.4)
85 < P_{total} ≤ 95	1039 (-9) (22.8%)	**90.7 (0)**	98.0 (+0.3)	95.1 (+1.9)	91.4 (-2.4)
75 < P_{total} ≤ 85	497 (+6) (10.9%)	**80.4 (-0.2)**	96.2 (+0.5)	89.2 (+3.8)	81.5 (-4.0)
P_{total} ≤ 75	920 (+235) (20.2%)	**53.8 (-4.5)**	94.6 (+1.0)	70.8 (+6.0)	54.7 (-12.0)
Total/average	**4560 (100%)**	**85.8 (-3.1)**	**97.9 (0)**	**91.5 (+0.4)**	**86.3 (-5.3)**

Table 4.9 Overview of the results in different operability classes for 15 m water depth (compared to 20 m)

The distribution of main drivers for 15 m water depth is given in Table 4.10. For 15 m water depth, 2656 (58.2%) locations have IG waves as their main driver, followed by a combination of short & IG waves for 1436 (31.5%) locations. In terms of water depth, our method is insensitive for wind speed and short-waves but sensitive for IG waves. Hence, ports with smaller water depths will have lower average operability potential due to larger IG waves.

Operability classes (%)	Main drivers			
	Wind (#)	Short waves (#)	Short & IG waves (#)	IG waves (#)
$P_{total} > 95$	343 (-78) (7.5%)	11 (-260) (0.2%)	1291 (-212) (28.3%)	459 (+318) (10.1%)
$85 < P_{total} \leq 95$	2 (-12) (0.0%)	70 (-423) (1.5%)	124 (-91) (2.7%)	843 (+517) (18.5%)
$75 < P_{total} \leq 85$	1 (-1) (0.0%)	40 (-211) (0.9%)	14 (-29) (0.3%)	442 (+247) (9.7%)
$P_{total} \leq 75$	1 (0.0%)	0 (-418) (0.0%)	7 (-24) (0.2%)	912 (+677) (20.0%)
Total	**347 (-91) (7.6%)**	**121 (-1312) (2.7%)**	**1436 (-356) (31.5%)**	**2656 (+1759) (58.2%)**

Table 4.10 Overview of main drivers in different operability classes for 15 m water depth (compared to 20 m)

4.4.3 Changes in metocean conditions

We test the sensitivity to possible local deviations in the metocean conditions as a result of our rough approach in selecting locations off the coast that are not too far away, but not too close either (see Chapter 3) and uncertainties in wave transformation. For example, changing winds due to the presence of land masses or changing waves due to bathymetric characteristics. To study the resilience of our approach we increased the metocean conditions from ERA5 with 5% for wind speed and short-wave height separately to examine the impact on the operability potential.

The overall average operability potential in terms of wind speed is 97.9%, by increasing the wind speed with 5% decreases the port operability potential in terms of wind speed to 97.1%. The overall operability potential will only decrease with 0.15%. The overall average operability potential in terms of short-wave height is 91.1%, increasing the short-wave height with 5% will decrease the average operability potential in terms of short-wave height with 1.4% and for IG waves it will decrease by 1.3%. The overall average operability potential will decrease with 1.7%. Hence, our approach is more sensitive to increasing short-wave height than wind speed, but generally robust when it comes to changes in metocean conditions.

4.4.4 Interannual trends

Interannual variations in the global ERA5 database are determined with intervals of one-year and a trendline with an average of 5 years. This enables us to identify global trends in port operability potential. Instead of looking at the average values of port operability over 40 years, we estimated the annual average port operability potential including duration and frequency. From this figure, we can conclude that the operability potential, duration and frequency all change over time. The average annual operability potential decreases by about 2% over a period of 40 years (Figure 4.8A). The average annual duration of exceedance events increases by about 2 hours (Figure 4.8B) and the average annual frequency by about 5 events per year (Figure 4.8C). Note that the year 2002 is ignored in the interannual analyses due to a significant outlier for the wind speed. What also stands out is the sharp decline in operability potential between 1990 and 1995.

In order to identify the driving forces behind those large global trends and the sharp decline in operability potential, we have analyzed the 95th percentile of different metocean parameters (wind speed, short-wave height and IG-wave height) over time in Figure 4.9. The annual average wind speed increases slightly over a period of 40 years and is insensitive (Figure 4.9A). The short-wave height (Figure 4.9B) shows a clear increase of about 5%, including a sharp increase between 1990 and 1995 which may explain the sharp decline in Figure 4.9A. For the correlated IG wave height, we observe an increase of more than 10% (Figure 4.9C), especially around 1990 and 1995, both are referred to as sensitive over time.

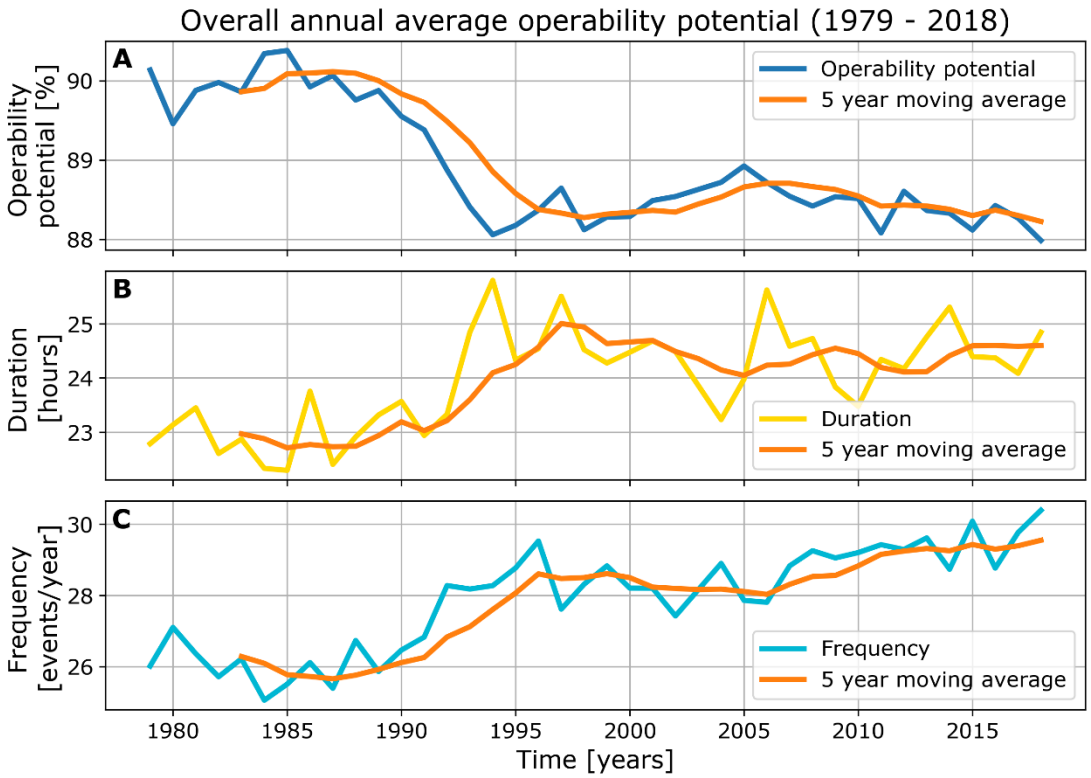

Figure 4.8 Global port operability for annual averages including characterizations

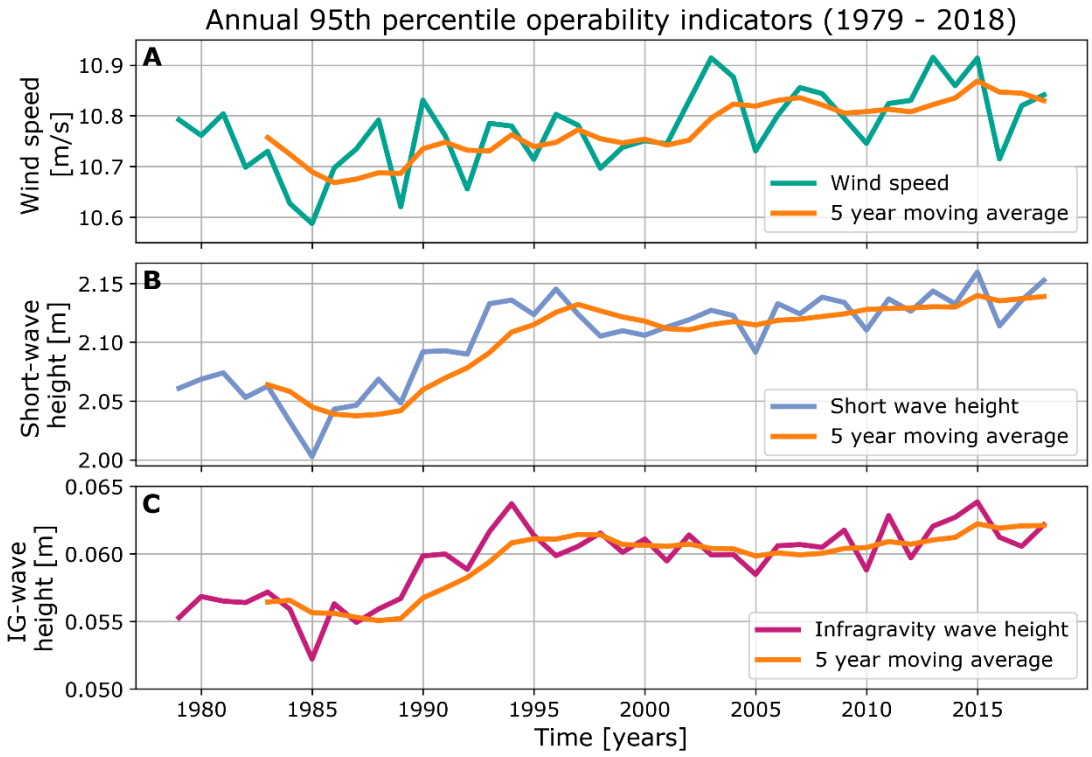

Figure 4.9 Global port operability potential for annual 95th percentiles for different metocean parameters

4.4.5 Seasonality

The sensitivity in the intra-annual time scale is studied via the seasonality divided into 4 individual seasons: DJF, MAM, JJA and SON with an overall average operability potential of 85.0%, 90.4%, 91.3% and 88.3% respectively (Table 4.11). The maximum absolute difference between a season (DJF) and the whole-time scale is 3.9%, which means that the sensitivity in terms of seasonality is robust. Short waves are the most critical indicator in terms of metocean conditions for the whole-time scale but during DJF the operability indicator for IG waves is slightly lower. The frequency (number of exceedance events per year) distributed over the different seasons shows an increase in DJF and SON, the same goes for the average duration of the exceedances. Note that the sum of the frequency and the average of the duration of the season is not equal to the values for the whole-time scale. By splitting the data into seasons and then applying our method season by season, the exceedance events are split at the beginning and end of a season.

Analyzed time period	Overall average operability potential (%)	Operability indicators			Frequency (events/ year)	Duration (hours)
		Wind (%)	Short waves (%)	IG waves (%)		
DJF	**85.0 (-3.9)**	96.4	88.6	88.5	8.9	23.0
MAM	**90.4 (+1.5)**	98.4	92.2	92.8	6.4	21.0
JJA	**91.3 (+2.4)**	99.0	92.7	93.7	5.1	21.0
SON	**88.3 (-0.6)**	97.7	90.7	91.2	7.9	21.8
1979-2018	**88.9**	97.9	91.1	91.6	28	24.5

Table 4.11 Sensitivity on seasonality for four individual seasons (DJF/MAM/JJA/SON)

We map out the different seasons in terms of operability on a global scale. From Figure 4.10 we can conclude that our model maps the different seasons properly. In the Northern Hemisphere there is a clear difference between winter (DJF) with low operability and summer (JJA) with high operability. It is also clearly visible that during JJA there is a low operability around the coastline of the Arabian sea and Bay of Bengal. This can be explained by the Indian monsoon period and starting to be strong in JJA with increasing swell wave heights. If we look at the southern Hemisphere we can see a clear trend that there is a low operability year-round which is probably due to the swell wave climate due to long fetches and year-round relatively larger wind speeds in the southern hemisphere than in the northern hemisphere.

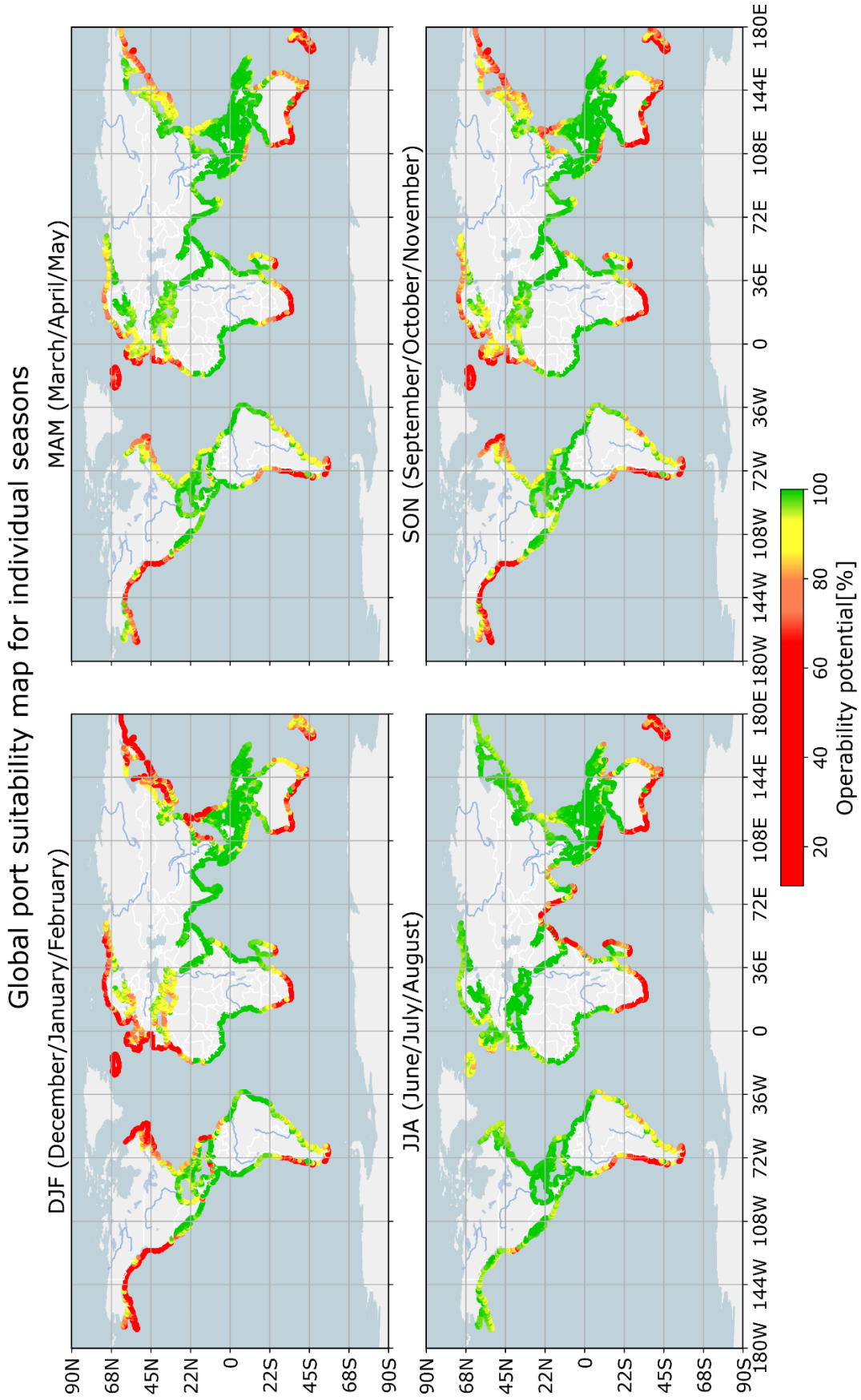

Figure 4.10 Global port operability maps for four different seasons (DJF/MAM/JJA/SON)

5 Discussion

In this chapter, the findings of our study are critically analyzed and interpreted. We reflect on the key limitations and assumptions regarding the operability indicators included in our study, the selected operability thresholds, methods for nearshore wave translation and selected grid points from the global dataset. Hereafter, we will discuss the interannual trends from the sensitivity analysis in Section 4.4.4 to demonstrate the potential of this study.

5.1 Limitations and assumptions

5.1.1 Selected factors for port suitability

We focus on operability indicators related to metocean conditions that are important for the operability and site selection of ports. Several studies have stressed the importance of these parameters for the operability of a port (Hattha & Hiraishi, 2017; Sánchez-Arcilla et al., 2016; Thoresen, 2014). However, there are more factors that could influence the suitability of a port location, for example, the presence of hinterland connections (Hales et al., 2016). There is also a shift towards more sustainable ports where port developments are in harmony with the ecosystem, for example, avoiding sedimentation and erosion in and around ports (De Boer et al., 2019). These considerations could all be relevant for the site selection of a port. Our results can be used complementary to the other relevant factors.

5.1.2 Selected indicators for port operability

In this study we selected three metocean parameters (i.e., wind, short waves, and infragravity waves) that are important for the operability of ports. A beam-on wind can push a vessel of the fenders, thereby reducing the fender friction, resulting in increased (surge) motions of the vessel (PIANC MarCom WG 115, 2012). Large short waves can hinder the tugboats and influence the roll motions of the ship. IG waves are hard to avoid inside ports due to the long wave lengths and swell wave periods could be near the natural motion periods (eigen periods) of a moored container vessel resulting in large vertical motions (Herbers et al., 1995; López & Iglesias, 2014; Sakakibara & Kubo, 2008). The layout of a port has a significant impact on ship motions, since particularly a port layout may provide shelter from waves or possibly amplify them (Miles & Munk, 1961). Port locations and layout are port specific and can be controlled to a certain extent. Metocean conditions cannot be controlled directly by the authorities or operators and are therefore the main important element for port designers who make the (economic) trade-off between the degree of protection from external conditions and the operability.

Water levels and currents are not included in our operability study. Due to different time scales, fluctuations in the water level as a result of the astronomical tide will not have a direct influence on the movements of a ship and the associated (un)loading operations. However, the water level data are relevant for the design of a port, the depth of the approach channel and the positioning of the fenders in relation to the ship (PIANC MarCom WG 121, 2014; Thoresen, 2014). Currents are in most cases the result of tides and exerted forces on the ship which depend on specific ship characteristics, the direction of the current relative to the ship and the keel clearance, this requires physical scale model tests (PIANC MarCom WG 115, 2012). Because of the case specific characteristics for water levels and currents we did not included these indicators in our study, however for some locations water levels and currents are the dominant factors. Via the Global Tide and Surge Model (GTSM) from GLOSSIS (Verlaan et al., 2015) we can include these indicators in our model.

Siltation is not included in our study, in approach channels and port basins it can lead to operational downtime and can also be expensive due to maintenance dredging (Winterwerp, 2005). It is influenced by the availability of sediment and the waves to mobilize those sediments (Sierra & Casas-Prat, 2014). In Appendix 7C a possible indicator, the wave power, is given to estimate the Longshore Sediment Transport (LST) potential as a proxy for siltation. There is no profound threshold found in literature and the outcomes of the wave power formula are summarized over time and cannot be evaluated together with the other metocean conditions per hour. Therefore, the wave power can only be used as a supporting indicator to create a first insight in terms of LST potential.

We also did not consider harbour seiching in our study. Safe and efficient (un)loading operations can be affected by vertical and horizontal movements (PIANC MarCom WG 115, 2012), in which the extent depends on the type of ship and cargo. The vertical oscillations of ships have typical natural periods of 10 – 15 s (depending on the actual mass of the ship) which can be classified in the range of swell periods. The horizontal oscillations of the ship have typical natural periods of 40 – 80 s (depending on the actual mass of the ship and the mooring system) which can be classified in the range of IG waves. To analyze the potential risks of harbour seiching without knowing the actual port layout, the mean or peak wave period from ERA5 dataset can be used as a first insight.

Hence, our study provides first insights into port operability indicators based on global data of metocean conditions. This can be used to identify operability risks and as a first hint on how to mitigate operability risks. These should be verified with detailed modelling studies and/or physical experiments for more accurate estimates and port designs.

5.1.3 Selected operability thresholds

The chosen operability thresholds for defining the operability limits in terms of wind, short waves and infragravity waves are based on literature. These are high-level thresholds bases on aggregated metocean data. In reality, the operability thresholds are determined by the maximum acceptable ship motions, that are induced by the metocean conditions, for safe and efficient operations. PIANC Working Group 115 (2012) sent out questionnaires to ports and terminal operators worldwide to obtain and collect data on local experiences with excess motions of container vessels and corresponding downtimes, also APM Terminals in The Hague has been contacted to obtain this type of information. Unfortunately, it is hard to obtain this type of information due to confidentiality and possible reputation damage issues. This limits the definition of more detailed operability thresholds. Therefore, the results of this study should be seen as a starting point to quickly classify, analyze and compare (port) locations and identify the main drivers for potential risks in terms of port operability potential based on metocean conditions.

In our study we started with fixed operability thresholds and in the sensitivity analysis we lowered and raised these thresholds by ~20-25%. We did not differentiate between the type of cargo and the corresponding operability thresholds. The increasing containerization of world trade and the fact that ships want to spend less time at berth in ports is accompanied by stricter operability thresholds. Our method can be applied for different thresholds as shown in Section 4.4.1, the operability potential for the lowered thresholds it decreases to 76.7% (-12.2) and for the raised thresholds it will increase to 93.5% (+4.6). But we cannot say something about the suitability of ports for specific cargo types because we used rough experience numbers based on literature for the port as a whole without exceptions for different types of cargo. Our model can be re-run with cargo specific operability thresholds to map the suitability for different cargo types based on metocean conditions.

5.1.4 Method for nearshore wave translation

For global information on the nearshore wave characteristics, we applied linear wave theory and assumed an alongshore uniform coast with parallel depth contours and a linear depth profile. This allowed us to gain a global picture on the nearshore wave characteristics within feasible computation times. Applying numerical wave models such as SWAN, would have resulted in more reliable nearshore wave information, as these models account for physical processes such as wind growth, white capping and bed friction. Nevertheless, also for these models we would have to rely on limited information on the bathymetry and the layout and, moreover, they would be much more computationally intensive. As linear wave theory still accounts for important wave physics, such as shoaling, refraction and breaking (using a breaker criterion), the methods is believed to be sufficiently accurate for this global scale analysis. Nevertheless, for local-scale studies it is recommended to apply numerical wave models together with local data on the bathymetry and port geometry to calculate the nearshore wave conditions more accurately.

5.1.5 Selected grid points from global dataset

The port suitability map from Figure 4.6 enables us to zoom in on continental or national level to compare locations in terms of operability indicators. This enables port authorities, operators and designers to identify potential operability risks and evaluate possible protective and mitigating measures. As an example, we take the Port of Salalah and its surroundings, which is also a location in our validation study. During an interview at the office of APM Terminals in The Hague, they indicated that they had problems with the container terminal in the port of Salalah. To identify the problems in terms of metocean conditions, the surroundings of the Port of Salalah are mapped in Figure 5.1. We discovered large differences between the ERA5 grid points in terms of operability potential, these differences are mainly caused by the underlying ERA5 dataset of this large differences in underlying and it is difficult to say something well-founded about port suitability.

Here it should be noted that the depth profile is of high importance in the evaluation of the short and IG waves. But a high-resolution depth profile is out of the scope of this study due to the global approach. The accuracy of our port operability potential estimates depends fundamentally on the accuracy of the ERA5 Re-Analysis dataset from ECMWF. We chose grid locations close but not too close to the coast due to the relatively large resolution of ERA5 which makes it unsuitable to capture small islands and small-size shallow flats/ridges or troughs. The ERA5 significant wave height shows a good agreement with measured buoy data in coastal and deep waters but during tropical cyclones the significant wave height is underestimated (Muhammed Naseef & Sanil Kumar, 2020). Bruno et al. (2020) did a performance assessment of ERA5 in the Arabian Sea using a wave buoy moored offshore Port of Salalah from early August to late December 2013 with a local depth of 30 m. The buoy wave data was compared via back-propagation approach to the nearest ERA5 grid node (50 km offshore). During the monsoon period the ERA5 data overestimates the buoy wave height by a root mean square error (RMSE) of 0.32 m, during the post-monsoon period the wave height overestimation is a RMSE of 0.19 m. From this we can conclude that the ERA5 global data is not accurate enough close to the coast in combination with monsoon periods.

Therefore, the port operability potential map can only be used as a first-order insights due to the limitations of global data in the nearshore. The ERA5 data differ significantly over a distance of 50 km between grid points. Hence, locations of the coast with a distance between 0.1° - 0.8° may still be too close. In further research we suggest using offshore locations with a minimum distance of 0.5° from the coast, because while looking at Figure 5.1 we observe less difference between locations further offshore than locations less than 0.5° offshore. But we still think that ERA5 is a reliable database to provide first-order operability estimates based on metocean conditions on a global scale.

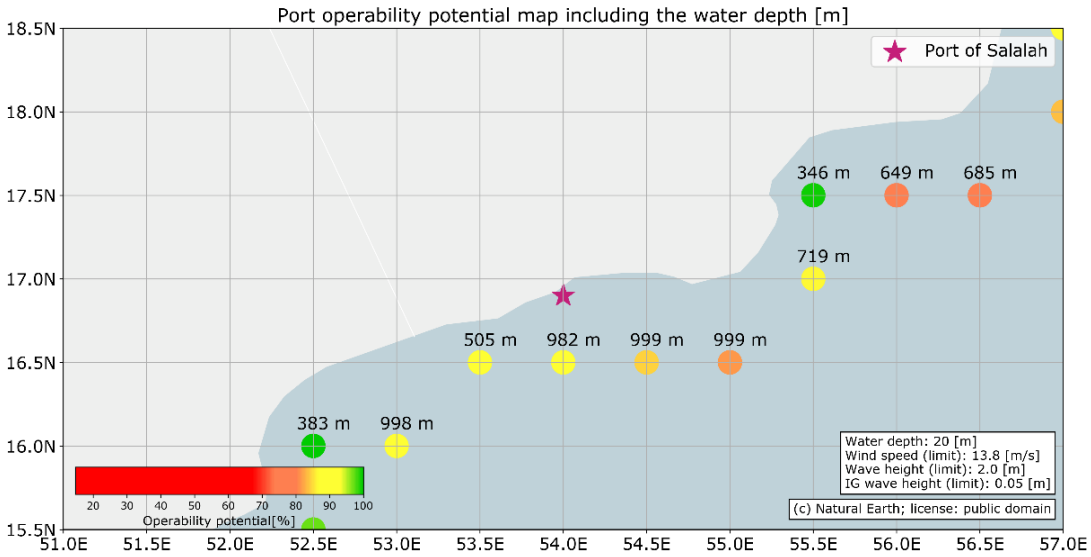

Figure 5.1 Port operability potential map around the port of Salalah including the water depth [m]

5.2 Mapping areas sensitive to changing metocean conditions in the near future

Port operability is sensitive to many factors, such as a changing climate, increasing ship sizes, modernized port facilities and changing cargo types. Our generic method is suitable to give (quick) first-order estimates on how changes in these factors could affect the operability risks geographically. By means of a sensitivity analysis in Section 4.4 we already looked at different operability thresholds (as a proxy for cargo/ship types), water depths and changing metocean conditions. Our method is most sensitive to lowering the operability thresholds (i.e., stricter operability criteria), for which the operability potential decreases. When lowering the operability thresholds with ~20-25%, only 26% (-25.2) of the world's coastline is potentially suitable as a port location (assuming an operability threshold of more than 95%). The distribution of locations across the operability classes changes radically, the majority (36.9%) of the locations is then classified as "low". For changing water depths, our method is insensitive to the average overall operability potential, but there is a shift between the operability indicators. Instead of short waves IG waves are now the lowest operability indicator, because the generation of IG waves is quadratically dependent on the water depth. We also found that our method is robust for changing metocean conditions with 5%.

After analyzing the interannual trends from the sensitivity analysis in Section 4.4.4 we combined those (historic) trends to identify areas sensitive to changing metocean conditions and sea-level rise via the relative change in the overall operability potential. The nearshore depth is adjusted with 1 m till 21 m water depth as a proxy for sea-level rise. The metocean parameters are increased, the wind speed by 1% and the short-wave height by 5%, both following the global trend of the past 40 years, see Figure 4.9A-B. The results are given in Table 5.1 and the global distribution of areas sensitive to change in the near future in Figure 5.2. The operability class with a very high operability potential decreases with 186 locations to 47.1% of all locations. The overall average port operability changes from 88.9% till 87.3% in the near future. The global average frequency increases with 2.2 (exceedance) events per year to 30.2 (exceedance) events. The average global duration increases with 2.3 hours to 26.8 hours per exceedance event.

Operability classes (%)	Locations (#)	Overall average operability potential (%)	Operability indicators			Frequency (events/ year)	Duration (hours)
			Wind (%)	Short waves (%)	IG waves (%)		
P_{total} > 95	2150 (-186) (47.1%)	**98.6 (-0.1)**	99.7 (0)	99.0 (-0.1)	99.3 (+0.1)	7.6 (+0.4)	13.3 (+0.3)
85 < P_{total} ≤ 95	1076 (+28) (23.6%)	**90.5 (-0.2)**	97.9 (+0.2)	92.8 (-0.4)	94.2 (+0.4)	35.6 (+0.5)	24.8 (-0.2)
75 < P_{total} ≤ 85	535 (-150) (11.7%)	**80.4 (-0.2)**	96.0 (+0.3)	84.8 (-0.6)	86.6 (+1.1)	53.3 (-1.2)	38.1 (+2.4)
P_{total} ≤ 75	799 (+114) (17.5%)	**57.1 (-1.2)**	93.6 (0)	63.1 (-1.7)	67.7 (+1.0)	68.5 (-0.5)	58.2 (+3.2)
Near future	**4560 (100%)**	**87.3 (-1.6)**	**97.8 (-0.1)**	**89.6 (-1.5)**	**91.0 (-0.6)**	**30.2 (+2.2)**	**26.8 (+2.3)**

Table 5.1 Overview of the results for 4560 locations across the world in the near future compared to 1979-2018

The relative change on port operability potential can provide insight into the possible influences of climate change on port operability on a global scale, we visualized the relative change in operability potential in Figure 5.2. What stands out is that (port) locations on the southern hemisphere are more sensitive to change in the near future than (port) locations on the northern hemisphere. It can also be concluded that locations which have a high-operability in the last 40 years are relative changing far less to nothing compared to locations which are denoted as low-operability, those locations changing relatively far more in terms of port operability. The main significant driver for sensitive areas in the near future are short waves, hereafter the IG waves and for small percentages the increased wind speed.

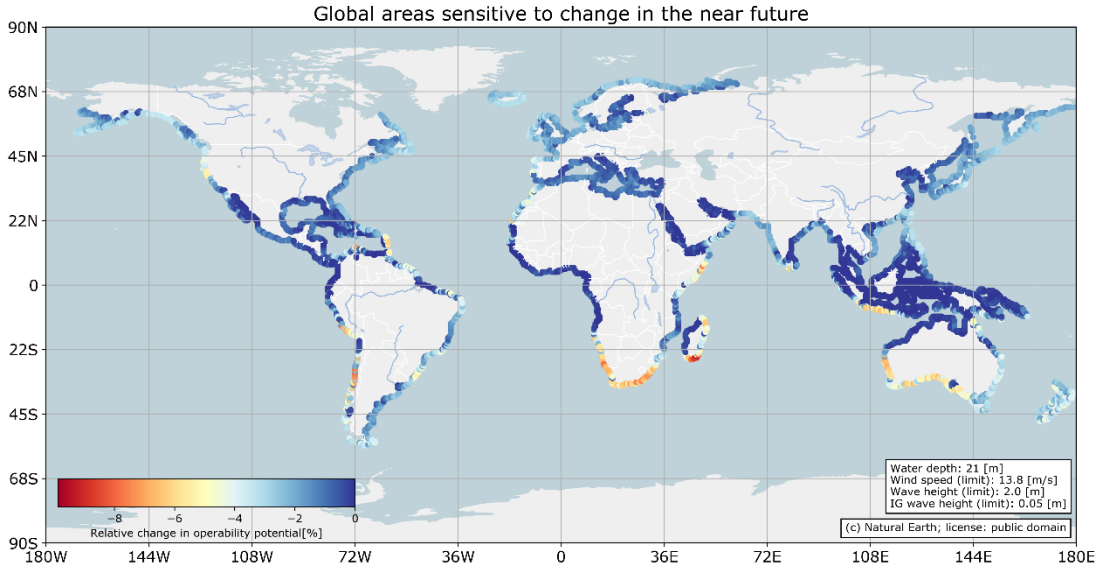

Figure 5.2 Geographical overview on areas sensitive to changes in metocean conditions in the near future. The red dots indicate locations which are very sensitive and the dark blue dots which are less sensitive to change.

6 Conclusions and recommendations

Ports are crucial nodes in the world's supply chain. The operability of a port can be affected by the ambient wave or weather conditions (i.e., metocean conditions). So far, no study has been done to create a global view on port operability based on metocean conditions, including the methods to analyze it. In this study we provide insights into which metocean indicators may influence port operability at which locations around the world. The main research question is: "How can global datasets of metocean conditions be used to assess and compare port locations in terms of port operability?". In this chapter we systematically answer the four sub-questions in Section 1.3 to formulate a conclusion of this study.

6.1 Conclusions

There are many factors that can influence the operability of a port. We evaluated a range of metocean indicators that are important for a port's operability: wind, short waves and infragravity waves. In this study we developed and validated a generic method based on the (global) ERA5 reanalysis data to analyze the port operability in terms of metocean conditions for the period 1979 to 2018. This resulted in the classification of (port) locations into different operability classes, identifying the driving operability indicators and creating a geographical overview.

For existing port locations, we can identify operability risks that can have a major impact on the assets in a port. Due to changing use of a port, the risk profile may also change over time. Increasing containerization, for example, makes the operability thresholds stricter and reduces the operability potential. On the other hand, metocean conditions may change as a result of possible climate change, which can be identified through sensitivity analysis. We can also identify "hotspot" port locations (operability potential ≤ 75%) where ships may have a high probability of delays.

Potential new port developments can benefit from this study due to analyzing and mapping 4560 locations equidistantly spaced along the world's coastline. Now we can easily identify which areas are more susceptible to operability risks from metocean conditions than others. We found that about half (51.2%) of the world's coastline is potentially suitable as a port location in terms of metocean conditions (operability potential > 95%). We can also find suitable (new) port locations where port operability risks are as low as possible, or when the location is already fixed, give an indication which risks have to be studied in more detail. On a global scale, short waves are the most critical indicator for potential operability risks, followed by IG waves, and the wind conditions are relatively less important. The results show large geographical differences in the operability risks of port locations. Around the equator and inland seas are generally more favorable for port locations.

This study also clearly shows the change over time of relevant metocean parameters, operability potential, average duration of exceedance events and number of exceedance events. From interannual trends we found that the overall average operability potential decreases by about 2% over a 40-year period. By extrapolating these global trends to the global metocean database, we estimate an average decrease of 1.6% for the overall average operability potential for the near future of 87.3%. This enables (future) port owners or operators to investigate if their planned and future investments coincide with possible risks and feasibilities from wave or weather conditions.

Global estimates should be seen as first-order insights and still be verified locally to consider the local bathymetry, influence of the port layout (wave breaking, sheltering, diffraction and reflections) and details of ship characteristics, cargo and mooring systems. Apart from this, the results provide insights into which regions and which type of operability risks can be expected for ports due to metocean conditions. This can be input for improved decision making for further analysis.

6.2 Recommendations

In Chapter 5, we discussed several limitations and assumptions that can be reduced by further research. In this section we will follow up on those limitations and assumption to make our model more accurate, widely usable and generate a broader perspective.

1. By extending the input parameters affecting the port operability with water level and current data from the Global Tide and Surge Model (GTSM) from GLOSSIS (Verlaan et al., 2015) we can create a better estimate on the port suitability. The data is available at Deltares on the same grid as ERA5 with values per hour, this allows our generic method to apply without adjustments after defining a common operability threshold for these parameters.
2. To make our model widely usable and adaptable for different operability thresholds and assumptions, we could use Google Earth Engine to create an online application in cooperation with the Deltares Global Data Services. All the relevant ERA5 data needs to be uploaded to the cloud, hereafter we apply our method on the different metocean parameters. In this way we could create an online application were port authorities, operators and designers can get real-time insights into operability indicators by filling in their own operability thresholds. This enable them to analyze existing port locations, search for locations to develop a new port with operability risks as low as possible or get more in-depth operability information with multiple figures like wave and wind roses, joint-occurrence-tables and seasonality information.
3. One remaining question is which operability thresholds port authorities and operators apply in relation to cargo operations. We could talk (again) with port operators because we are convinced that our model and outcomes could benefit them to set up a partnership. By working together with the university, research institute and a port operator, we would be able to verify first-order insights and combine global data with local specific (buoy) data and operability figures which benefits everyone.
4. Ports have a variety of socio-economic impacts on the global economy but can also be seen as an accelerator for local economic development. Especially in emerging economies there are new port developments with large investments and a strongly growing population. In addition to the wave and weather conditions, it is also possible to look at the socioeconomic well-being of port regions and the hinterland, in order to analyze the feasibility of a port location in a broader perspective. Instead of selecting port locations based on harbor size from the WPI, we can also look at cargo throughput and revenue of ports to create a better benchmark and selection of “hotspots”. Hereafter, we can substantiate our analysis based on the sensitivity to change with socioeconomic factors, e.g., population growth around port regions and estimated economic growth, to identify locations sensitive to changes in metocean conditions and socio-economics in the near future.

7 Bibliography

African Development Fund. (2008). Doraleh Container Terminal Port Project. Retrieved 21 January 2020, from https://www.afdb.org/en/documents/document/djibouti-doraleh-container-terminal-port-project-esia-summary-12938

Airy, G. B. (1845). Tides and Waves. In *Encyclopaedia Metropolitana* (Vol. 5, p. 156).

Bakermans, B. A. (2014). *Open Ports for Container Vessels: An exploratory study into the possibilities for offshore and exposed container ports*. MSc. Thesis - Delft University of Technology.

Battjes, J. A., & Stive, M. J. F. (1985). Calibration and verification of a dissipation model for random breaking waves. *Journal of Geophysical Research: Oceans*, *90*(C5), 9159–9167. https://doi.org/10.1029/JC090iC05p09159

Bellotti, G. (2007). Transient response of harbours to long waves under resonance conditions. *Coastal Engineering*, *54*(9), 680–693. https://doi.org/10.1016/j.coastaleng.2007.02.002

Bont, J. De, Molen, W. Van der, Lem, J. Van der, Ligteringen, H., Mühlestein, D., & Howie, M. (2010). Calculations of the Motions of a Ship Moored With Moormaster ™ Units. *Proceedings of the 32nd PIANC International Navigation Congress*, 622–635.

Booij, N., Holthuijsen, L. H., & Ris, R. C. (1997). `SWAN' wave model for shallow water. *Proceedings of the Coastal Engineering Conference*, *1*, 668–676. https://doi.org/10.1061/9780784402429.053

Bruno, M. F., Molfetta, M. G., Totaro, V., & Mossa, M. (2020). Performance Assessment of ERA5 Wave Data in a Swell Dominated Region. *Journal of Marine Science and Engineering*, *8*(3). https://doi.org/10.3390/jmse8030214

Bruun, P. (1989). *Port Engineering, Volume 1, Harbor Planning, Breakwaters, and Marine Terminals* (4th ed.). Houston: Gulf Publishing Company.

Campos, Á., García-Valdecasas, J. M., Molina, R., Castillo, C., álvarez-Fanjul, E., & Staneva, J. (2019). Addressing long-term operational risk management in port docks under climate change scenarios-A Spanish case study. *Water (Switzerland)*, *11*(10). https://doi.org/10.3390/w11102153

Carr, C. M., Yavary, M., & Yavary, M. (2004). Wave agitation studies for port expansion - Salalah, Oman. *Port Development in the Changing World, PORTS 2004, Proceedings of the Conference*, (Port Development in the Changing World), 71–80. https://doi.org/10.1061/40727(2004)8

Christodoulou, A., Christidis, P., & Demirel, H. (2019). Sea-level rise in ports: a wider focus on impacts. *Maritime Economics and Logistics*, *21*(4), 482–496. https://doi.org/10.1057/s41278-018-0114-z

De Boer, W. P., Mao, Y., Hagenaars, G., De Vries, S., Slinger, J., & Vellinga, T. (2019). Mapping the Sandy Beach Evolution Around Seaports at the Scale of the African Continent. *Journal of Marine Science and Engineering*, *7*(May). https://doi.org/10.4121/uuid

De Boer, W. P., Slinger, J. H., Wa Kangeri, A. K., Vreugdenhil, H. S. I., Taneja, P., Addo, K. A., & Vellinga, T. (2019). Identifying ecosystem-based alternatives for the design of a seaports marine infrastructure: The case of tema port expansion in Ghana. *Sustainability (Switzerland)*, *11*(23), 1–19. https://doi.org/10.3390/su11236633

Del Estado, P. (2007). *Desing of Maritime Configuration of Ports, Approach Channels and Harbour Basins* (Vol. 53; P. Del Estado, Ed.). V.A. Impresores S.A.

Deltares. (2016). PHAROS - Lockfill - User & Technical Manual. Retrieved from www.oss.deltares.nl

DHI. (2017). MIKE 21 SW - Spectral Wave Model Short Description. In *DHI Water and Environment*. Horsholm, Denmark.

ECMWF. (2019). Copernicus Climate Change Service (C3S) (2017): ERA5: Fifth generation of ECMWF atmospheric reanalyses of the global climate. Retrieved 1 November 2019, from Copernicus Climate Change Service Climate Data Store (CDS) website: https://cds.climate.copernicus.eu/cdsapp#!/home

Guo, J. (2002). Simple and explicit solution of wave dispersion equation. *Coastal Engineering*, *45*(2), 71–74. https://doi.org/10.1016/S0378-3839(02)00039-X

Hadijah, S. (2013). *Assessing the feasibility of open container ports*. MSc. Thesis - UNESCO-IHE.

Hales, D., Lam, J. S. L., & Chang, Y. T. (2016). The balanced theory of port competitiveness.

Transportation Journal, *55*(2), 168–189. https://doi.org/10.1353/tnp.2016.0010
Hasselmann, K. (1962). On the non-linear energy transfer in a gravity-wave spectrum: Part 3. Evaluation of the energy flux and swell-sea interaction for a Neumann spectrum. *Journal of Fluid Mechanics*, *12*(4), 481–500. https://doi.org/10.1017/S002211206300032X
Hasselmann, K., Barnett, T. P., Bouws, E., Carlson, H., Cartwright, D. E., Eake, K., … Walden, H. (1973). *Measurements of wind-wave growth and swell decay during the joint North Sea wave project (JONSWAP). 46*(8).
Hattha, W., & Hiraishi, T. (2017). Berth Operability and Port Downtime Due to MetOcean in Eastern Thailand. *The 27th International Ocean and Polar Engineering Conference*, p. 8. San Francisco, California, USA: International Society of Offshore and Polar Engineers.
Herbers, T. H. C., Elgar, S., & Guza, R. T. (1994). Infragravity-frequency (0.005-0.05 Hz) motions on the shelf. Part I: forced waves. *Journal of Physical Oceanography*, *24*(5), 917–927. https://doi.org/10.1175/1520-0485(1994)024<0917:IFHMOT>2.0.CO;2
Herbers, T. H. C., Elgar, S., & Guza, R. T. (1995). Generation and propagation of infragravity waves. *Journal of Geophysical Research: Oceans*, *100*(C12), 24863–24872. https://doi.org/10.1029/95JC02680
Holthuijsen, L. H. (2007). Waves in oceanic and coastal waters. In *Waves in Oceanic and Coastal Waters* (Vol. 9780521860). https://doi.org/10.1017/CBO9780511618536
ICS. (2020). Shipping and World Trade. Retrieved 2 April 2020, from https://www.ics-shipping.org/shipping-facts/shipping-and-world-trade
JMA. (2013). JRA-55: Japanese 55-year Reanalysis, Daily 3-Hourly and 6-Hourly Data. Retrieved from Research Data Archive Computational & Information Systems Lab website: https://rda.ucar.edu/
JOC. (2014). The Trends , Outlook and Market Forces Impacting Ship Turnaround Times. In *JOC Group Port Productivity*.
Kalnay. (1996). The NCEP/NCAR 40-year reanalysis project. Retrieved from NOAA Physical Sciences Laboratory website: https://psl.noaa.gov/data/gridded/index.html
Kassimi, A. (2016). *Design tool for an offshore harbour*. MSc. Thesis - Delft University of Technology.
Ligteringen, H., & Velsink, H. (2017). *Ports and Terminals* (2nd ed.). Delft: Delft Academic Press.
Longuet-Higgins, M. S., & Stewart, R. W. (1962). Radiation stress and mass transport in gravity waves, with application to 'surf beats'. *Journal of Fluid Mechanics*, *13*(January), 481–504.
López, M., & Iglesias, G. (2014). Long wave effects on a vessel at berth. *Applied Ocean Research*, *47*, 63–72. https://doi.org/10.1016/j.apor.2014.03.008
Massey, T. C., Anderson, M. E., Smith, J. M., Gomez, J., & Jones, R. (2011). STWAVE : Steady-State Spectral Wave Model User ' s Manual for STWAVE , Version 6.0. *Erdc/Chl Sr-11-1*, (September), 90.
Miles, J., & Munk, W. (1961). Harbour Paradox. *Journal of the Waterways and Harbors Division*, *87*(3), 111–132.
Mol, A., Ligteringen, H., & Waanders, A. J. (1986). Motions of moored vessels, a statistical approach. *In: First Australasian Port, Harbour & Offshore Engineering Conference 1986, (Sydney, Australia: Sep. 29-Oct. 2, 1986), Barto*, (86–10), 141–145.
Molina-Sanchez, R., Campos, Á., de Alfonso, M., de los Santos, F. J., Rodríguez-Rubio, P., Pérez-Rubio, S., … Álvarez-Fanjul, E. (2020). Assessing Operability on Berthed Ships. Common Approaches, Present and Future Lines. *Journal of Marine Science and Engineering*, *8*(4), 255. https://doi.org/10.3390/jmse8040255
Muhammed Naseef, T., & Sanil Kumar, V. (2020). Climatology and trends of the Indian Ocean surface waves based on 39-year long ERA5 reanalysis data. *International Journal of Climatology*, *40*(2), 979–1006. https://doi.org/10.1002/joc.6251
Munk, W. (1949). Surf beats. *Eos, Transactions American Geophysical Union*, *30*(6), 849–854. https://doi.org/10.1029/TR030i006p00849
Munk, W. (1950). Origin and Generation of Waves. *Coastal Engineering Proceedings*, *1*(1), 1–4. https://doi.org/10.9753/icce.v1.1
Natural Earth Data. (2020). Natural Earth. Retrieved 8 April 2020, from Free vector and raster map data website: https://www.naturalearthdata.com/
PIANC MarCom WG 115. (2012). *Report No. 115 Criteria for the (un)loading of container vessels*. Brussels.
PIANC MarCom WG 121. (2014). *Report No. 121 Harbour Approach Channels Design Guidelines*. Brussels.

PIANC MarCom WG 24. (1995). *Report No. 24 Criteria for movements of moored ships in harbours – A practical guide*. Brussels.

Rabinovich, A. B. (2009). Seiches and Harbor Oscillations. In *Handbook of Coastal and Ocean Engineering* (pp. 193–236). https://doi.org/10.1142/9789812819307_0009

Rawat, A., Ardhuin, F., Ballu, V., Crawford, W. C., Rawat, A., Ardhuin, F., … Corela, C. (2014). *Infragravity waves across the oceans*. 7957–7963. https://doi.org/10.1002/2014GL061604.Received

Rienecker, M. M., Suarez, M. J., Gelaro, R., Todling, R., Bacmeister, J., Liu, E., … Woollen, J. (2011). MERRA: NASA's Modern-Era Retrospective Analysis for Research and Applications. Retrieved from Journal of Climate website: https://rda.ucar.edu/

Sakakibara, S., & Kubo, M. (2008). Characteristics of low-frequency motions of ships moored inside ports and harbors on the basis of field observations. *Marine Structures*, *21*(2–3), 196–223. https://doi.org/10.1016/j.marstruc.2007.11.002

Sánchez-Arcilla, A., Sierra, J. P., Brown, S., Casas-Prat, M., Nicholls, R. J., Lionello, P., & Conte, D. (2016). A review of potential physical impacts on harbours in the Mediterranean Sea under climate change. *Regional Environmental Change*, *16*(8), 2471–2484. https://doi.org/10.1007/s10113-016-0972-9

Sierra, J. P., & Casas-Prat, M. (2014). Analysis of potential impacts on coastal areas due to changes in wave conditions. *Climatic Change*, *124*(4), 861–876. https://doi.org/10.1007/s10584-014-1120-5

Symonds, G., Huntley, D. A., & Bowen, A. J. (1982). Two-dimensional surf beat: Long wave generation by a time-varying breakpoint. *Journal of Geophysical Research: Oceans*, *87*(C1), 492–498. https://doi.org/10.1029/JC087iC01p00492

The Open University. (1999). *Waves, Tides and Shallow-water Processes* (2nd ed.; Open University Course Team, Ed.). Oxford: Butterworth-Heinemann.

Thoresen, C. A. (2014). Port Designer's Handbook. In *Port Designer's Handbook*. https://doi.org/http://dx.doi.org/10.1680/pdh.60043.099

U.S. Army Corps of Engineers Coastal Engineering Rersearch. (1984). Shore Protection Manual. *Coastal Engineering Research Center*, *I*(4th), 337. https://doi.org/10.5962/bhl.title.47830

Van den Bos, W. (2011). Wind influence on container handling, equipment and stacking. *Port Technology International*, *29*, 89–95.

Van der Molen, W., & Moes, H. (2009). General characteristics of South African ports and the safe mooring of ships. *Proceedings of the 28th Annual Southern African Transport Conference*, (July), 308–314.

Van der Molen, W., Monárdez, P., & Van Dongeren, A. (2006). Numerical simulation of long-period waves and ship motions in Tomakomai Port, Japan. *Coastal Engineering Journal*, *48*, 59–79. https://doi.org/10.1142/S0578563406001301

Van Dongeren, A., De Jong, M., Van der Lem, C., Van Deyzen, A., & Den Bieman, J. (2016). Review of long wave dynamics over reefs and into ports with implication for port operations. *Journal of Marine Science and Engineering*, *4*(1), 1–10. https://doi.org/10.3390/jmse4010012

Van Marle, G. (2015). Measuring port performance. Retrieved 8 March 2020, from LongRead website: https://theloadstar.com/wp-content/uploads/The-Loadstar-LongRead-Port-productivity1.pdf

Verlaan, M., De Kleermaeker, S., & Buckman, L. (2015). GLOSSIS: Global storm surge forecasting and information system. *Australasian Coasts & Ports Conference 2015: 22nd Australasian Coastal and Ocean Engineering Conference*.

Winterwerp, J. (2005). Reducing Harbor Siltation. I: Methodology. *Journal of Waterway Port Coastal and Ocean Engineering-Asce - J WATERW PORT COAST OC-ASCE*, *131*. https://doi.org/10.1061/(ASCE)0733-950X(2005)131:6(258)

WPI. (2019). World Port Index (Pub 150). Retrieved 11 December 2019, from https://msi.nga.mil/Publications/WPI

A Linear Wave Theory

For the nearshore wave translation, an alongshore uniform coast with parallel depth contours and a linear depth profile is assumed. When entering shallower waters, the amplitude and direction is affected by the limited water depth. The waves change over the longitudinal direction (of propagation) due to variations in the group velocity which is called shoaling. This generally results in an increase of wave height near the coast. Another phenomenon is the changing wave direction due to depth-induced variations in the phase speed in the lateral directions (along the wave crest) which is called refraction. For waves propagating around obstacles, the wave amplitude can vary rapidly across the geometric shadow line. The offshore wave climate is translated nearshore based on shoaling, refraction and wave-breaking criterium which results in a nearshore wave climate via the following formula:

$$H_s = K_s K_r H_0 \tag{7.1}$$

A.1 Shoaling

Harmonic waves, propagating into coastal regions will retain its frequency but due to dispersion relation, decreases the wave length and phase speed (if the depth decreases). The dispersion relation says that waves with a given frequency must have a certain wavelength.

$$\omega^2 = gk \tanh(kd) \tag{7.2}$$

Where g is the acceleration due to gravity (in m/s^2), k is the wave number (in rad/m) and d the water depth (in m) resulting in ω the angular frequency (in rad/s).

The wave velocity (in m/s) is calculated in deep/offshore and shallow/nearshore water:

$$\mathrm{c} = \frac{\omega}{k} = \sqrt{\frac{g}{k} tanh(kd)} \tag{7.3}$$

Hereafter, the group wave velocity (in m/s) in deep and shallow water is calculated:

$$c_g = \mathrm{nc} \quad \text{with} \quad \mathrm{n} = \frac{1}{2}\left[1 + \frac{2kd}{sinh(2kd)}\right] \tag{7.4}$$

And finally, the shoaling coefficient is defined:

$$K_{sh} = \frac{H}{H_0} = \sqrt{\frac{c_{g,0}}{c_g}} \tag{7.5}$$

Where $c_{g,0}$ is the wave group velocity for deep/offshore water and c_g is the wave group velocity in shallow/nearshore water (in m/s). The subscript 0 refers to deep water conditions.

The wave number k is dependent on the wave length λ (in m). Calculating the wave length for deep and shallow water waves is an iterative process, too speed up this process first an approximation is calculated based on Guo (2002) which has a maximum error of about 0.7% after which two iteration are done to accurately calculate the linear dispersion relation for surface gravity water waves.

$$k = \frac{2\pi}{\lambda} \tag{7.6}$$

$$\lambda = \frac{g\,T^2}{2\pi}\tanh\left(\frac{2\pi}{\lambda}d\right) \tag{7.7}$$

$$kd = \frac{\omega^2 d}{g}\left(1 - \mathrm{e}^{-\left(\omega\sqrt{d/g}\right)^{5/2}}\right)^{-2/5} \tag{7.8}$$

The shoaling coefficient depends on the relative water depth d/L_0. The shoaling coefficient is smaller than 1 (implicating a smaller wave amplitude nearshore) for $0.05 < d/L_0 < 0.5$.

A.2 Refraction

Due to the depth variation along the wave crest with a corresponding variation in phase speed along that crest. The crest moves faster in deeper water than it does in shallow water. While assuming parallel depth contours a simple alternative is used: Snell's law to calculate the wave angle at a certain location after calculating the phase speed c.

$$\frac{\sin\theta_0}{c_0} = \frac{\sin\theta}{c} \tag{7.9}$$

Where θ is the angle of propagation, between the wave ray and the normal to the depth contours.

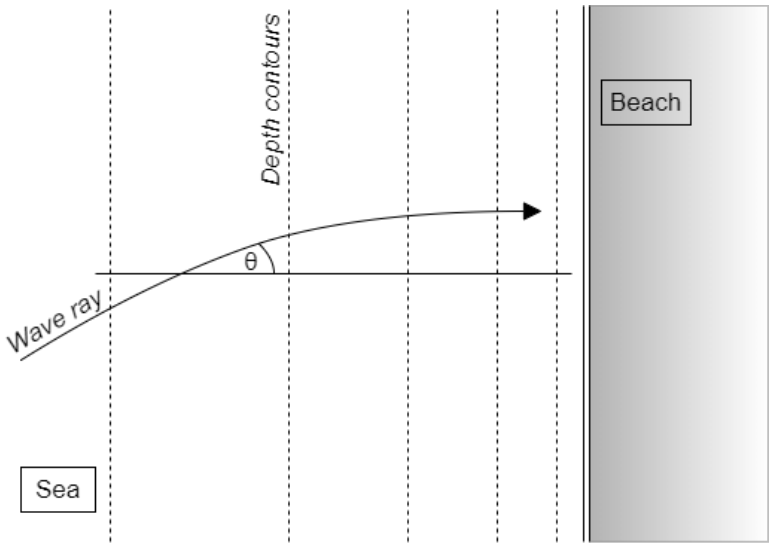

Figure 7.1 Refraction of the wave ray with the angle θ between the wave ray and the normal to the straight and parallel depth contours (Holthuijsen, 2007)

To calculate θ, we need the wave direction and coastline orientation. The wave direction (°) is extracted from ERA5. Defining the coastline orientation to define the normal to the depth contours is challenging. In this study we estimate the coastline orientation across the world via physical coastline vectors from Natural Earth Data (2020). From the ERA5 grid point the closest coordinate on the coastline vector is found. Left and right from this coastline point the 4 closest coordinates are averaged. Via the averaged coordinate left and right from the coastline vector point the coastline orientation is calculated which is converted to the normal of the coastline to calculate the angle of propagation. This method will have some inaccuracies, but it is not feasible to manually derive the coastline orientation for 4560 locations. Based on multiple manual checks this automatic shoreline orientation method seems to provide relatively reliable outcomes.

For parallel depth contours the wave rays will refract the same way, the distance between given wave rays, measured parallel to the depth contours, remain constant with the refraction coefficient:

$$a = \frac{b}{\cos\theta} = constant \tag{7.10}$$

$$K_r = \sqrt{\frac{\mathrm{b}_0}{\mathrm{b}}} = \sqrt{\frac{\cos\theta_0}{\cos\theta}} \tag{7.11}$$

Where b is distance between the parallel wave rays and a is the distance between wave rays parallel to the coast.

A.3 Wave breaking

Shoaling would increase the wave height until infinity, but because of wave breaking this is prevented. Due to the application of shoaling and refraction which is mainly based on 'rule-of-thumbs' it is important to check the output if it makes sense. There are two criteria to determine if a wave will break. First, a limit to the wave steepness and the second is based on depth-induced wave-breaking. The area of interest in this study is in the range of 30 – 10 m water depths. The wave steepness criterion based on Miche (1944) better describes steeper waves which is usually limited to smaller water depths close to the coast (surf zone). Therefore, the ratio between wave height and water depth is used via a general guideline: the breaker index $\gamma_b = H_b/h_b = 0.73$ (based on the average best values from (Battjes & Stive, 1985)), where H_b is the breaking wave height and h_b is the water depth at the breaking point. If there are waves in the output of our model exceeding the maximum allowable wave height based on the assumed nearshore water depth (20 m) these waves are scaled down to the maximum wave height just before breaking.

Another aspect worth mentioning is wave reflection. Ports consists of quays with vertical walls which reflect incoming waves and result in standing waves in the harbor basin and form hindrance for port operations. For accurate operability estimates waves in ports need to be modelled properly to understand the wave reflection and possible measures to mitigate via permeable structures which are very effective. This is also out of the scope of this research due to the case specific character of wave reflection in ports and we thrive for a global approach on port operability. (Holthuijsen, 2007)

B Visualization of metocean parameters and operability indicators

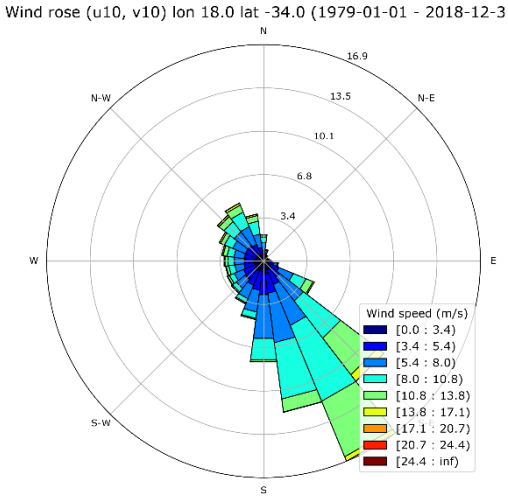

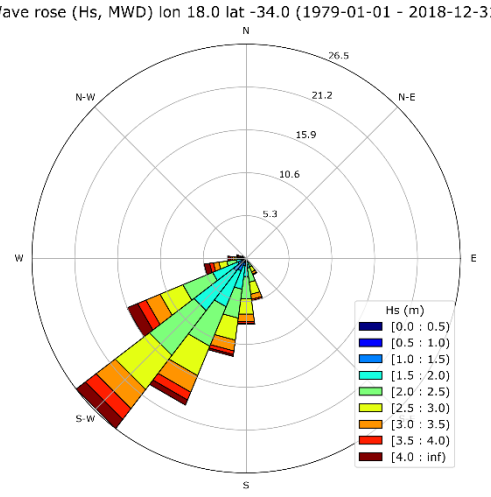

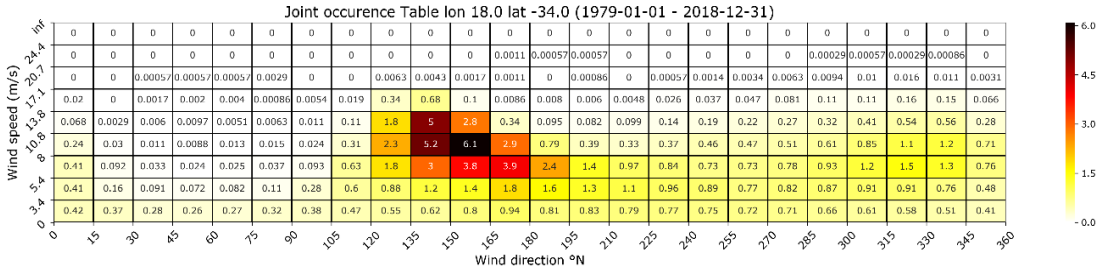

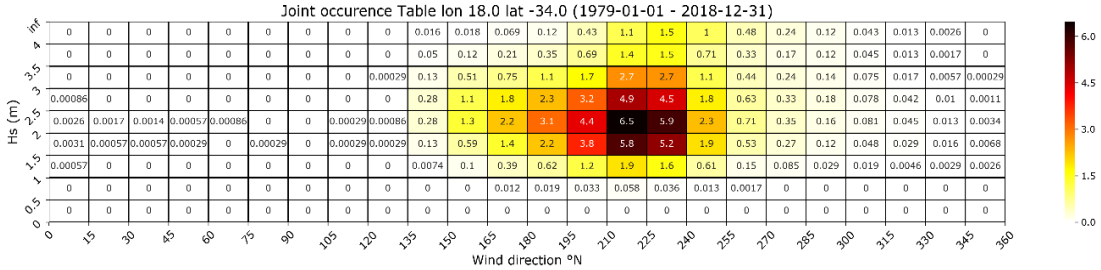

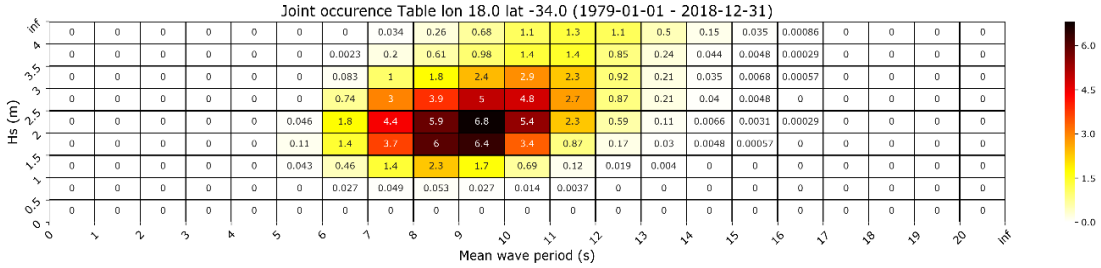

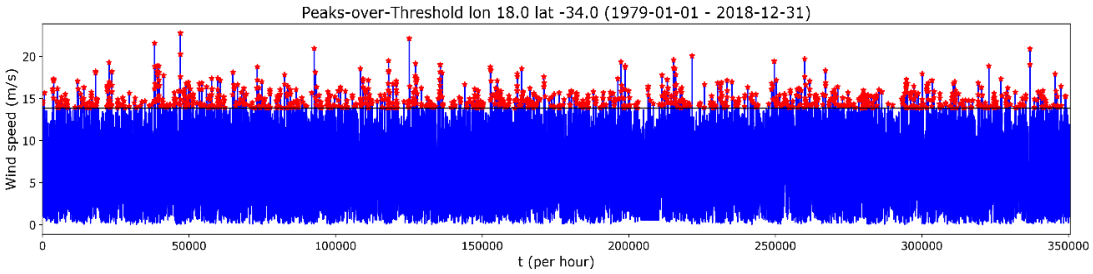
Peaks-over-Threshold lon 18.0 lat -34.0 (1979-01-01 - 2018-12-31)
Wind speed (m/s)
t (per hour)

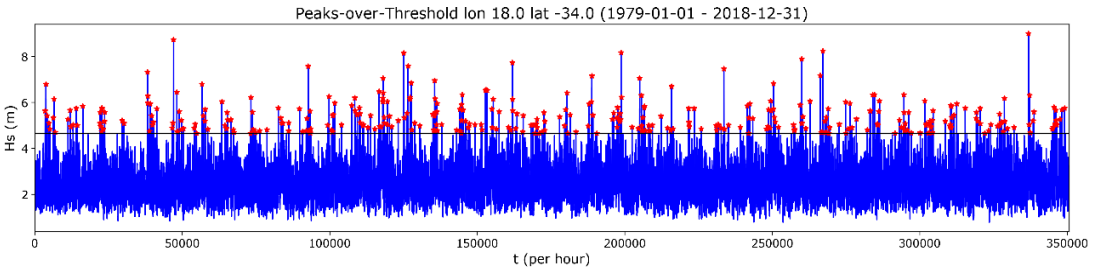
Peaks-over-Threshold lon 18.0 lat -34.0 (1979-01-01 - 2018-12-31)
Hs (m)
t (per hour)

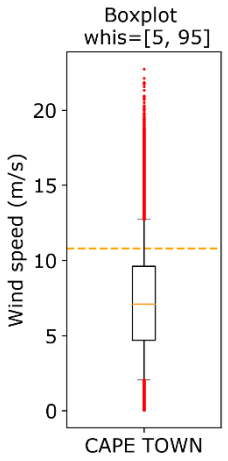
Boxplot
whis=[5, 95]
Wind speed (m/s)
CAPE TOWN

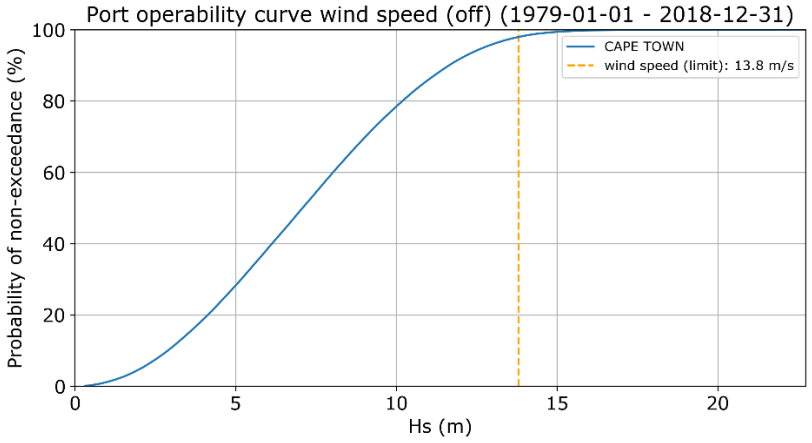
Port operability curve wind speed (off) (1979-01-01 - 2018-12-31)
CAPE TOWN
wind speed (limit): 13.8 m/s
Probability of non-exceedance (%)
Hs (m)

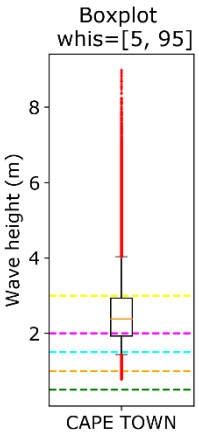
Boxplot
whis=[5, 95]
Wave height (m)
CAPE TOWN

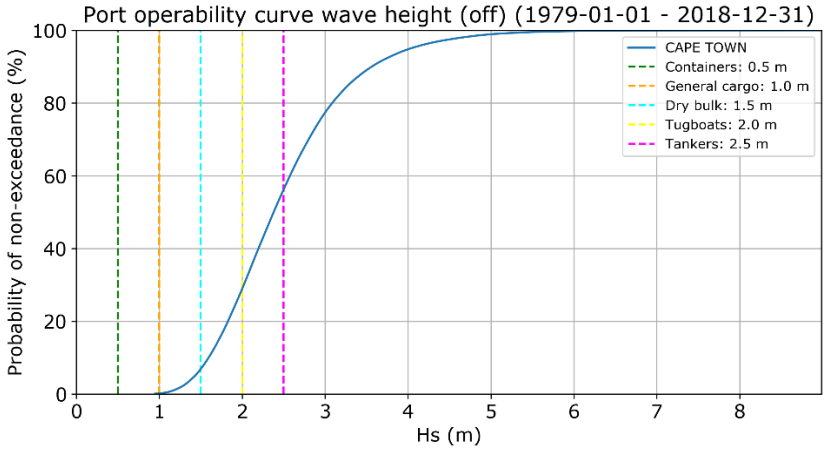
Port operability curve wave height (off) (1979-01-01 - 2018-12-31)
CAPE TOWN
Containers: 0.5 m
General cargo: 1.0 m
Dry bulk: 1.5 m
Tugboats: 2.0 m
Tankers: 2.5 m
Probability of non-exceedance (%)
Hs (m)

C Wave power

Siltation is an important process in approach channels and port basins which entails expensive maintenance dredging to require enough depth. The cause consists of several processes: tidal exchange, eddy exchange and density exchange (Winterwerp, 2005) which are affected by sediment availability and wave influences to mobilize those sediments. (Sierra & Casas-Prat, 2014) Inside the port there are much less wave influences, so a low dynamic environment resulting in the perfect sediment trap. Besides operational downtime it will also highly influence the economics of the port because maintenance dredging is expensive. Breakwaters and traditional ports block the longshore sediment transport (LST) for a portion. The rate of LST can be estimated via a wave energy flux, the longshore component of the wave power as an indicator for longshore sediment transport potential. To do this the CERC (Coastal Engineering Research Center) sediment transport formula is used to derive the wave power which is approximated by (U.S. Army Corps of Engineers, 1984) as follows:

$$WP \sim H_{s,br}^{2.5} \, sin(2\theta_{br}) \qquad (7.12)$$

Where WP is the longshore wave power ($m^{2.5}$), $H_{s,br}$ is the significant wave height at breaking (m) and θ_{br} is the mean wave angle of incidence at breaking (°). Because of the bathymetry not being accurate enough due to the large grid it is impossible to determine the location where the waves will break and the subsequent wave height. Therefore, the nearshore significant wave height calculated in Section 3.1.3 is used instead of the significant wave height at breaking $H_{s,br}$, the same holds for the angle of incidence θ_{br} as a first estimate for the wave power.

Waves heading offshore are already filtered out of the nearshore wave climate, the wave power can have positive and negative values, because $sin(2\theta_{br})$ will range from -1 till 1. All the separate values for the wave power are summed up as absolute numbers for every individual location as the gross longshore wave power indicator $WP_{gross} = |WP_1| + |WP_2|$ because we are interested in the potential of the longshore sediment transport, hereafter the P_{gross} is averaged over the timeseries. Because the wave power is only an indication for the LST potential, it is not feasible to set any substantiated criteria, the wave power is also not analyzed via our generic method as the previous 3 parameters by means of the 4 characterizations due to summing up to a gross longshore wave power indicator. Therefore, the wave power is only given as a supporting indicator for operability.

There is also a clean distinction for the wave power (Table 7.1) between the 5 open layout locations, gross averaged wave power < 1.0 and the 5 locations known for their downtime, gross averaged wave power > 1.0.

Ports with open layout	Wave power ($m^{2.5}/s$)	Ports known for their downtime	Wave power ($m^{2.5}/s$)
Doraleh	0.28	Long Beach	1.56
Jiddah	0.67	Tomakomai	1.74
Hay Point	0.47	Salalah	1.05
Shanghai	0.22	Cape Town	8.24
Hadera	0.51	Geraldton	7.23

Table 7.1 Wave power for 10 validation locations

We can also observe a strong correlation between low operability port locations and large wave powers (Figure 7.2). Which can indicate a larger longshore sediment transport potential at port locations with low operability, which can result in siltation in port and limit the uptime even more due to maintenance dredging.

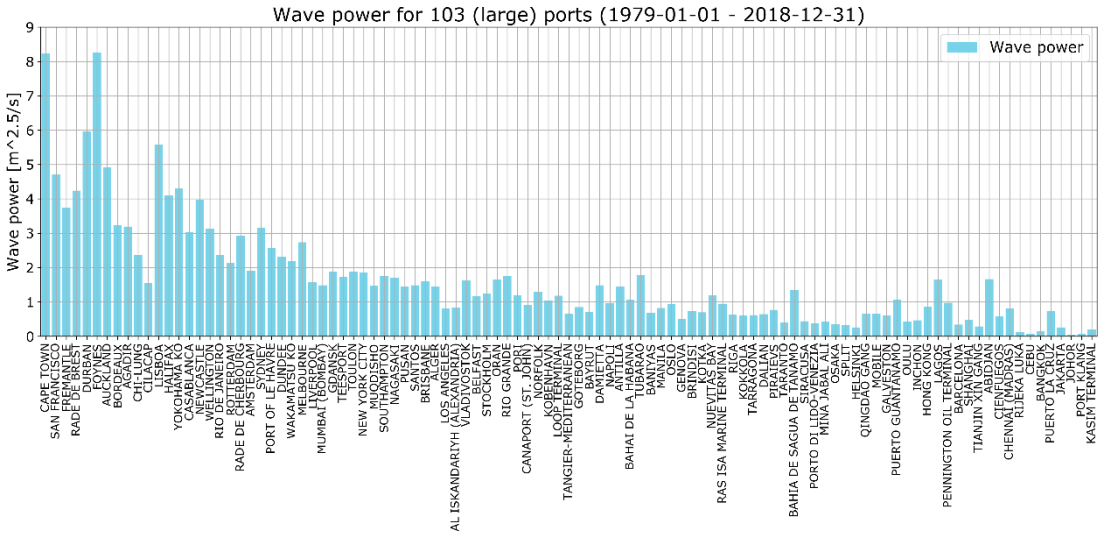

Figure 7.2 Overview on wave power for 103 (large) ports

D Global mapping of port operability indicators

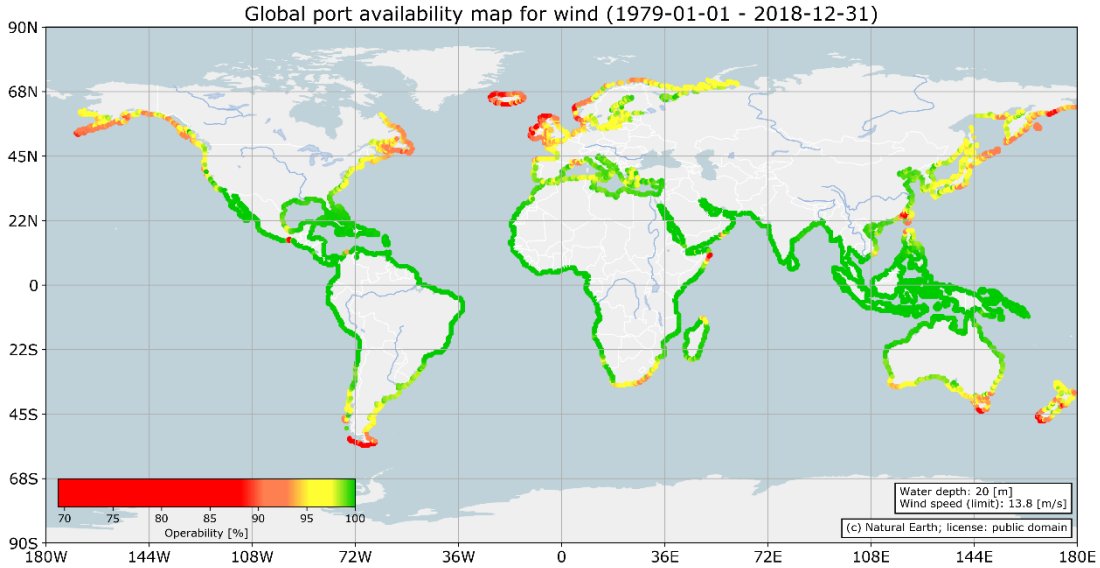

Figure 7.3 Graphical overview on port operability in terms of wind speed

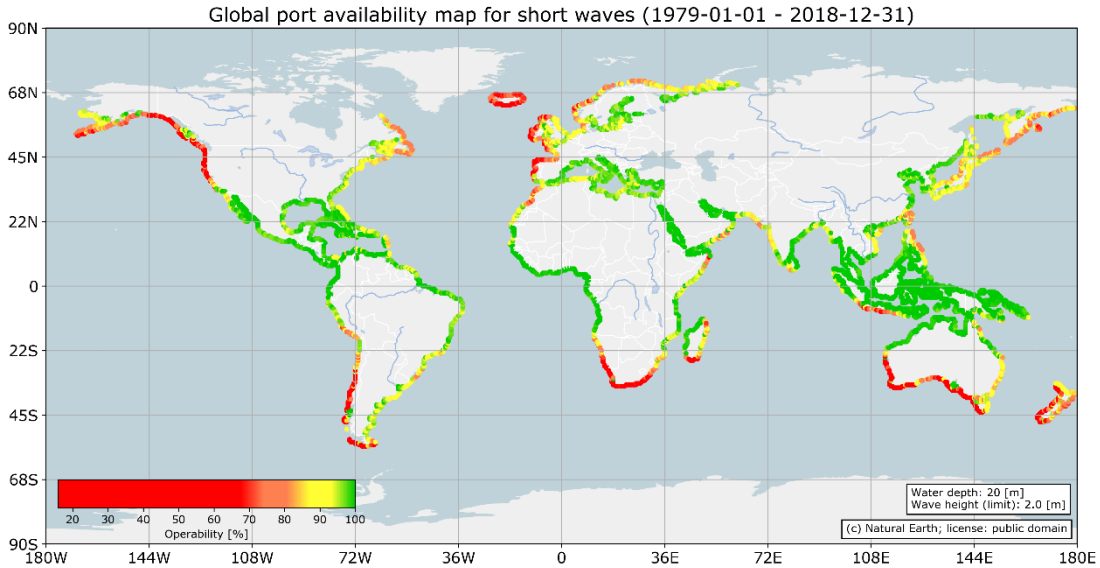

Figure 7.4 Graphical overview on port operability in terms of short waves

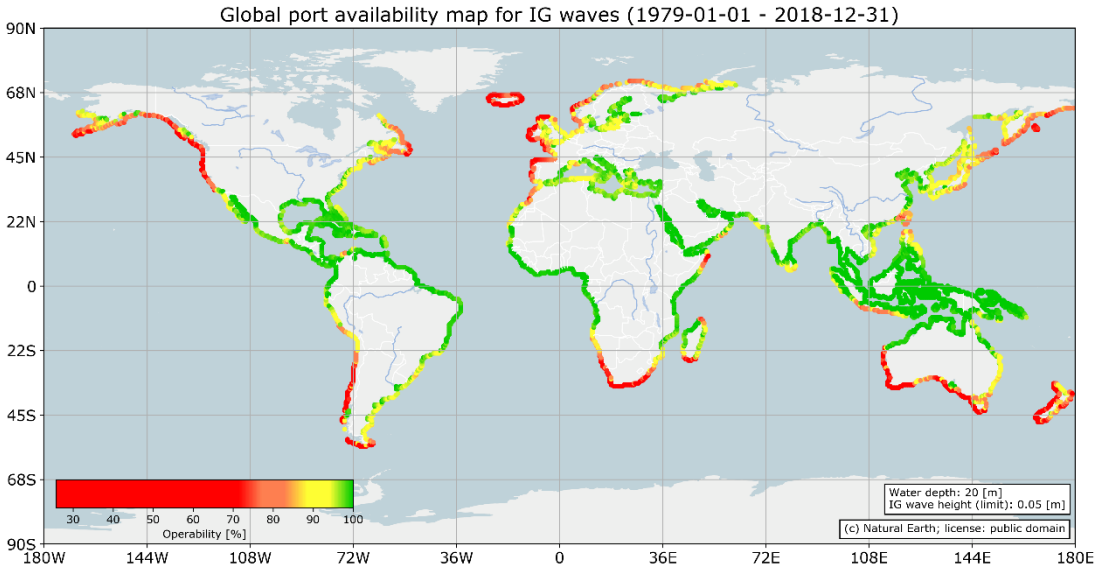

Figure 7.5 Graphical overview on port operability in terms of infragravity waves

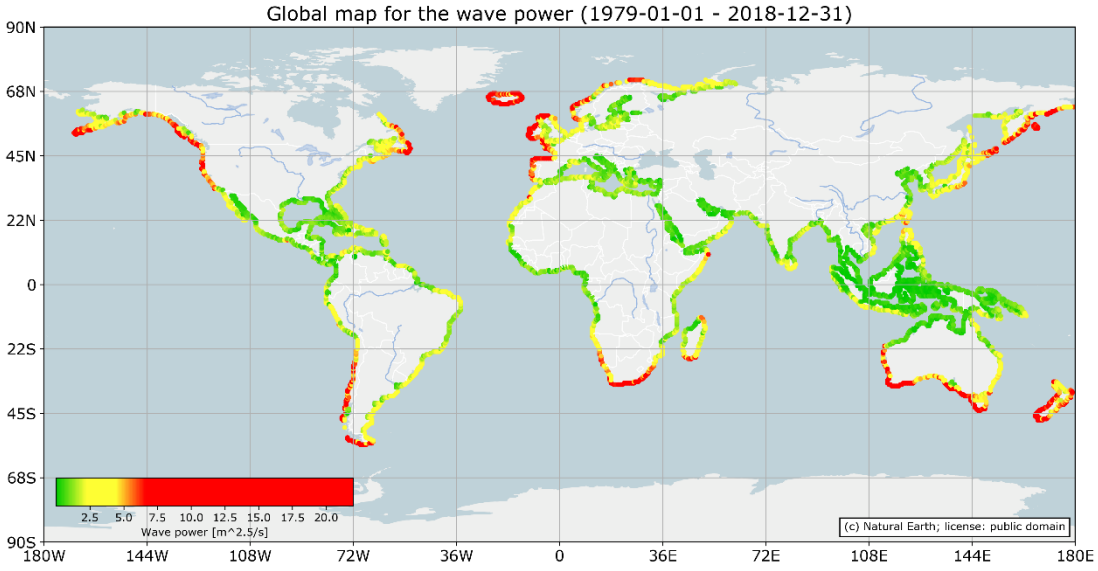

Figure 7.6 Graphical overview on port operability in terms of wave power

E Code archive

GitHub repository for this study

Main model

Yearly model

Output for sensitivity analysis

Output for 10 ports

Output for 103 ports

Output for the world's coastline